Molecular Beam Epitaxy of Monocrystalline GaAs on Water-Soluble NaCl Thin Films

Brelon J. May,[1] Jae Jin Kim,[2] Evan W. K. Wong,[1] Patrick Walker,[1] William E McMahon,[1] Helio R. Moutinho,[1] Aaron J. Ptak,[1] and David L. Young[1]

1 National Renewable Energy Laboratory
2 Shell

NREL is a national laboratory of the U.S. Department of Energy
Office of Energy Efficiency & Renewable Energy
Operated by the Alliance for Sustainable Energy, LLC

This report is available at no cost from the National Renewable Energy Laboratory (NREL) at www.nrel.gov/publications.

Contract No. DE-AC36-08GO28308

Technical Report
NREL/TP-5900-83678
February 2023

Molecular Beam Epitaxy of Monocrystalline GaAs on Water-Soluble NaCl Thin Films

Brelon J. May,[1] Jae Jin Kim,[2] Evan W. K. Wong,[1] Patrick Walker,[1] William E McMahon,[1] Helio R. Moutinho,[1] Aaron J. Ptak,[1] and David L. Young[1]

1 National Renewable Energy Laboratory

2 Shell

Suggested Citation

May, Brelon J., Jae Jin Kim, Evan W. K. Wong, Patrick Walker, William E McMahon, Helio R. Moutinho, Aaron J. Ptak, and David L. Young. 2023. *Molecular Beam Epitaxy of Monocrystalline GaAs on Water Soluble NaCl Thin Films*. Golden, CO: National Renewable Energy Laboratory. NREL/TP-5900-83678. https://www.nrel.gov/docs/fy23osti/83678.pdf.

NREL is a national laboratory of the U.S. Department of Energy
Office of Energy Efficiency & Renewable Energy
Operated by the Alliance for Sustainable Energy, LLC

This report is available at no cost from the National Renewable Energy Laboratory (NREL) at www.nrel.gov/publications.

Contract No. DE-AC36-08GO28308

Technical Report
NREL/TP-5900-83678
February 2023

National Renewable Energy Laboratory
15013 Denver West Parkway
Golden, CO 80401
303-275-3000 • www.nrel.gov

NOTICE

This work was authored by the National Renewable Energy Laboratory, operated by Alliance for Sustainable Energy, LLC, for the U.S. Department of Energy (DOE) under Contract No. DE-AC36-08GO28308. Funding provided by Shell International Exploration and Production Inc., Houston, USA. The views expressed herein do not necessarily represent the views of the DOE or the U.S. Government.

Molecular Beam Epitaxy of Monocrystalline GaAs on Water Soluble NaCl Thin Films

Brelon J. May[1], Jae Jin Kim[2], Evan W. K. Wong[1], Patrick Walker[1], William E McMahon[1], Helio R. Moutinho[1], Aaron J. Ptak[1], David L. Young[1]

[1]National Renewable Energy Laboratory, Golden, USA
[2]Shell International Exploration and Production Inc., Houston, USA

PROJECT SUMMARY

- Monocrystalline solar cell devices were grown on water-soluble NaCl thin films which functioned as a release layer for separation from the GaAs substrate
- GaAs/NaCl/GaAs templates were grown on GaAs (100) substrates by molecular beam epitaxy (MBE)
- The NaCl layers were found to be highly crystalline with the surface reconstruction of the underlying GaAs having an effect on the preferred orientation of the NaCl during the early stages of deposition
- The NaCl thin films begin to strongly desorb from the substrate at temperatures >300°C, which is much lower than typical GaAs growth conditions by MBE
- The morphology and crystallinity of GaAs deposited on NaCl thin films were dependent on the temperature at which the GaAs was first nucleated
- Exposure of the *in-situ* electron beam during growth (both during and between deposition steps) had profound effects on the morphology and crystallinity of the GaAs overlayers
- Monocrystalline GaAs templates on continuous NaCl layers were achieved by combining exposure of the bare NaCl surface to the electron beam prior to nucleation of GaAs, separating growth into low temperature nucleation and high temperature growth steps, and shutter pulsing techniques during the GaAs nucleation step
- GaAs templates on NaCl were verified to be epitaxial using transmission electron microscopy and electron back scatter diffraction
- NaCl layers as thin as 3 nm facilitated near-immediate liftoff of GaAs overlayers by submerging in water; thicker NaCl films allowed for separation of the substrate without water
- Photovoltaic devices were grown on monocrystalline GaAs/NaCl/GaAs templates using MBE and hydride vapor phase epitaxy (HVPE)
- Devices were able to be removed from the substrate and fully fabricated using standard cleanroom processing techniques
- The surfaces of the original substrate remained locally smooth after liftoff of the overlayer, but for samples with prolonged high temperature deposition, micron sized defects were seen on the surface resultant from holes in the overlayer film
- The holes in the overlayer film prevented fabrication of a working device
- The density of the hole defects can be tuned through engineering of the template layer, with thinning of the NaCl layer and increasing the growth rate of the during GaAs nucleation having the largest effects

TABLE OF CONTENTS

1. BACKGROUND AND SUMMARY

The goal of this project was to demonstrate the feasibility of employing an epitaxial NaCl thin film as a water-soluble release layer for III-V photovoltaic devices and GaAs substrate reuse. Over the course of this project efforts were focused on:

- achieving crystalline NaCl thin films on GaAs (100) substrates
- exploring the growth parameters for subsequent GaAs on NaCl thin films in effort to improve crystallinity of the semiconductor layer
- deposition and removal of single crystalline solar cell devices from the parent substrate
- improving morphology and reducing large scale defects in the removed layers to fabricate a working a solar cell device

There was no previous work on direct integration of GaAs/NaCl/GaAs heterostructures at the time of this study. We used molecular beam epitaxy (MBE) to deposit both the alkali halide salt and subsequent III-V material in the same chamber, with no vacuum break. Single crystalline GaAs films were achieved on NaCl layers through careful tuning of the growth parameters and exposure to the reflection high energy electron diffraction (RHEED) beam. Dissolution of the NaCl layer in water provided rapid release of the semiconductor layer from the substrate. Monocrystalline solar cells were grown on the III-V templates using MBE and dynamic hydride vapor phase epitaxy (HVPE). However, the extended time at elevated temperatures required for the cell growth resulted in large area defects from fusion of the semiconductor overlayer to the substrate, causing shorts in fabricated devices. By changing the way that the template layer was grown, the density of these defects could be reduced. Unfortunately, the defects were not reduced to a level allowing for fabrication of a working device.

1.1. Achieving NaCl thin films on GaAs substrates

The first necessary step in achieving a high quality overlayer would be the formation of a crystalline intermediate layer, in this case NaCl. There was limited older work regarding NaCl deposition on GaAs to build from.[1–5] We were able to discern highly crystalline NaCl layers using transmission electron microscopy (TEM). However, X-ray diffraction (XRD) pole figures revealed that these films were not monocrystalline. While some of the material is commensurate to the substrate, the presence of two other surface normal orientations (with 4 equivalent 90° azimuthal rotations) are also observed. The amount of misoriented material could be reduced through growth on different GaAs surface reconstructions, specifically the Ga-rich 4×2 surface. RHEED showed the presence of rings indicating polycrystallinity, during the early stages of growth on As-rich c(4×4) and 2×4 surfaces. These rings were not observed at any point during the growth on the Ga-rich surface. However, XRD pole figures still indicate a smaller amount of misoriented material.

1.2. Effects of electron beam exposure on NaCl films and subsequent growth

Analysis of bare NaCl films *ex-situ* is marred by complications from the film decaying in ambient atmosphere. Additionally, investigation of NaCl layers using electron beam microscopy techniques is difficult as the material decays under the exposure. A less direct observation of this effect is also seen when exposing a bare NaCl surface to the RHEED beam for *in-situ* analysis during growth; prolonged exposure shows a transition in the diffraction pattern from streaky (indicating a smooth surface) to spotted (indicating a rough surface). Exposure of the bare NaCl surface to this electron beam allows for condensation of amorphous As on the surface and changes the nucleation rate of subsequent GaAs. The discovery and implementation of this effect was key to achieving single crystalline GaAs overlayers while maintaining a full NaCl layer which is

necessary for removal of the template layer. The importance of the exposure of the NaCl surface to the RHEED prior to nucleation of the GaAs eventually became clear, as the GaAs overlayers in areas without RHEED exposure fused to the substrate and were not able to be removed.

1.3. Improving the crystallinity and liftoff of GaAs grown on NaCl thin films

Over the wide variety of growth parameters investigated for GaAs growth on NaCl, a variety of different morphologies with a range of crystallinities were observed. Exclusively low temperature deposition resulted in amorphous films with smooth interfaces. As the deposition temperature was increased, the film morphology changed from chunky films to discrete islands with highly textured orientations. The NaCl is volatile and rapidly desorbs from the substrate at the elevated temperatures required to get improved crystallinity. However, by combining a separate lower temperature nucleation step with a higher temperature growth step and utilizing growth schemes to enhance adatom mobility (such as migration enhanced epitaxy and metal modulated epitaxy) monocrystalline films were achieved on complete NaCl layers. These monocrystalline layers were used as templates for photovoltaic device growth using both MBE and HVPE.

As long as a cohesive NaCl layer remained beneath the overlayer, submersion in water resulted in the ability to quickly remove the film/device form the substrate. Layers as thin as ~3 nm were able to facilitate near immediate liftoff. In the case of thicker NaCl layers, the overlayer could also be peeled from the substrate without submersion in water. Solar cell devices were successfully lifted off from the original substrate. However, the extended time at higher temperature required for device deposition in MBE (~2.5 hours at 580°C) resulted in the formation of large-scale hole-like defects which hinder the ability to fabricate a working device. Additional work with thinner NaCl layers, capped with material using a higher effective growth rate, and reducing the highest temperature required was shown to reduce the propensity of formation of these defects.

1.4. Details of deposition and analysis methods

Thin films of NaCl and GaAs were deposited on GaAs (100)±0.1° substrates in an Epi930 MBE reactor with base pressure of 4×10^{-9} torr without any vacuum break. Band-edge thermometry is used to verify the substrate temperature using a kSA BandiT. A beam energy of 15 kV for RHEED which was employed both as an *in-situ* diagnostic tool as well as a source of high energy electrons to help promote nucleation of GaAs on NaCl.[6] To ensure a clean and oxide free surface for subsequent GaAs and NaCl deposition, the GaAs substrates were heated to 620°C for 25 minutes under exposure to excess As flux (~1.68× the 1:1 As flux) from a valved cracker source. Following this, a 300 nm GaAs buffer layer was deposited at 580°C with a As/Ga = 1.68, and subsequently cooled for NaCl deposition. The NaCl (5N, Sigma Aldrich) was supplied from a conventional effusion cell operating at ~480°C which gave a growth rate of 3 nm/min, unless otherwise noted. After NaCl deposition was complete, the sample was heated at a rate of 20-50°C/min to the desired temperature for GaAs deposition. Unless otherwise noted, GaAs was deposited at a growth rate of ~33 nm/min (with co-deposition) measured using RHEED oscillations at 580°C.

The growth morphology and epitaxial relationships of the different layers were investigated using various methods of electron microscopy. Cross sectional SEM was performed on a Hitachi S-4800 using accelerating voltages from 3-7 kV and a beam current of 5-7 nA. EBSD data was acquired with the sample tilted at 70° using an Oxford system with a Symmetry detector and CMOS sensor technology and an acquisition voltage of 20 kV. TEM imaging, electron diffraction

patterns, and energy dispersive X-ray spectroscopy (EDX) were carried out with JEOL 2100F/Oxford Instruments X-Max EDX at 200 kV. The GaAs substrate was tilted so that incident electrons are along <110>. Bright field TEM imaging was performed to show both overall layers and atomic structure of defects. Electron diffraction within area of 100 nm in diameter was acquired to identify the local phases and crystalline orientation. To minimize damage from long electron beam dwell times during EDX map acquisitions, the average information across regions of interest was collected. EDX mapping was conducted with Aztec in ≤ 10 min. Subsequently the counts of the EDX map were summed along the horizontal line perpendicular to the growth direction to achieve line profiles of elemental distribution. High-resolution x-ray diffraction (XRD) and pole figures were collected using a Rigaku Smartlab. For removal of the GaAs film from the substrate, Kapton tape was first attached to the film and then placed in water to dissolve the NaCl layer.

2. TECHNICAL RESULTS AND DISCUSSION

2.1. Deposition of crystalline NaCl thin Films on GaAs substrates

The growth of crystalline NaCl on GaAs (100) substrates is first investigated. This section will cover the growth conditions specific to the growth of the NaCl layers focusing on the growth temperature and surface reconstructions of the underlying GaAs. The crystallinity of the NaCl films is investigated using XRD and TEM. This section will also cover the fragility of bare NaCl to both air and electron beams. Because of this *ex-situ* analysis of NaCl layers is difficult, but the effects of an electron beam will be proved to be useful in later sections.

2.1.1. Deposition of NaCl thin films on GaAs (100) substrates

The first step is to understand the growth of crystalline NaCl on GaAs (100) substrates. First, a 300 nm GaAs buffer layer is grown at 580°C; after completion, RHEED reveals the typical As-terminated 2×4 surface reconstruction. The diffraction pattern converts to a symmetric c(4×4) as the sample is then cooled under an As-overpressure (~1×10^{-6} Torr) until ~340°C. The sample is cooled to the desired temperature for the growth of NaCl (T_{NaCl}). A nominally 30-nm-thick layer of NaCl is deposited using a NaCl deposition time (t_{NaCl}) of 10 minutes and a growth rate of ~3 nm/min. If the As-source remains open when the substrate temperature is < 320°C, the RHEED pattern begins to go diffuse as a result of the condensation of small amounts of amorphous As. In this case, a ring-like pattern quickly appears upon opening of the NaCl shutter which does not revert back to a streaky single-crystalline pattern with further NaCl deposition (Figure 1(a1)). Blurry arcs superimposed on the rings signal some degree of fiber texturing,[7] which in the absence of a crystalline surface on which to nucleate, would suggest that NaCl has a preferred growth direction.

The remaining images of Figure 1 show RHEED patterns viewed along the [110] and [100] directions of 30 nm of NaCl deposited at various T_{NaCl} starting on clean c(4×4) GaAs surfaces and a chamber pressure less than <7×10^{-8} Torr. Deposition at 100°C (Figure 1(b)) is most closely lattice matched with GaAs and displays a streaky pattern with slight undulations indicating small island growth.[8] Figure 1(c) shows patterns from deposition of NaCl at 150°C. The streaks become brighter and Kikuchi patterns become visible indicating that the surface becomes increasingly well-organized and smooth despite a slight increase in the lattice mismatch (which increases from ~0% at 100°C to 2.9% at 580°C) due to the difference in thermal expansion between the materials. Figure 1(d) shows that deposition of NaCl at 175°C results in a dimmer pattern overall which could be for two reasons which will be discussed more in sections 2.3.1. First, the exposure of the NaCl

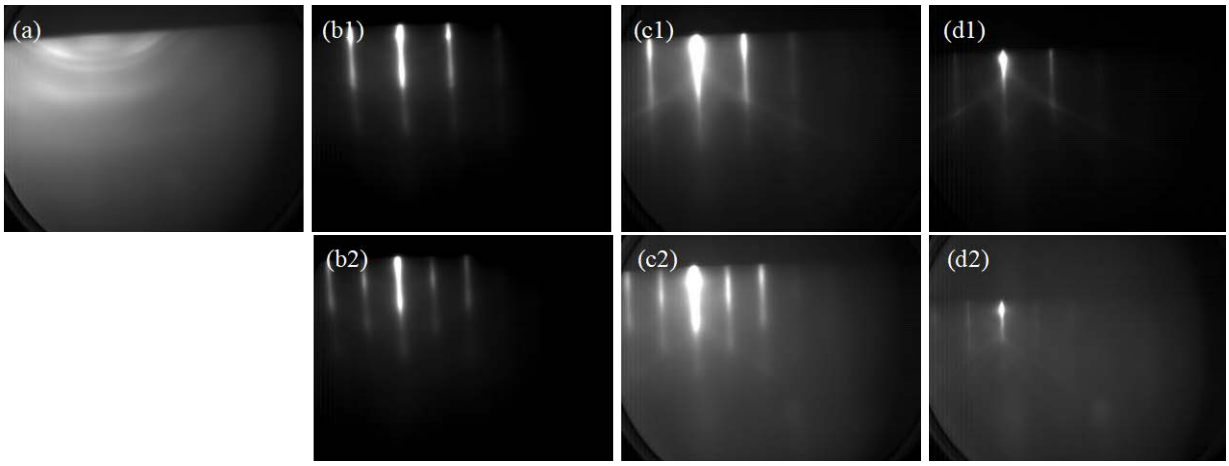

Figure 1: RHEED images of different samples with 10 minutes (roughly 30 nm) of NaCl deposition on (a) a GaAs substrate at 100°C with a small amount of excess As on the surface, and on clean GaAs surfaces at (b) 100°C, (c) 150°C, and (d) 175°C. Top row (1) taken along the [100]. Bottom row (2) taken along [110].

to the RHEED beam begins to have substantial effects on the salt layer at higher temperatures. Second, as the substrate temperature is increased, the NaCl layer begins to decompose. Thus, the nucleation of NaCl at temperatures >175°C was not studied. When deposition occurs on clean GaAs surfaces (Figures 1(b-d)), the ratio of the spacing between streaks along the [110] and [100] directions is proportional to $\sqrt{2}/2$. Additionally, the [110] and [100] patterns of the NaCl are parallel to the [110] and [100] directions of the GaAs, indicating that the NaCl has a cubic symmetric crystalline surface.

2.1.2. Effect of GaAs surface reconstructions on NaCl growth

The deposition of NaCl on three primary GaAs surface reconstructions was investigated. A c(4×4) (Figure 2(a1)) is easily achieved through cooling the sample to ~350°C while maintaining a high As background pressure (around 1×10^{-6} torr). A (2×4) pattern (Figure 2(b1)) is achieved by cooling and closing the As-valve immediately after the GaAs buffer deposition at 580°C; residual As in the chamber keeps a Ga-rich surface from forming. Because of this residual As background, the Ga-rich (4×2) surface reconstruction (Figure 2(c1)) is more difficult to achieve. The As-valve is again closed immediately following buffer layer deposition at 580°C; but the temperature is held constant while the chamber is allowed to pump out for several minutes. Then ~2 monolayers (MLs) of Ga are deposited and the RHEED pattern (observed along <110>) transitions from 2× to 4×, signifying formation of a Ga-rich surface. As the sample cools, As more readily condenses on the surface and the pattern slowly begins to revert back to 2×. This is mitigated through subsequent Ga-flashes until the sample temperature is cooled to ~530°C. Any supply of Ga at temperatures below this results in a more diffuse diffraction pattern (not shown), because the surface mobility of the Ga adatoms is too low to facilitate reconstructions.

The evolution of the RHEED patterns during a ten-minute NaCl deposition at 150°C on each of the reconstructed surfaces are shown in Figures 2(a-c). There is a notable difference in the patterns of the resulting NaCl during the early moments of growth. After 15s (~2.5 ML) of NaCl deposition on the As-rich c(4×4) surface, the reconstructions disappear, and faint rings begin to become present signifying some degree of polycrystallinity at this early stage. The streaks broaden

and become spottier, representative of slight azimuthal rotations (mosaic islands) of small crystallite [8] (Figure 2(a2)). After 30 s (1.5 nm) of deposition, the pattern looks similar (Figure 2(a3)). However, upon further deposition (9 nm, Figure 2(a4)) the rings have disappeared, streaks have become tighter and less spotted, and Kikuchi lines begin to be observed, all indicating a smoother more crystalline material. This trend continues and eventually the pattern becomes very streaky (Figure 2(a5)).

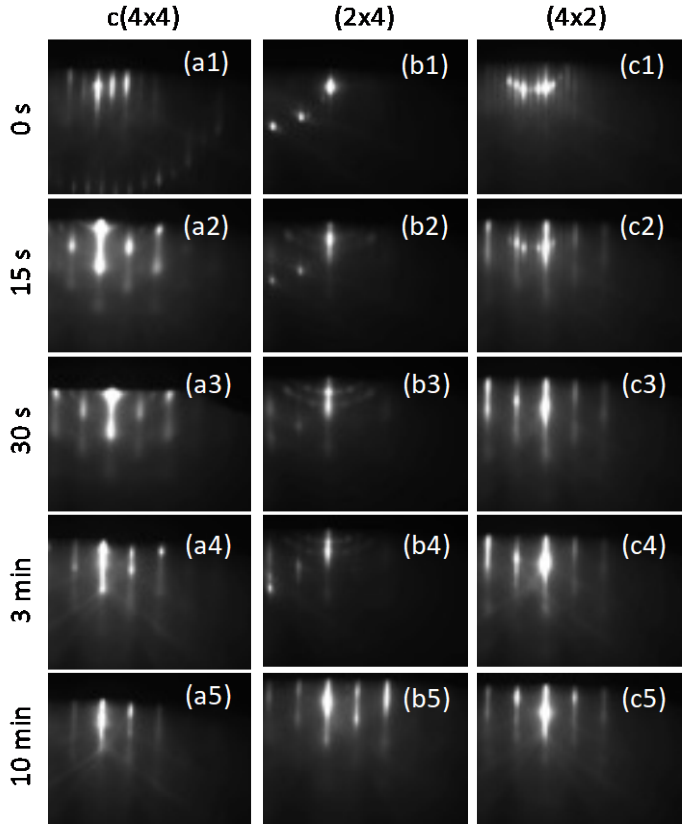

Figure 2: RHEED patterns taken (1) prior to, and after (2) 15s, (3) 30s, (4) 3 min, and (5) 10 min of NaCl deposition on GaAs (100) substrates taken parallel to (a) the [$1\bar{1}0$*] direction on a c(4×4), (b) the [*$1\bar{1}0$*] direction on a (2×4), and (c) the [110] direction on a (4×2).*

The initial moments of growth on As-rich 2×4 surfaces again show weak ring like characteristics (Figure 2(b2)), but in this case they get more pronounced and spotted during the first few nm of deposition (Figure 2(b3)). By 9 nm of deposition (Figure 2(b4)) the rings have started to fade, but unlike the previous case are not yet gone completely, and the pattern has become streakier. After 30 nm of deposition (Figure 2(b5)) the pattern is streaky and there are no ring-like characteristics. However, there are still faint spots that could be indicative of residual 45° misoriented domains as a result from twinning or an additional crystalline phase.

In contrast to the As-rich cases, the initial growth on a Ga-rich 4×2 (Figure 2(c2)) does not show any ring like characteristics. The original reconstruction seems to fade more slowly, and the pattern is only marginally more spotted. However, after only a few more nanometers any trace of the original reconstruction has disappeared (Figure 2(c3)); the pattern is already similar to the end-case scenario for growths on As-rich surfaces. No substantial changes are observed with further

growth (Figures 2(c4-5)) aside from becoming brighter, and Kikuchi lines more prominent. It must also be noted that with deposition on any reconstruction, a pattern with 4-fold rotational symmetry is observed. This fits with the expected symmetry and crystal alignment where the [100] and [110] directions of NaCl are parallel with the respective [100] and [110] directions of GaAs. Each NaCl layer was subsequently capped with GaAs to protect them for *ex*-situ measurements.

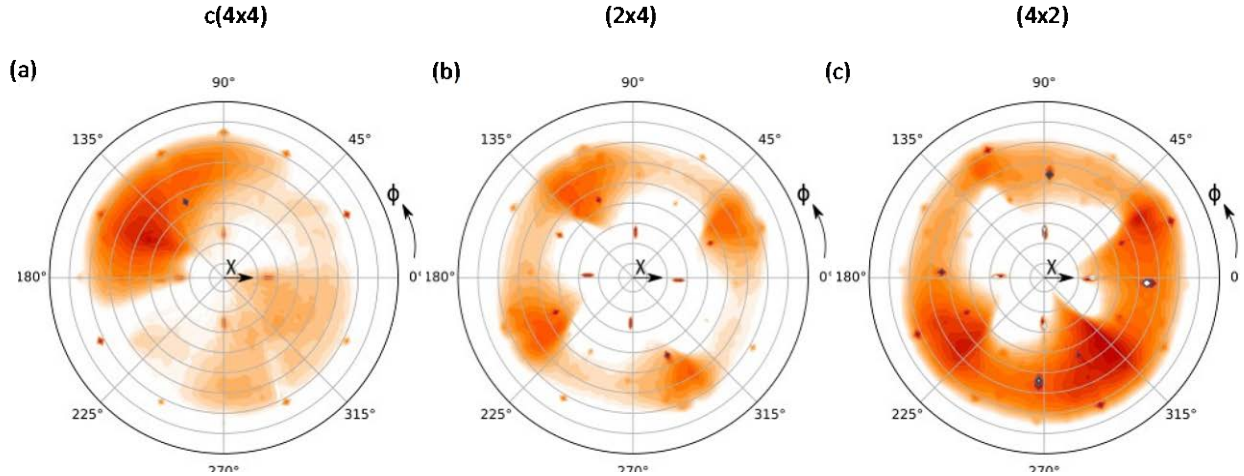

Figure 3: XRD pole figures of the (222) reflection of NaCl deposited on (a) c(4×4), (b) (2×4), and (c) (4×2) GaAs reconstructions

Both GaAs and NaCl have very similar lattice constants at room temperature. Thus, to avoid any spurious signal from the GaAs cap, XRD pole figures are taken of the NaCl (222) peak as the corresponding GaAs reflection should be forbidden. The results show highly textured patterns with 4-fold rotational symmetry in each case (Figure 3). The peaks corresponding to epitaxial NaCl are more intense relative to the other peaks in the sample using the Ga-rich reconstruction (Figure 3(c)). This contrasts with the final RHEED patterns observed for each case, where the NaCl displayed 4-fold rotational symmetry and spacing between peaks nearly identical to the GaAs (100) substrate. It is possible that the other orientations are buried near the substrate/NaCl interface and are visible in the RHEED pattern as the spotted/partial ring structure in the early stages. The additional peaks observed in each case correspond to four 90° rotations of grains that are tilted ~25° from {111} toward {011} but are difficult to index precisely. These peaks have similar symmetry to planes that are observed in EBSD pole figures of textured GaAs films grown on NaCl in Section 2.3. The reason behind the formation of these misoriented grains is still unknown. We believe, based on the RHEED observations, that any of these misoriented grains are at the interface with the substrate and are mostly, if not completely, overgrown and provide a monocrystalline surface on which to nucleate subsequent GaAs.

TEM measurements in Figure 4(a) show a <2 nm layer of material at the interface with the substrate which appears to be amorphous. However, there is only one distinct orientation observed in any NaCl above this layer; fast Fourier transforms (FFTs) of both the NaCl film and GaAs substrate reveal only a single matching pattern suggesting high crystallographic alignment. The reason behind the structural differences between NaCl deposited on As-rich vs Ga-rich are not known. However, both the surface stoichiometry and structure vary between the GaAs surface reconstructions. The reconstruction of the GaAs surface has been shown to have an effect on the size and shape of nuclei in other systems[9] and changes in the growth surface have stabilized non-

traditional facets of NaCl.[1] Because the c(4×4) surface reconstruction is the most consistently achievable of the three discussed, it is used as the platform for the remaining NaCl layers in the investigation of subsequent GaAs deposition in the next section.

Figures 4(b,c) show a lower magnification STEM image and the corresponding EDX line profile. The image reveals the presence of a similar upper GaAs/NaCl interface but the EDX shows that the interface with the substrate is compositionally sharper than this upper interface. There is no Ga or As observed in the bulk of the NaCl layer. Additionally, the Cl is also well contained in the NaCl and no appreciable outward diffusion is seen. The signal for Na is not plotted here because the main K-peak overlaps the dominant Ga L-peak; the Ga signal is taken using the K-family peaks to avoid contamination from any Na signal. Thus, the Cl data combined with the TEM is used to verify the presence of a NaCl layer and is only present within the bright layer. A slight increase in oxygen levels at both interfaces is observed, which is likely due to the growth pauses between the buffer layer and the NaCl, and the NaCl and the GaAs cap. This could also be related to the interfacial layers at both interfaces observed in the STEM image. The only presence of C is in the protective layer deposited during sample preparation, as also marked by the Pt signal.

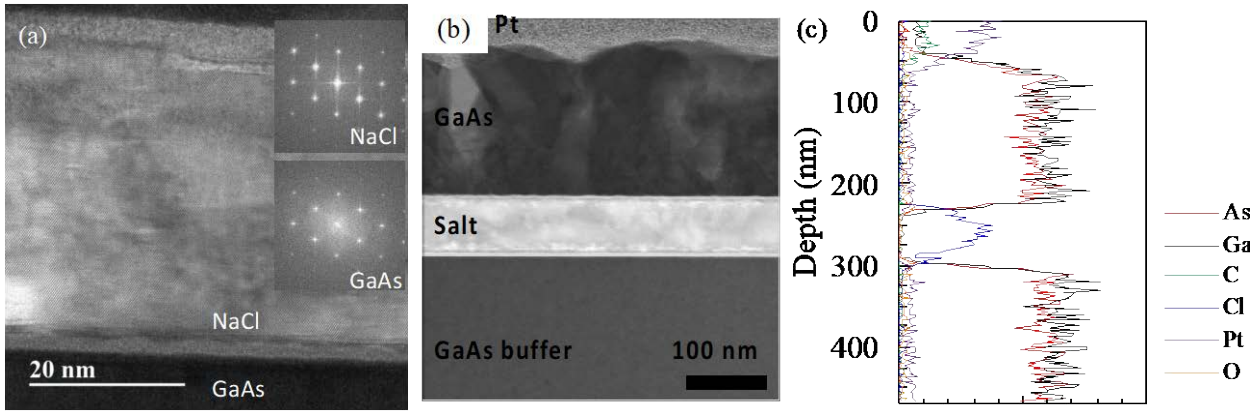

Figure 4: (a) TEM image of a NaCl grown on a c(4×4) GaAs surface with insets showing FFTs of the NaCl (top) and GaAs (bottom) (b) STEM image of a NaCl layer capped with GaAs, and (c) EDX maps of the NaCl layer contained between GaAs layers, and (d) line scans for each element.

2.2. Fragility of NaCl layers

The *in*-situ RHEED beam used for characterization has effects on the NaCl layer. However, bare NaCl layers are also extremely difficult to measure using *ex-situ* diagnostic tools. The {100} facets may be the low energy facet, and mostly stable in air, as one can see when using normal table salt. However, there are effects at small length scales that happen rapidly when removed from vacuum which has proved difficult for doing detailed analysis of bare NaCl layers. Figure 5 shows a variety of plan view SEM images of a 90 nm bare NaCl film deposited on a GaAs substrate. Figure 5(a) shows an image of the sample immediately after growth, and exposed to air while moving to the SEM. The surface is not as smooth as RHEED images would suggest. Some holes are also observed, it is not known whether these holes go all the way to the GaAs substrate, whether they form during growth or the walk over to the SEM. Figure 5(b) shows the same sample after storage in a nitrogen drybox for 4 days. The density and size of holes is now much larger. The sample is mounted with a cleaved {110} edge parallel to the sample holder, and these holes show very specific edges, which at ~45°, are likely the low energy {100} facets of NaCl.

It is known that NaCl dissolves readily in water, but the extent to which thin films can be removed, and at what speed was tested here. The dissolution of NaCl was also investigated by partially submerging a piece of the bare NaCl (after storage in the drybox for 4 days). The sample was dipped in room temperature water by hand and immediately removed and blown dry with nitrogen before doing additional plan view SEM (Figure 5(c)). In the lowest magnification image (Figure 5(c1)) the right side of the image was dipped in water and the left was not; there are three clearly different contrast regions. Furthest from the water, in area (2), the NaCl surface still shows a large density of square holes resembling those seen in Figure 5(b). Moving further right, closer to the dipped area, the prevalence of the holes increases, and eventually the sample is only ~50% covered with salt (area (3)). Here, the NaCl still shows preferential directions with right angle faceting. Moving even closer to the edge (area (4)), one is left with discrete NaCl islands. These islands still have similar 90° edges and is likely right on the edge of where the water reached. Moving further right into the middle area, the islands no longer have such strong faceting or relationship to the substrate as seen in the left side of Area 5. This could be due to either the significantly higher vapor pressure of water at <1 mm from the surface in a dry environment (Denver, CO), instability during the water dip, or in the meniscus of the water surface, which could dissolve the NaCl, but then recrystallize as the highly NaCl-rich solution that was purely at the surface is dried. Beyond this line, nothing appearing like NaCl is observed suggesting that it is fully dissolved. There is some contrast/scratching on the GaAs surface, but it is believed that a GaAs surface similar to the as-received case could be achieved by more carefully rinsing the surface with water, and subsequent thermal cleaning in vacuum and buffer layer growth. This all suggests that NaCl could provide a suitable release layer, but also that the study of bare layers in high humidity environments would be extremely difficult.

The final effect discussed in this section pertains to Figure 5(d) and is the fragility of the NaCl under exposure to electron beams. Here, another plan view SEM image is shown, taken with an accelerating voltage of 3 kV and beam current of 6.2 nA. Prior to acquisition of this low magnification image, the beam was focused in the two regions at a higher magnification (top) and medium magnification (bottom) which show significant effects from the electron beam. One can watch the surface move and evolve in real time while focused on these areas at higher magnification. Adjusting the focus and stigmation of the incoming beam i.e., oscillating the depth of focus, results in faster decay of the surface and deep holes can be made. It is not known whether this material is ablated, moved aside, or is different in crystallinity or composition than the original material. Additionally, as with the medium magnification area, using a long exposure time can result in degradation of the entire area. Thus, in order to acquire an image of a lesser damaged surface, one must move from the focused area to a new area and acquire the next image quickly. These effects are seen at accelerating voltages 3-5× lower than what is used in RHEED. It is possible that even though the electron beam in RHEED is at a glancing angle, rather than directly impinging on the NaCl surface, the degradation (such as observed and will be discussed in Section 2.3.1.c.i)) could be because of a similar mechanism. The roughening of the surface observed via SEM could be comparable to what is happening when the surface is exposed to RHEED during the growth as well.

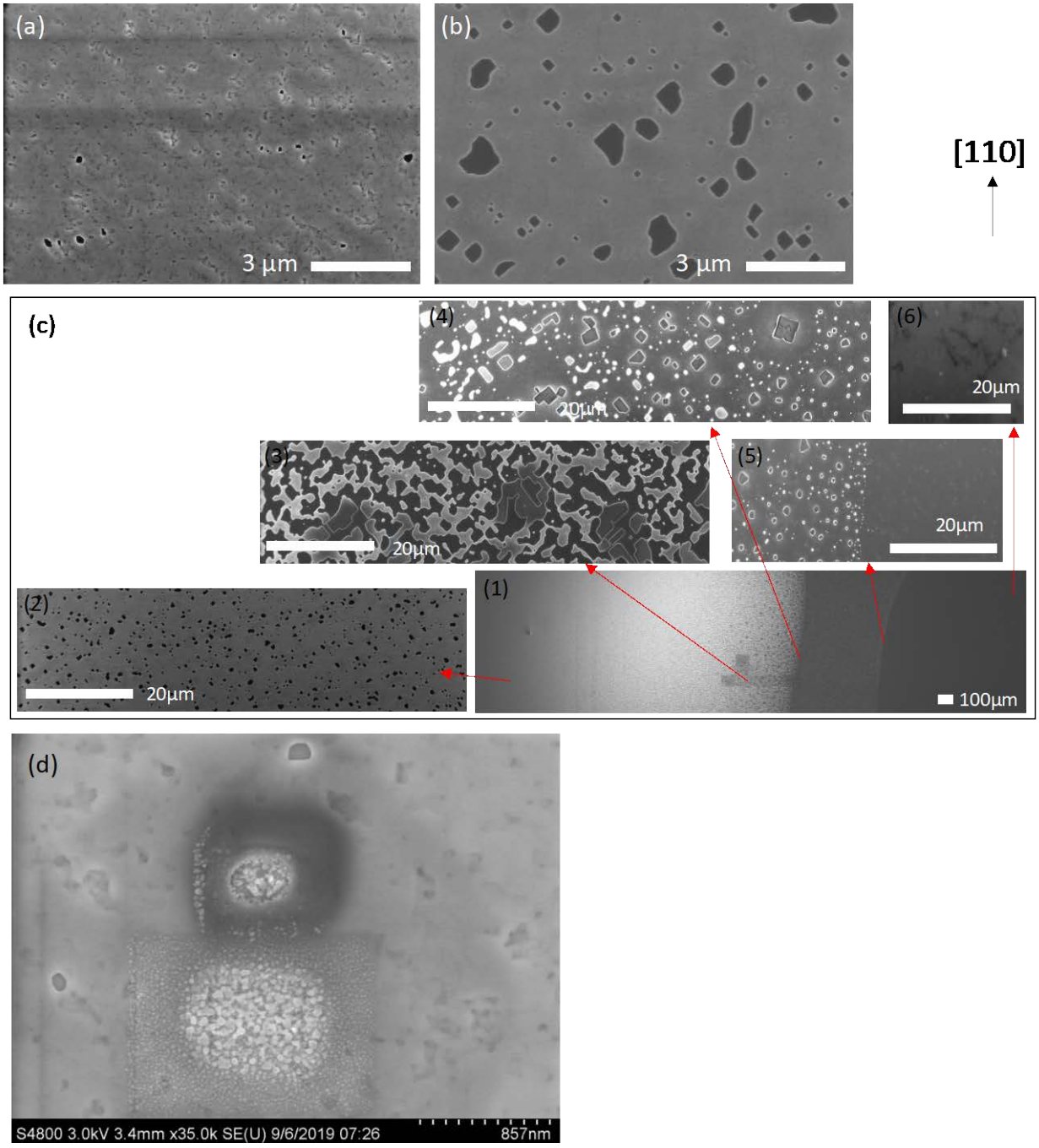

Figure 5: Plan view SEM images of a bare NaCl thin film deposited on GaAs. (a) Image of the sample the day of growth and (b) 4 days after growth with most of the time in a nitrogen dry box. (c) Images of the sample the day of growth that was partially dipped in water for ~1s. (1) The low magnification image shows three distinct regions with the right side being the side dipped into water. Higher magnification images of the different regions (2-6) show lighter colored NaCl and the darker GaAs substrate. (d) Images of a NaCl surface with a 3kV beam at low magnification showing regions that were roughened form exposure at higher magnification

2.3. Deposition of GaAs on NaCl thin films

This section will cover the deposition of GaAs overlayers on NaCl films. Different growth schemes will be discussed such as deposition while continuously ramping the temperature, deposition at constant temperature, and separate low-temperature and high-temperature deposition steps. The effects of the RHEED electron-beam on the nucleation of the GaAs will also be discussed, both exposure during the GaAs deposition as well as exposure of the bare NaCl surface at low temperature under an As-flux. The latter proves to be a critical component to maintain continuous NaCl thin films below monocrystalline GaAs layers. Different growth techniques for the growth of GaAs, specifically during the nucleation stages are also investigated, such as co-deposition, migration enhanced epitaxy (MEE), and metal modulated epitaxy (MME).

2.3.1. Co-deposition of GaAs

This project first used co-deposition of GaAs to study the growth on NaCl thin films. In other words, both Ga and As atomic species are supplied concurrently. This is how typical GaAs material is grown using MBE. Most of the efforts of this project were done using this growth scheme and different growth schemes were employed. During this portion of work, we discovered some complexities in the integration of these two materials such as the volatility of NaCl layers at temperatures much lower than typical deposition temperatures of GaAs and the effects of the RHEED beam on the growth of GaAs.

2.3.1.a. Growth with continuous temperature increase

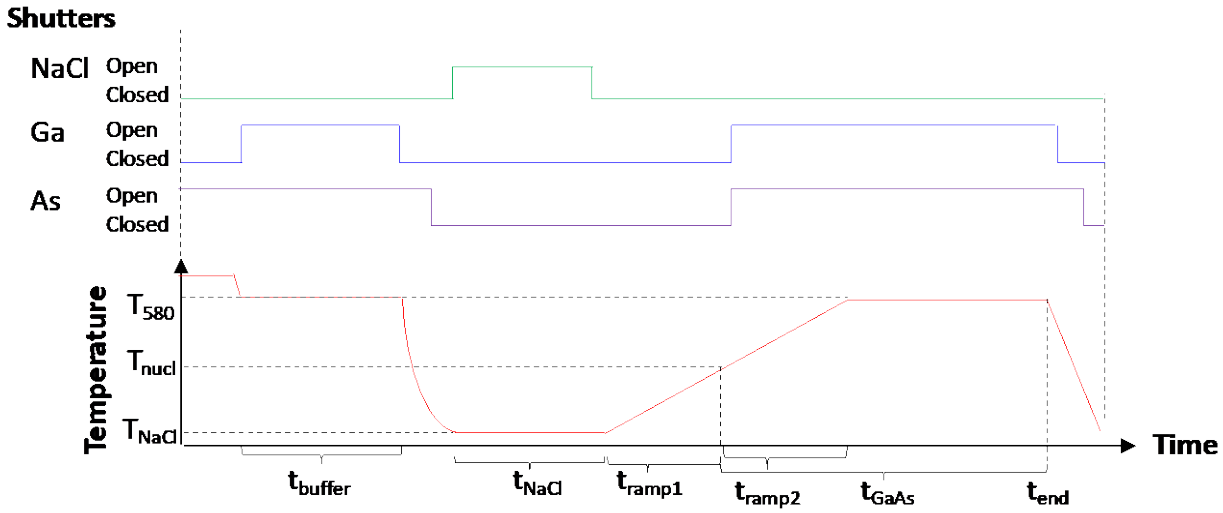

Figure 6: Growth schematics showing shutter positions for NaCl (green), Ga (blue), and As (purple), with growth temperature (red) as a function of time for the growths discussed in Figure 7

Figure 6 represents the growth scheme for the samples shown in Figure 7. Table 1 lists all of the variables used in the growth schemes that will be discussed in this study. The shutter sequences for NaCl (green), Ga (blue), and As (purple) are shown in conjunction with the temperature of the substrate (red), as a function of time beginning from the oxide desorb step at 620°C, where the As shutter is already open. All samples go through this identical step, as well as the same time for a buffer layer (t_{buffer}) of 9 minutes to achieve a thickness of ~300 nm at 580°C (T_{580}), prior to cooling rapidly under an As flux until ~340°C. The samples are all then cooled until

the temperature at which NaCl deposition begins (T_{NaCl}). The salt deposition time (t_{NaCl}) is varied between studies, and sometimes persists into the time taken to ramp temperature (t_{ramp1}) to the GaAs nucleation temperature (T_{GaAs1}). The substrate temperature ramp rate post-NaCl deposition is either 20 or 50°C/min depending on the sample set.

Table 1: Definition of variables outlined in Figure S2

Variable	Definition
T_{580}	580°C
T_{NaCl}	Temperature of starting NaCl deposition
T_{GaAs1}	Temperature at which the first GaAs deposition begins
t_{buffer}	time of buffer layer GaAs deposition (9 minutes)
t_{NaCl}	time of NaCl deposition
t_{ramp1}	time taken to increase temperature from initial NaCl deposition temperature (T_{NaCl}) to GaAs nucleation temperature (T_{GaAs1})
t_{ramp2}	time taken to increase temperature from the GaAs nucleation temperature (T_{GaAs1}) to 580°C
t_{GaAs1}	total time of first initial GaAs deposition
t_{GaAs2}	total time of second GaAs deposition
t_{soak}	time taken to sweep RHEED across NaCl surface under As-flux
t_{end}	end of growth

The NaCl is deposited only at low temperature. For these growths the ramp rate after NaCl deposition is 50°C/min. Thus, the time to ramp from T_{NaCl} to T_{GaAs1} (t_{ramp1}) and from T_{GaAs1} to T_{580} (t_{ramp2}) are both dependent on the T_{GaAs1} chosen; $t_{ramp1}+t_{ramp2}\approx(580°C-T_{NaCl})/(\text{ramp rate})$. However, this is only approximately equal because it can take up to 5 minutes before the heater actually increases the substrate temperature. Additionally, the GaAs deposition time (t_{GaAs1}) is also dependent on T_{GaAs1} as it includes t_{ramp2} and the time of growth at 580°C. However, the time at 580°C is lengthened/shortened in an effort to keep the total thickness of the layers the same between sample comparisons, i.e., t_{GaAs} is attempted to be kept the same for all samples. For these samples, once T_{GaAs1} is reached, both the As and Ga shutters are opened simultaneously. The Ga shutter remains open for t_{GaAs1}, before closing and cooling the sample at the end of growth (t_{end}). The sample cools under an As-overpressure until ~340°C when the As shutter is also closed.

The subsequent deposition of GaAs layers on NaCl thin films was carried out in the same MBE chamber without any vacuum break. The first investigation involves varying the initial GaAs nucleation temperature (T_{GaAs1}) for GaAs deposition on a NaCl layer. A schematic of this growth process is given in the Figure 6. After growth of the high-temperature buffer layer, nominally 90 nm of NaCl is deposited at 110°C. The NaCl shutter is closed, and the temperature is increased at a rate of 50°C/min to the nucleation temperature under test. GaAs deposition begins once T_{GaAs1} is reached at a rate of ~33 nm/min (calibrated using RHEED oscillations during homoepitaxial GaAs growth) by simultaneously opening both the Ga and As sources while the substrate temperature is continuously increased to 580°C. The resulting thicknesses of each sample are slightly different because the total GaAs deposition time (t_{GaAs1}) depends on the nucleation temperature and the ramp rate (samples with lower T_{GaAs1} are thicker).

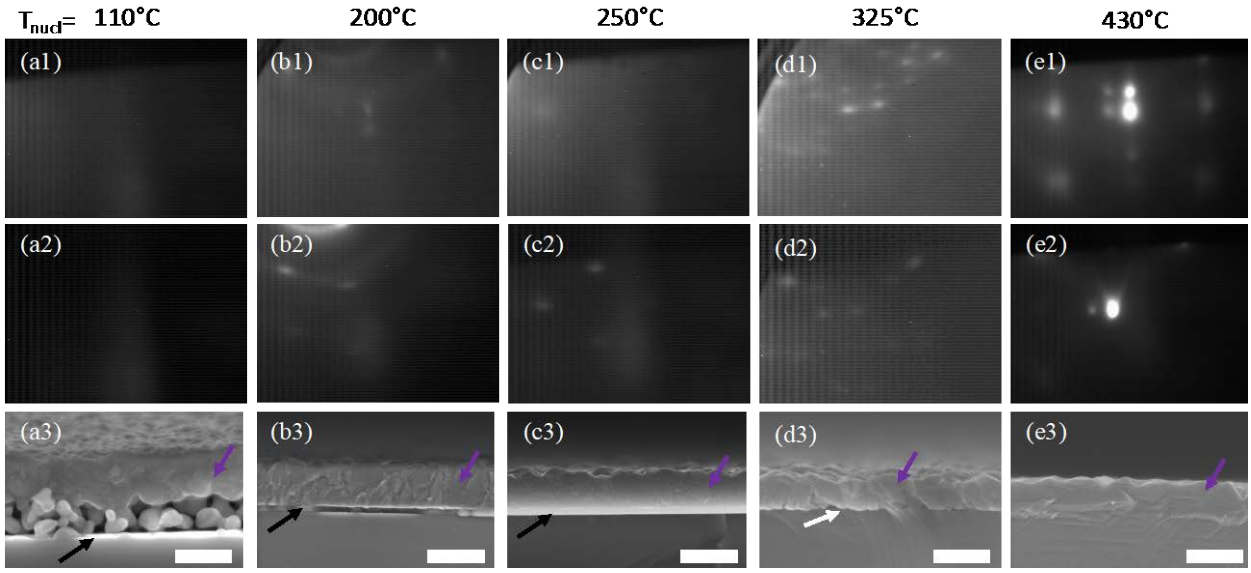

Figure 7: RHEED images taken with a <100> beam direction during (1) the initial and (2) the final moments of GaAs deposition and (3) cross-sectional SEM of the finished sample (scale bar is 600 nm) after 30 minutes of salt deposition capped with GaAs initially at a temperature of (a) 110°C, (b) 200°C, (c) 250°C, (d) 325°C, and (e) 430°C and ramped to 580°C. Purple, black, and white arrows mark the GaAs overlayer, an NaCl layer, and any voids between the substrate and overlayer, respectively.

Figure 7 shows RHEED patterns at the onset and at the end of GaAs deposition with corresponding cross section SEM images from a series of growths with various T_{GaAs1}. The additional spots in the RHEED patterns located to the left of the primary and first order spots here are artifacts of the incident RHEED beam, and not indicative of any surface reconstructions or twin grain structure. When GaAs deposition begins at 110°C (Figure 7(a)) the RHEED pattern goes diffuse very quickly, signifying a lack of crystalline order. Due to the increased surface roughness and spontaneous delamination of the film from the substrate, the pattern gets darker upon continued growth and heating, as even diffuse reflections are blocked. In contrast to the other samples in this figure, the sample in Figure 7(a) has an additional ~90 nm of GaAs at T_{GaAs1} (110°C) prior to heating to 580°C. Without this longer initial low-temperature deposition the film completely delaminated from the substrate during the growth. Cross sectional SEM reveals an extremely porous interface with a coalesced top layer. *Ex-situ* TEM measurements (not shown) reveal the smaller particles between the substrate and film to be crystalline GaAs, with the overlayer being a dense polycrystalline film with grains on the order of 100 nm. Additionally, if the temperature is not increased from 110°C, the film remains smooth, but fully amorphous and As-rich. Additional samples (not shown) showed that changing the thickness of the initial 110°C deposition results in proportional changes in the thickness of the porous section. However, the coalesced top region remains similar in thickness, and without any observed improvements in the crystallinity. Thus, it can be assumed that the porous structure is a result of the low-temperature, As-rich, amorphous deposition and the coalesced layer is due to the growth at elevated temperatures.

The formation of a porous interface can be avoided by increasing the T_{GaAs1} to 200-250°C (Figures 7(b,c)). In both cases the RHEED develops a spotty ring pattern upon initial GaAs deposition, which persists throughout growth indicating a textured polycrystalline film. The

presence and persistence of the polycrystalline rings decreases as T_{GaAs1} is increased. SEM shows the presence of a smooth ~70-nm-thick NaCl layer maintained beneath a fully dense ~500 nm GaAs overlayer. *Ex-situ* TEM and EBSD measurements reveal that these films are indeed polycrystalline, in agreement with the RHEED observations.

If the NaCl film is heated to temperatures ≥325°C prior to initiating the GaAs deposition (Figure 7(d-e), the RHEED immediately begins to turn spotty, indicating Volmer-Weber style growth. Little change is observed throughout the deposition at 325°C. However, using a T_{GaAs1}=430°C, the pattern at the end of the GaAs deposition shows spots with chevrons indicating shallow surface facets. In either case with T_{GaAs1} ≥325°C, SEM measurements no longer show the presence of a NaCl layer. Instead, large gaps between the substrate and a rough GaAs surface layer are observed. As the T_{GaAs1} is increased, the large gaps become smaller pores, and eventually disappear altogether. The NaCl film begins to rapidly decompose as the sample is heated above 300°C; as a point of reference the NaCl effusion cell temperature is operating ~480°C.

The observation of the initial spotty RHEED in each scenario indicates that initial GaAs on NaCl growth proceeds via three-dimensional island growth. This results in incomplete coverage of the NaCl until all islands coalesce. This enables the NaCl to continuously desorb at the higher temperatures even during GaAs deposition. This happens especially quickly at higher temperatures where both the nucleation of islands is slower and the NaCl desorbs more rapidly. For example, at 300°C some GaAs is seeded on the NaCl before desorbing, but not quickly enough to form a cohesive film before the NaCl is completely desorbed, leaving behind large voids. By delaying GaAs deposition until 430°C, most of the NaCl has already desorbed from the surface. It is likely that by this point the NaCl layer is either very thin, or has completely disappeared, and many of the initial GaAs atoms are impinging directly on a GaAs surface, resulting in homoepitaxy. Any remaining NaCl escapes through pinholes or gaps between GaAs islands and the result is small pores in a mostly homoepitaxial structure. XRD and TEM measurements (not shown) confirm the RHEED measurements that the GaAs overlayers of any previously discussed case, with a persistent salt layer or large voids (T_{GaAs1} ≤325°C), are polycrystalline. Additionally, using a T_{GaAs1}=580°C, the NaCl is completely desorbed prior to GaAs nucleation. In this case the RHEED remains very streaky, regains the typical reconstructions observed with MBE growth, and cross-sectional SEM shows no evidence that a NaCl layer was ever deposited. Intriguingly, this suggests that any NaCl can be thermally cleaned, and regrowth on substrates which once had salt deposited on them is possible.

2.3.1.b. Growth at a single temperature: persistent NaCl layers

Figure 8 is a somewhat simpler scheme pertaining to the samples in Figure 9. The first part of the growth is the same as outlined in Figure 6. However, in this case t_{NaCl} also includes t_{ramp1} as the NaCl shutter is kept open while ramping the substrate temperature, and a ramp rate of 20°C/min is used. Thus, the thickness of the NaCl deposited is necessarily dependent on both t_{NaCl} and the T_{GaAs1} chosen. The temperature stops increasing once T_{GaAs1} is reached. At this point the NaCl shutter is closed, and both Ga and As are immediately opened. The Ga shutter remains open for t_{GaAs1}. Once the growth is completed, the Ga shutter is closed. If T_{GaAs1}>340°C, the sample is cooled to ~340°C prior to closing the As shutter. If T_{GaAs1}<340°C, the Ga and As shutters are closed simultaneously.

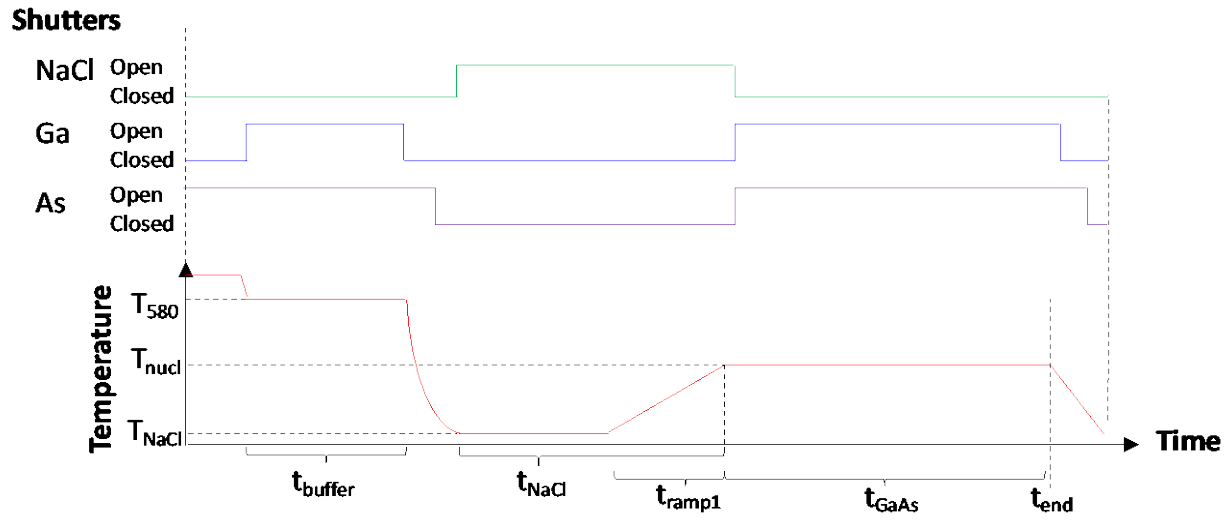

Figure 8: Growth schematics showing shutter positions for NaCl (green), Ga (blue), and As (purple), with growth temperature (red) as a function of time for the growths discussed in Figure 9

RHEED and cross-section SEM patterns are used to analyze the growth of GaAs on the thick continuously deposited NaCl films. Figures 9(a1-d1) show the RHEED patterns during the initial moments of GaAs deposition at various T_{GaAs1}. Samples with $T_{GaAs1} \leq 450°C$ show complex RHEED patterns with symmetric shadow spots and chevrons within the first ~10 s of deposition. The extra set of spots symmetric about the primary reflections are expected to be due to twins, likely rotations about the {111} which will be discussed more in Section 2.3.2. The shallow angle chevrons as viewed along this <110> direction correspond to {111} faceting of the GaAs. However, at $T_{GaAs1} = 500°C$ the RHEED during initial growth remained streaky and it took nearly 60 s to display a RHEED pattern similar to what was observed at the lower temperatures (Figure 4(d1)). In this case, it is possible that the initial GaAs islands are more epitaxially oriented and have a lower degree of twin formation. However, it is more likely that the longer time before a similar pattern is observed is due to a slower nucleation and growth of GaAs at this elevated temperature.

The middle row of Figure 9 shows the RHEED patterns at the end of the GaAs deposition at the different temperatures. For $T_{GaAs1} = 350°C$ (Figure 9(a2)), the pattern at the end of the ~300 nm deposition is spotted and ring-like, indicating a textured polycrystalline film, in contrast to the original pattern. Figure 9(b2) also shows a spotty ring pattern for the growth at $T_{GaAs1} = 400°C$. The rings are comparatively less pronounced than the spots, but the pattern is dimmer overall. This indicates a higher degree of crystalline order compared to growth at lower temperature, but still a very rough film. It was impossible to discern a pattern at the end of the growth for depositions at $T_{GaAs1} \geq 450°C$. The pattern become steadily darker as the growth temperature is increased, likely due to the formation of increasingly discrete islands. Electrons at RHEED energies have a mean free path on the order of a few tens of nanometers. Thus, these glancing-angle electrons are completely blocked by the islands which are hundreds of nanometers in size, and the pattern on the phosphor screen becomes dark.

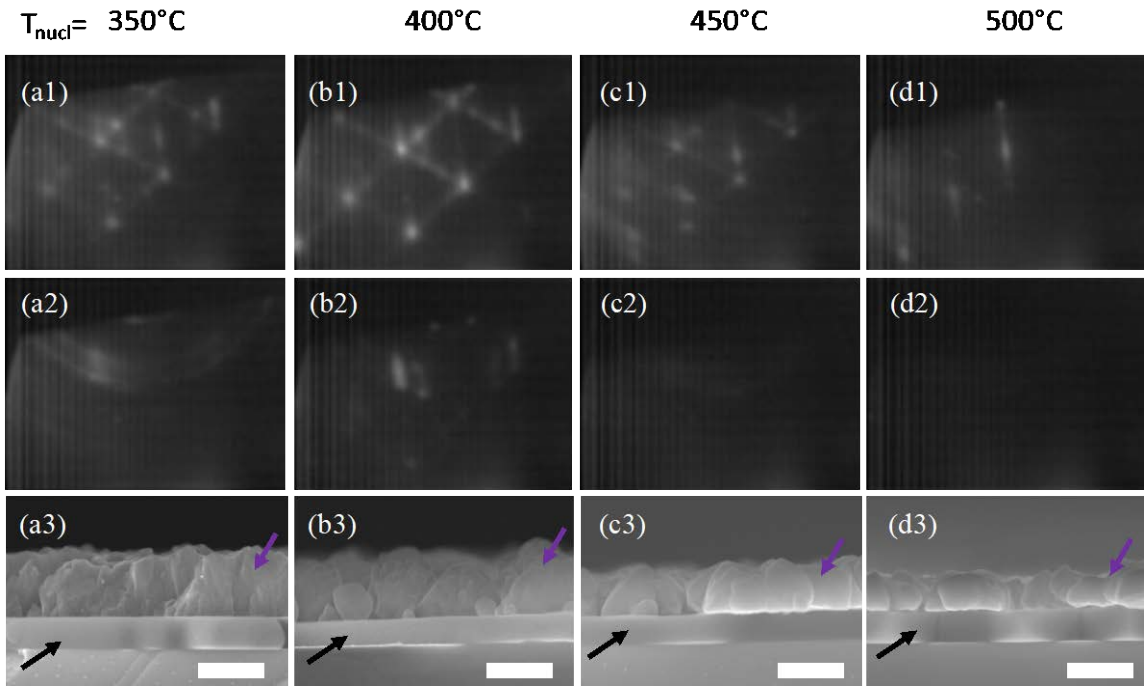

Figure 9: RHEED images of (1) initial and (2) final GaAs deposition on thick NaCl and (3) the corresponding SEM images of samples with NaCl deposition beginning at 110°C and continuously until initializing the GaAs cap at (a) 350°C, (b) 400°C, c) 450°C, d) 500°C. Purple and black arrows mark the GaAs overlayer and NaCl layer, respectively. (scale bars are 300 nm)

The bottom row of Figure 9 shows the corresponding SEM images of the previously discussed samples. All samples have the same t_{GaAs1} and growth rate (33 nm/min) and thus should have the same target thickness of 300 nm. Figure 9(a3) shows that GaAs deposited at 350°C is dense and approximately equal to the target thickness. As T_{GaAs1} increases, the morphology trends toward the formation of more discrete faceted islands, in agreement with the RHEED observations from the early portions of the growth. Additionally, as the T_{GaAs1} goes higher than 450°C the islands become smaller and more discrete. This also corresponds with the darkening of the RHEED pattern at these temperatures, because an array of disconnected ~200-nm-tall islands is essentially a very rough film. Figure 9(d3) shows that with T_{GaAs1}=500°C, the islands are thinnest (~190 nm), only ~60% of the targeted thickness. The reason behind this reduction in thickness, or apparent growth rate, with increasing temperature is not fully understood. It is possible that the rapid desorption of the NaCl surface at these higher temperatures creates chemical complexes, such as $GaCl_3$, which are more volatile and halt further growth or that impinging Ga and As atoms have difficulty remaining on such an actively desorbing surface, because the temperature of the substrate temperature is now higher than the NaCl effusion cell.

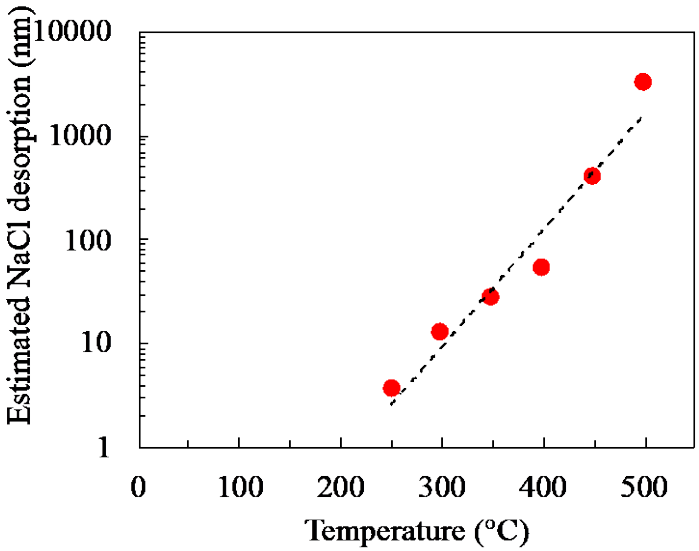

Figure 10: Amount of salt desorption as a function of GaAs capping temperature

Despite the NaCl thickness all appearing similar in these images, there are significant differences between the total amount of NaCl deposited. While the estimated and observed thickness of NaCl is similar when $T_{GaAs1} \leq 250°C$ (not shown), they begin to strongly diverge as the temperature increased. Figure 10 shows the estimated amount of total NaCl desorption using the difference between the expected thickness (from measured low temperature growth rates and total NaCl deposition time) less the thickness observed in the SEM images from Figure 9. As mentioned earlier, the thickest NaCl layer was deposited for $T_{GaAs1}=500°C$ (~3.3 µm), and the observed thickness is only ~160 nm. Thus, >3 µm of material had desorbed during the growth of this sample. The initial NaCl thickness required to maintain a persistent film until the end of growth increases exponentially as the growth temperature is increased. The actual desorption rate of the NaCl is temperature dependent, but lower and upper bounds on the desorption rate can be made by making two generous assumptions using the sample with $T_{GaAs1}=500°C$: the NaCl decomposition either occurs (1) over the entire 29 minutes at which the sample is >110°C or (2) exclusively during the 9 min growth at 500°C. These would result in an average desorption rate somewhere in the range of 112-362 nm/min. This desorption rate would be in the range of 3.4-11× the growth rate of GaAs used in this study. This presents an obvious challenge for achieving growth at typical GaAs deposition temperatures which are even higher.

2.3.1.c. Effects of RHEED on the growth of GaAs on NaCl

Maintaining a continuous NaCl layer is critical for enabling removal of the overlayer from the substrate. In order to protect the NaCl from desorption at higher temperatures, a conformal GaAs layer must be deposited at a lower temperature. This low-temperature GaAs has poor crystallinity. Thus, one must balance the low-temperature GaAs deposition with the desorption of the NaCl at high-temperatures. Because GaAs growth on NaCl proceeds by growth of 3D islands instead of layer-by-layer, a thick low-temperature GaAs layer would be required, but that would result in difficulties achieving monocrystalline templates. This section will introduce RHEED as more than a diagnostic tool, and as something that can have profound effects on the nucleation of GaAs. The effects of the RHEED beam were originally discovered when depositing Ge on NaCl films (Section 5.1.1) and then applied to the deposition of GaAs.

2.3.1.c.i. Effects of RHEED immediately prior to and during GaAs deposition

As demonstrated throughout the earlier sections, RHEED is a critical tool for *in-situ* observation, but the presence of the electron beam during growth actively affects the growth surface, which has been seen in other material systems.[10,11] In an attempt to elucidate the effects of the presence of the electron beam, a sample was grown where the beam was moved across the surface at different points during the growth, resulting in different levels of exposure and exposure starting at different times during the growth process. The growth process used here was similar to that discussed in Section 2.3.1.b, i.e., 10 min of initial NaCl deposition at 110°C, then continuously deposited NaCl while heating to 300°C, at which point GaAs is deposited at a rate of 33 nm/min to reach a nominal thickness of 100 nm.

A picture of the sample in Figure 11(a) shows distinct color differences from the presence of the 15 kV RHEED beam at different portions of the growth. In the picture of the sample, areas exposed prior to GaAs deposition (lines 1 and areas above) appear relatively similar, while the three regions at different points during the GaAs growth (4, 5, and 6) have drastically different colors. Figure 11(b) outlines the portion interest for the growth of this sample, neglecting oxide desorb and buffer layer growth steps, while highlighting the timing of the RHEED exposure in relation to the NaCl and GaAs deposition. The time axis is roughly to scale. The RHEED was not open for the entirety of the time marked by region 1 and was turned on and off throughout this portion. However, for the remaining sections the RHEED was left on without any beam blanking. Note that contrary to all other growths, NaCl is deposited for a considerable time (~270 s) at 300°C, t_{NaCl} spans beyond the temperature increase. This is the reason for further NaCl deposition on top of areas 1 and 2. After the 90 s roughening that occurs for area 3, the NaCl shutter is closed, RHEED moved to area 4, and GaAs deposition initialized. The RHEED stays in each of the following 3 locations for 1 min before moving to the next without any pause in GaAs deposition.

Figures 11(c-k) show RHEED patterns taken from areas 1-5 during the growth. Area 0 has no RHEED pattern because it was never exposed, and Area 6 was blocked by the clip so no pattern could be obtained. However, for Area 6 there was a region near the edge of the sample where the clip no longer shadowed the beam that was used for the plan-view SEM discussed in Figure 12. Figure 11(c) shows the pattern after 10 min of NaCl deposition at 110°C, it appears streaky as was observed in other growths. Once the 10 min deposition was complete, the RHEED was moved to the edge of the sample (top of sample in Figure 11(a)) and turned off while the sample was heated (with continuous NaCl exposure). Figure 11(d) shows the brightened pattern of a fresh area of NaCl (during deposition) once the temperature reached 300°C. The beam is left on and unmoved while constantly monitoring for any change. Under continuous NaCl growth, it takes ~3 minutes for the RHEED pattern to begin to go spotty as shown in Figure 11(e) signifying that the surface was roughened. At this point the beam was moved to position 3 where it is left on for 90s. The pattern after holding the beam at Area 3 for 90s is Figure 11(f), and unsurprisingly looks like it would fall between Figures 11(d and e).

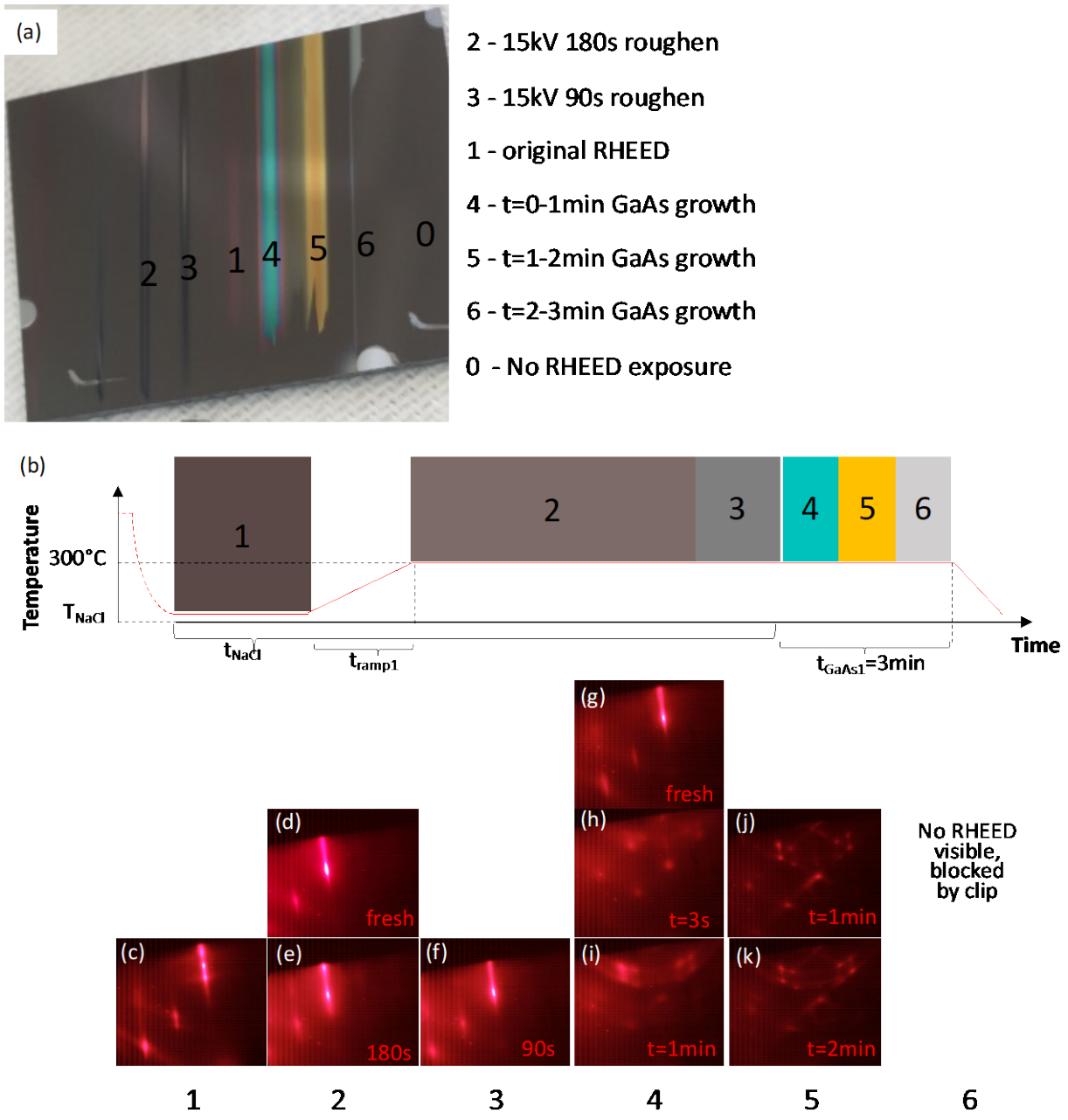

Figure 11: (a) Image of a sample after removal of the chamber showing distinct lines from exposure to the RHEED beam during different portions of the growth (labeled 0-6). (b-j) RHEED patterns from the different stages of growth in regions 0-6. (k) A representation of timing of the RHEED exposure for areas 1-6 from the sample shown in (a).

GaAs deposition began immediately once the beam was moved to the fresh NaCl surface in Area 4 (Figure 11(g)), which at first looks bright and streaky. The pattern after 3s of GaAs deposition (Figure 11(h)) shows the formation of new dim spots, with faint chevrons and shadow spots. After 1 minute (Figure 11(i)) the pattern has transitioned to spotty rings. This signifies that the growth starts out oriented but three dimensional, and after 1 minute of growth with continuous

RHEED exposure ends up as a textured polycrystalline film. The beam is then moved to area 5 (Figure 11(j)) which does not show any ring-like characteristics. Rather, a spotty pattern similar to the onset of GaAs deposition with RHEED exposure (Figure 11(h)) is observed. However, the pattern is much less blurred, and the spots and chevrons are seen clearly. After a minute of continues deposition with exposure, rings start to appear again (Figure 11(k)). This signifies that upon further deposition with RHEED exposure the growth starts to go more polycrystalline. Without the presence of the RHEED beam during nucleation, the clearer pattern observed suggests that the RHEED may be worsening the crystallinity of the nucleation layer. However, even without constant exposure to the RHEED beam, further deposition at 300°C would be polycrystalline, similar to Figure 9(a2) which was a longer growth performed at 350°C.

Figure 12 shows plan-view SEM images of the seven distinct areas on the same sample with various degrees of RHEED exposure (RE) at different times throughout the growth at low and high magnification, top and bottom rows, respectively. The first column (Figures 12(a1, a2)) shows an area with no RHEED exposure (NRE) at any point throughout the growth. There are two different areas observed: a dark area and a light area. In this case the dark area is the NaCl, and the light area is GaAs. This was inferred from the continuous degradation and movement of this surface under the presence of a tightly focused electron beam in the SEM (details in Section 2.2). The difference in smoothness of the dark surface can be seen between the low and high magnification images; it was impossible to acquire a high magnification image without some roughening of the NaCl layer. However, the light areas, do not degrade. The composition of these areas is not known, but they are highly ordered, with the long axis nearly perpendicular to the <110> direction (all images in Figure 12 are oriented the same).

The images from the next three columns show areas exposed to the RHEED beam prior to GaAs deposition. Figure 12(b) shows an area with RE during the initial low temperature NaCl deposition but eventually covered with ~20 nm of fresh NaCl at 300°C while the RHEED beam was moved to the next areas. This area looks very similar to the area with NRE; it seems like 20 nm of NaCl deposition negates any effect from previous RHEED exposure. The area in Figure 12(c) was exposed to the beam for 180 s, which was just enough to see the RHEED pattern go slightly spotty (Figure 11(e)). Once the transition in the RHEED pattern was observed, the beam is moved to the next location, and 4.5 nm of NaCl was subsequently deposited on this location (in Figure 12(c)) prior to GaAs deposition. These images look mostly similar to the previous areas; there is a similar density of lighter islands contrasting against a dark NaCl background. However, the NaCl (dark) area in the low magnification image (Figure 12(c1) shows two slightly different contrast areas with cracks between. This is presumed to be a roughening of the NaCl layer due to the constant exposure of the RHEED beam at 300°C. Again, this is not seen in the area that was similarly exposed yet had ~20 nm of new NaCl deposition (Figure 12(b)). Thus, it appears that 5-20 nm of subsequent NaCl deposition can hide any effects of the RHEED on the original NaCl layer. It took 180 s of constant exposure (during continuous NaCl deposition) for a change to be seen in the RHEED at 300°C. To observe a similar change at lower temperatures takes significantly longer or is never seen. It is expected that because this significant difference is seen with 180 s of exposure, similar changes that may not be observable in SEM or RHEED are likely happening with shorter exposures and/or at lower temperatures.

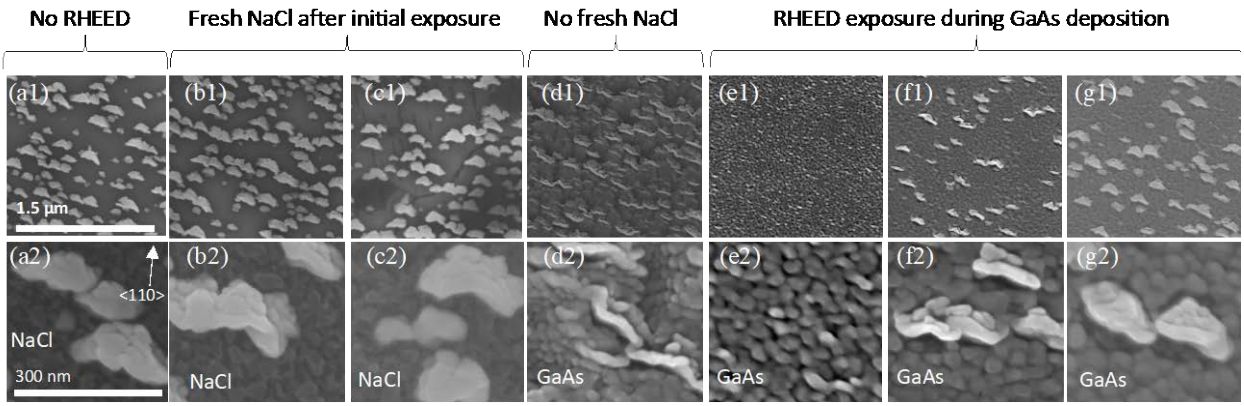

Figure 12: Plan view SEM images of 100 nm of GaAs deposited on a NaCl film at 300°C at (1, top row) low and (2, bottom row) high magnification. (a) was not exposed to RHEED at any point during the growth. (b) was exposed to RHEED during NaCl deposition and covered with >20 nm of NaCl without RHEED exposure. (c) NaCl exposed to RHEED for 180s and covered with 4.5nm of NaCl without exposure. (d) NaCl exposed to RHEED for 90s immediately prior to GaAs deposition. RHEED exposed to the area during the (e) initial, (f) second, and (g) third minute of GaAs deposition

The images in Figure 12(d) are different from all the others, supporting the hypothesis that there are effects with shorter exposures. This area was exposed to the RHEED beam for 90 s while continuously depositing NaCl (not long enough to see a change in the RHEED pattern) up until the final moment prior to GaAs deposition. Thus, this region has no fresh NaCl deposition, and is the reason for the additional 4.5 nm of NaCl in the area shown in Figure 12(c). Here, the morphology of both the light and dark regions are distinctly different. The lighter features are thinner than in the previous case, but still have similar directionality. The darker region shows some larger, scale-like undulations that could be related to a rougher underlying NaCl layer and no longer degrades under the presence of the SEM electron beam, similar to the next figures.

The location of the RHEED beam was moved to three different areas for the first, second, and third minute of GaAs deposition (Figures 12(e-g)). The dark background from each of these areas is similar and comparable to Figure 12(d) without the large-scale undulations. The rough island-like morphology is also observable at low and high magnifications, does not degrade under the presence of the RHEED beam at any high focus conditions, and looks similar to previous studies of stoichiometric GaAs.[12] Figure 12(e) shows the area with RE during the first minute; the presence of the light islands is completely suppressed. Figure 12(f) shows that exposure during the second minute results in light islands with a similar shape to that observed in the area with RE just prior to GaAs deposition (Figure 12(d)). However, the density of these islands is lower compared to areas with NRE. Figure 12(g) shows the area with RE during the final minute of GaAs deposition; the density of light islands is similar to regions that were never exposed at all or had fresh NaCl after exposure.

The composition and mechanism behind the formation of these light islands are still unknown and a subject of investigation. The RHEED observations in Figure 11(c-k) support 3-D textured polycrystalline growth in all regions from Figures 12(e-g). Based on the results presented, it seems that the presence of a RHEED beam, either immediately prior to or during GaAs deposition, facilitates the growth of the small dark islands in these regions (likely GaAs). The

formation of the light islands seems to start immediately upon GaAs exposure but begins to stagnate after the first minute. These could be similar to the discrete GaAs islands observed in Section 2.3.1.b. The presence of RHEED facilitates nucleation of dark GaAs islands, which suppresses the formation of the light islands. Electron bombardment of NaCl surfaces was seen to promote nucleation in metal films.[6] However, if RE is withheld until light islands have already formed (Figures 12(f,g)), the smaller darker GaAs islands grow around them, and suppress formation of further light islands. There is no observable density of the dark GaAs islands in areas with >4.5 nm of fresh NaCl. This suggests that <5 nm of fresh NaCl is enough to erase the effects of RHEED, and suppresses the nucleation of islands with this morphology at 300°C. The effects of the RHEED beam were not limited to the growth of binary material but were also seen in the deposition of Ge on NaCl films (Section 5.1.1), where RHEED exposure also enhanced the nucleation density of the Ge islands. The presence of an electron beam during material deposition results in a uniform surface morphology underneath the millimeter-wide beam. However, this would not be a practical way of achieving any large area uniformity because the nucleation of GaAs is highly sensitive to the time exposed to the RHEED beam, both total duration and the point during the deposition.

2.3.1.c.ii. RHEED induced As-adsorption at low temperature

Another growth scheme was developed to achieve uniform nucleation in areas larger than the millimeter-wide RHEED beam by utilizing RHEED exposure only prior to GaAs deposition. A representative growth schematic and RHEED images are outlined in Figure 13. The different points throughout the growth labeled 1-11. The first three steps are identical for all other growths in this study. Moving sequentially through the growth, we begin with a 25-minute oxide desorb and the first 3 steps are the same

1. After a few minutes at 620°C under a high As background pressure (6.9×10^{-6} torr), the GaAs surface which was once covered with an oxide and did not give a good RHEED pattern, now shows a bright pattern typical of an oxide free surface. The sample is cooled to 580°C and a 300 nm GaAs buffer is grown to clean up the surface.
2. The RHEED now shows a bright streaky 2×4 pattern (shown here along the $<\bar{1}10>$) at the end of the buffer layer signifying a smooth, well-ordered and As-stabilized surface. The sample is kept under a lower As background pressure ($\sim1.0\times10^{-6}$ torr) while cooling until ~340°C before closing the As and cooling fully to T_{NaCl}.
3. A c(4×4) reconstruction appears with cooling under a constant As-flux at intermediate temperatures and persists down to T_{NaCl} without losing any broadening of dimming of the peaks.

The following two images are of NaCl deposition at T_{NaCl}=150°C, however the trends observed are relatively similar for other T_{NaCl} shown in the main text of this study. More details on the NaCl deposition can be found in Section 2.1.

4. Upon opening the NaCl shutter the GaAs reconstruction disappears quickly, and the pattern is replaced by spotty streaks. There are also faint rings present during the early stages. This suggests that during the formation of the first few MLs of deposition the NaCl is not perfectly smooth and has some degree of polycrystallinity.
5. With further NaCl deposition the streaks become tighter and Kikuchi lines become visible. The surface becomes smoother and appears single crystalline with the spacing between streaks similar to that of the original GaAs.

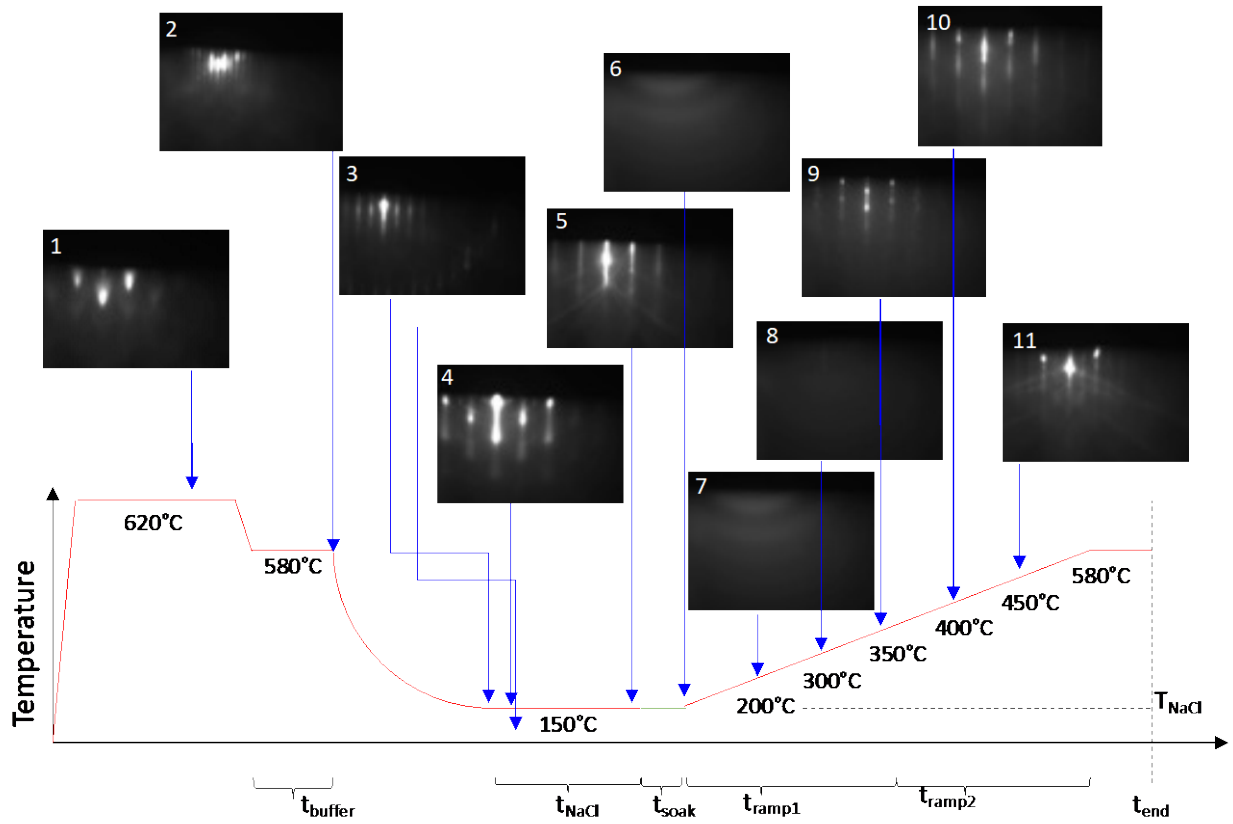

Figure 13: Growth schematic and RHEED images at different points throughout the growth of a sample using RHEED-assisted As-adsorption

The following steps pertain only to growths with the RHEED induced As-adsorption.

6. The NaCl shutter is closed, and the temperature is held constant. An As flux= 1.22×10^{15} atoms/cm^2/s (matching that of the Ga-flux used for 33 nm/min deposition rates) is supplied to the surface. Under constant RHEED exposure, the pattern transitions over the course of a few seconds from streaky (5) to diffuse (6) suggesting the condensation of amorphous material. However, when the location of the RHEED beam is moved pattern 5 (bare NaCl) is again observed, but it immediately begins to fade until a pattern matching (6) is observed. This stepping of the RHEED beam (which is ~1mm wide) is repeated until the amount of desired area is covered and appears diffuse. Examples of the stark differences caused in areas scanned by the RHEED can be seen in the images of 2×2 cm samples pictured in Sections 2.3.2 and onward.
7. Once the desired amount of surface is exposed to the RHEED beam, the sample is heated (at a rate of 20°C/min) under the same As-flux. The pattern remains unchanged with heating to 200°C.
8. Heating further to 300°C, a very faint primary streak starts to appear.
9. Once the temperature reaches 350°C the pattern reveals obvious spotty streaks that match perfectly with the NaCl. Excess As desorbs from GaAs at ~320°C, thus we believe the same thing is happening with material on a NaCl surface. However, one must be careful because any additional exposure of the RHEED beam at temperatures <320°C can re-condense amorphous material, leading to the false assumption that there is still amorphous

material everywhere, when in reality areas that were not re-exposed have fully desorbed all condensed material and would already display a pattern similar to (9).

10. By the time the sample is heated to 400°C the spots present at lower temperatures have transitioned into a brighter, streakier pattern. Even though NaCl adsorption is high at these temperatures, cross-section SEM images of samples where GaAs deposition begins at this temperature (as will be discussed in Figure 16) reveals continuous NaCl layers. Thus, this pattern is representative of a NaCl surface.
11. Further heating to 450°C shows the brightening of the primary spot, and the reappearance of reconstructions. Because of the reintroduction of the surface reconstructions, we believe that in this pattern is now representative of the GaAs surface. It is worth noting that the t_{NaCl} for this growth is 10 minutes, and the NaCl thickness is only ~30 nm and does not take long to desorb. Cross section SEM in this case shows only smooth GaAs and no evidence that a NaCl layer was ever deposited.

    If t_{NaCl} is increased to 60 minutes (~180 nm) the RHEED pattern does not yet show reconstructions at this point because not all of the NaCl has desorbed. Despite the RHEED signifying the presence of NaCl at the onset of nucleation at 450°C in this case, there is no observable NaCl layer via SEM measurements. Instead, small holes are observed at the interface. Thus, because the NaCl is still so volatile, it fully desorbs prior to coalescence of a full GaAs film to protect it.

Figure 14 shows the RHEED patterns, SEM, and electron back-scatter diffraction (EBSD) maps of a sample utilizing this growth scheme. After ~30 nm of NaCl deposition, the RHEED was moved across the surface in the center portion of the sample under an As-flux prior to heating. Once heated to 350°C, GaAs growth was initialized and deposited while continuously heating to 580°C. The first column in Figure 14 shows the area with the RHEED assisted As-adsorption post-NaCl deposition. The second column shows the area with NRE. The RHEED patterns were taken at the end of growth and reveal slight chevrons in both cases. In the area with RE (Figure 14(a1)), the pattern is mostly spotty, with dimmer chevrons but slight streaking indicating a surface that isn't quite smooth and has a lower degree of any specific faceting. The dim secondary spots suggest some sort of twin-related secondary orientation. This contrasts with the pattern from the area with NRE (Figure 14(a2)) which was taken only at the end of growth to avoid any influence on the structure. Here, the chevrons are much brighter and shallow angle (similar to those observed in Figure 9), with brighter shadow spots, suggesting a higher degree of twin formation. The cross-section SEM images (Figures 14(b1,b2)) reveal similar thickness of both the GaAs and the underlying NaCl. Perhaps the roughness in the area with NRE could correlate with the spottier RHEED pattern as well.

However, plan view EBSD (Figures 14(c1,c2)) reveals significantly different crystalline textures between the two areas. There are a number of different orientations observed in the area with RE, where As condensed on the surface. A portion of the grains have the same {100} out of plane orientation as the substrate (red). The shades of purple and blue are results of different 90° azimuthal rotations of {122} grains and {322} grains, respectively. Quantitative {100} pole figures (Figure 14(d1)) reveals that all {100} grains have the same azimuthal orientation as the substrate and that the prevalence of each 90° rotation of {322} is approximately equal. However, one of the rotations of the {122} grains is favored more than the other three. The EBSD data for the area with NRE shown in Figure 14(c2) reveals more area oriented commensurate to the substrate (red), and significantly fewer {322} grains (purple). The quantitative pole figure of this image (Figure 14(d2)) shows that there is an extreme preference for the same single rotation of the

{122} grain (blue) that was observed in the area with RE. Because the substrates used in this study have a maximum of 0.1° offcut, the distance between atomic steps would be at minimum 160 nm. Therefore, it is possible that there is some contribution from the step edges on the grains which are only hundreds of nanometers in size. The presence of these additional grains could also explain the shadow spots observed in the RHEED patterns at the end of growth. The root cause of the grain formation, as well as the single preferential orientation of these grains is the subject of an ongoing investigation.

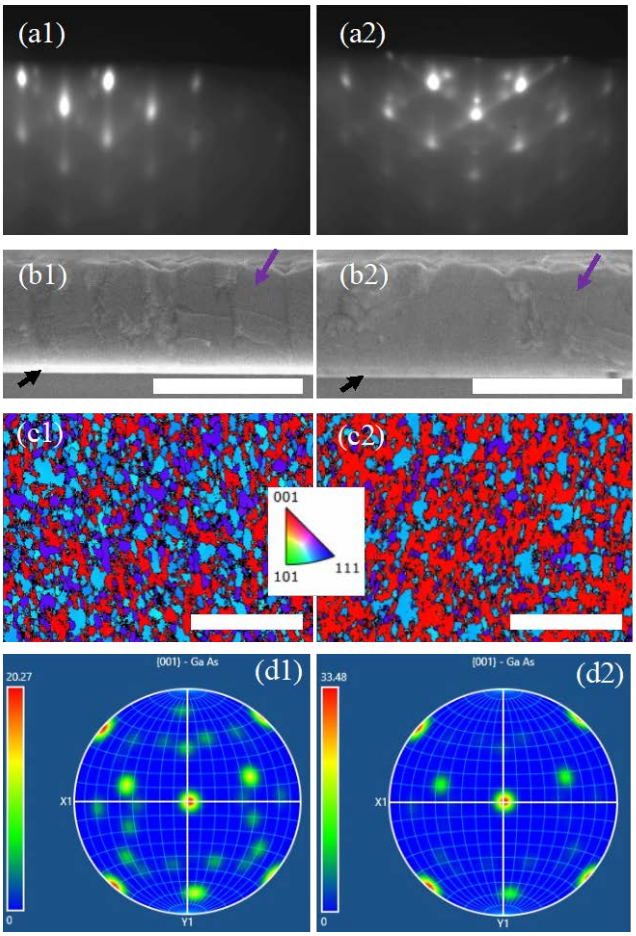

Figure 14: GaAs growth initialized at 350°C and ramped to 580°C (a) RHEED images, (b) SEM (scale bar 600 nm, purple and black arrows mark the GaAs overlayer and NaCl layer, respectively.), (c) EBSD maps of areas (scale bar 5 μm), and (d) corresponding quantitative {100} pole figures of areas (1) exposed to RHEED and (2) not exposed to RHEED until growth was completed.

From the data shown thus far, one could assume that the presence of RHEED was purely detrimental for the growth of near single crystal GaAs on NaCl. However, as temperature is increased the growth process with RHEED gets more complicated. The NaCl film is highly volatile and can completely desorb if not sufficiently capped before heating to elevated temperatures. A continuous NaCl layer must be maintained if one hopes to achieve liftoff of the overlayer. Section 2.3.1.c.i shows that RHEED promotes the faster nucleation of GaAs, which would enable more rapid coalescence to protect the NaCl at higher temperatures.

2.3.2. Separate nucleation and growth layers

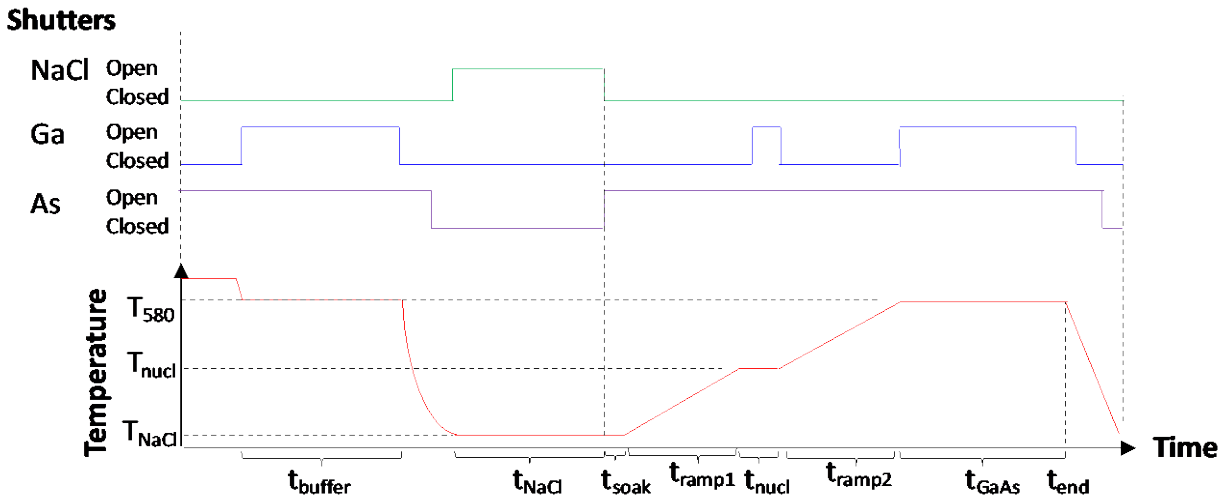

Figure 15: Growth schematics showing shutter positions for NaCl (green), Ga (blue), and As (purple), with growth temperature (red) as a function of time for the growths discussed in Figure 16.

Table 2: Growth parameters for GaAs films grown on NaCl thin films

	NaCl Deposition		GaAs Nucleation			GaAs Growth		
	Time (min)	Temp (°C)	Time (min)	As/Ga	Temp (°C)	Time (min)	As/Ga	Temp (°C)
Sample A	15	150	3	1	400	9	1.68	580
Sample B	15	150	3	1	375	9	1.68	580
Sample C	25	150	3	1	375			
Sample D	25	150	17	MEE	350	1	1	400

Figure 15 outlines a two-step GaAs deposition scheme which also utilizes an As-adsorb step. The time it takes to move the RHEED beam manually across the surface to effectively dim the diffraction pattern is t_{soak}. During this time, the As shutter is opened while the sample is still at T_{NaCl}. The As shutter remains open using an As flux with a As/Ga ratio = 1 (calibrated at 580°C) while heating the sample to T_{GaAs1} at 20°C/min (which takes a predictable amount of time (t_{ramp1}). Once the T_{GaAs1} is reached, the temperature stabilizes, and then the Ga shutter is opened for a short time (t_{GaAs1}) to form a thin layer at this lower temperature. The As shutter remains open as it is heated to T_{580} using the same ramp rate (which takes t_{ramp2}) at which point the As flux is increased and the Ga shutter is opened for a secondary GaAs deposition time (t_{GaAs2}). Once complete, the same cooling procedure as outlined earlier is then applied.

Four GaAs films deposited on NaCl layers are chosen for comparison in this section and 2.3.3; the growth parameters are outlined in Table 2. All samples had a NaCl deposition rate of 3 nm/min and a Ga-flux that gave a growth rate of 33 nm/min when supplied concurrently with arsenic.

Figure 16(a) shows an image of sample A after removal from the vacuum chamber. A relatively uniform area larger than just the width of the RHEED beam was able to be achieved because the RHEED sweep was done prior to any GaAs deposition. When inside the chamber, the RHEED beam was incoming from the direction perpendicular to the top edge of the sample. The

area exposed to the RHEED appears darker marked by the light blue lines. The red lines point out areas that were not exposed to RHEED, either deliberately or because the glancing angle beam was blocked by the sample holder clips or flakes on the sample holder. In the absence of any flakes present on the holder (as was observed with other samples), the beam can be scanned across the entirety of the sample during the As-adsorb step to provide a relatively uniform large area. The presence of a shadow from the sample holder clip is not avoided with a single scan, but if the sample were rotated 90° and the beam moved across again it could cover that area. This was not attempted.

The RHEED patterns from areas with RE and NRE are shown in Figures 16(b1,b2). The pattern from the area with RE is slightly streakier, while the pattern from the area with NRE shows faint steeper chevrons. This suggests that the area with NRE has a rougher faceted surface compared to the area with RE. Both areas are a bit dimmer but have substantially fewer additional spots than the samples in Section 2.3.1.c.ii that were grown continuously from the nucleation at lower temperatures. Figures 16(c1,c2) display SEM images which show a stark contrast between the two regions. A complete NaCl layer of the expected thickness is still present in the areas with RE. Conversely, in the area with NRE, there is no more NaCl and the overlayer has fused to the substrate. The area with NRE is unsurprisingly similar to samples grown at similar temperatures discussed in Section 2.3.1 (such as Figure 7 which showed fusion with the substrate when nucleating as cold as 325°C), while the area with RE is quite different. By utilizing the RHEED exposure at low temperature, GaAs was nucleated more quickly at 400°C, resulting in more rapid coverage of the NaCl, which was protected even during the high temperature deposition.

The EBSD maps and quantitative pole figures in Figure 16(d1,e1) show that there are only two predominant grain orientations in the RE area, those oriented commensurate to the substrate and a single orientation of the {122}. The {322} grains that were previously observed previously in Figure 14, have been fully suppressed. The origin of this orientation must be a result of the lower GaAs nucleation temperature or the continuously depositing GaAs while heating. Figures 16(d2,e2) show a EBSD map and the corresponding pole figure from the area with NRE revealing monocrystalline GaAs. Because the material in this region does not show a complete NaCl layer, this could be a result from the bonding to the substrate, either homoepitaxy, recrystallization, or a combination of both. Without the presence of a NaCl layer it will not be possible to be simply removed from the substrate anyway.

Both pole figures show the angle of {100} planes with respect to the surface normal. The central spot (at 0°) is indicative of the red areas present in the EBSD orientation maps. The additional set of 4 spots located at 90° from the center, and ~45° from the X and Y axes correspond to the other planes of a single (100) oriented crystal. The 45° misorientation is because the samples are mounted with the cleaved {110} edge parallel to the sample holder edge (which is used as the x-y reference). A completely (100) (red) oriented surface could also be observed with each grain being azimuthaly misoriented (fiber oriented). In a case such as this a full ring would be observed around the outside if there was zero rotational registry with the underlying material, or multiple sets of spots could be observed around the edge if specific rotations were preferred. Here, only a single set of 4-fold rotationally symmetric spots are observed, and because the samples are 0±0.1° offcut, we can say these grains are exactly aligned with the substrate.

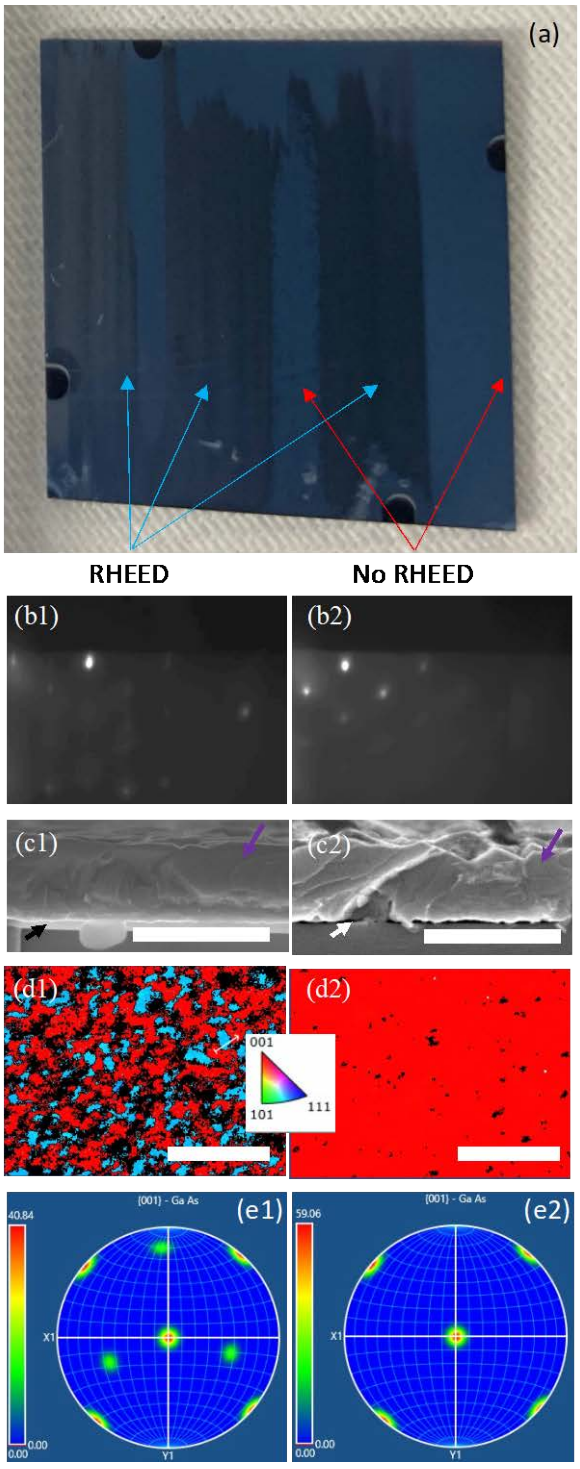

Figure 16: (a) Image of sample A after removal from the chamber with (b) RHEED images at the end of growth, (c) SEM images where purple, black, and white arrows mark the GaAs overlayer, NaCl layer, and voids between the substrate and overlayer, respectively (scale bars 600 nm), (d) EBSD maps of areas (scale bars 5 µm), and (e) the corresponding quantitative {100} pole figures for areas (1) exposed to RHEED and (2) not exposed to RHEED until growth was completed

For sample B, GaAs is first deposited on a NaCl film at a lower temperature (~100 nm, 375°C) with As/Ga =1 (calibrated at 580°C), followed by a traditional As-rich GaAs deposition (300 nm, 580°C). Upon removal from the chamber, the central portion of the sample exposed to the RHEED beam is visibly darker, and slightly more specular than the areas along the edges of the sample which were not exposed (Figure 17(a)). Cross-sectional STEM images were taken from areas inside the green circle and the purple square, to look at regions without (Figure 17(b) and with (Figure 17(c)) RHEED exposure, respectively. Diffraction patterns were taken at different locations throughout the thickness of each region of the GaAs overlayer: (1) at the top, (2) near the middle, and (3) near the GaAs/NaCl interface and can be compared to the diffraction pattern of the substrate (inset of Figure 17(a)).

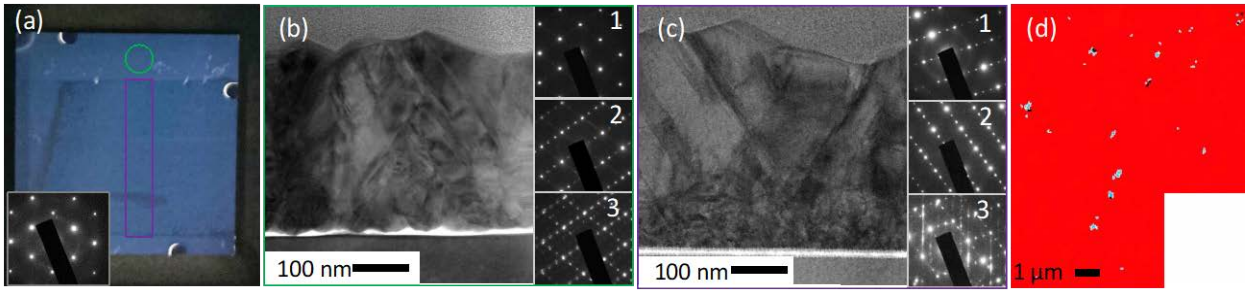

Figure 17: (a) image of the sample B showing the central area exposed to the RHEED beam prior to GaAs deposition (inset) STEM diffraction pattern of the substrate. STEM images of areas (b) never exposed to RHEED (from green circle) and (c) exposed to RHEED prior to GaAs deposition (from purple square) and the corresponding diffraction patterns from (1) the top of the film, (2) the center of the film, and (3) near the NaCl interface. (d) EBSD orientation map from the RHEED exposed area.

Without any exposure to RHEED (Figure 17(b)) the NaCl layer is rough and incohesive, with the GaAs overlayer coming in close proximity (or attached) to the substrate. This is likely because the surface prior to capping more completely at high temperature, as will be shown more in the following section. The grains appear slightly tapered, with smaller grains near the interface and larger grains near the top. The diffraction patterns near the NaCl interface show highly textured grains with the $(\bar{1}\bar{1}1)$, (111), (220), and (100) planes parallel to the same respective plane in the substrate. The extra spots observed in patterns from this area correspond to grains that are {122} oriented in the growth direction, with different azimuthal registry to the NaCl/GaAs substrate. Moving toward the top surface, the texturing trends toward a (100) oriented film until a single set of spots nearly identical to the substrate pattern is observed.

In the region exposed to the RHEED (Figure 17(c)), the NaCl layer remains flat and cohesive, with no indication that the overlayer is attached to the substrate. The GaAs just above the NaCl consists of smaller grains than in the areas without RHEED exposure, but again taper outward with a larger grain structure at the surface. The thicknesses of the small and large grain regions roughly correlate to the low and high temperature depositions, respectively. The diffraction patterns reveal that the grains in this area are highly textured with orientations similar to the area without RHEED exposure, but the high degree of streaking suggests a high stacking fault density. Above the small-grained region, the patterns are increasingly textured, and the stacking fault density is reduced. The intensity of intermediate spots decreases as one approaches the top surface of the film, suggesting an increase in the texture and grain size. EBSD images of this area (Figure 17(d)) show that most of the RHEED exposed area is (100) oriented, but with small {122}

inclusions separated by CSL Σ3 boundaries: 60° rotations of the crystal about a [111] direction. The small-grained low-temperature section has a higher degree of grain misorientation, which can provide seeds for the tapered columnar growth, leading to these inclusions.

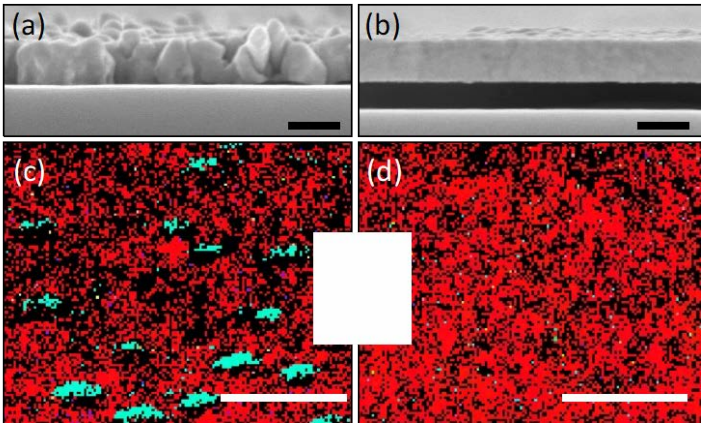

Figure 18: SEM images of regions of Sample C (a) without and (b) with RHEED exposure (scale bars 100 nm). EBSD orientation map from regions of the same sample (c) without and (d) with RHEED exposure (scale bars 5 µm)

Sample C was grown to investigate the crystallinity of the low-temperature GaAs. It consists of an identical RHEED exposure process after the NaCl deposition and low temperature GaAs deposition (100 nm at 375°C, Table 1), but without the high temperature growth or heating to the elevated temperature. Cross sectional SEM was performed in regions of the sample without and with RHEED exposure. Without RHEED exposure (Figure 18(a)), the low temperature GaAs capping layer is chunky, rough, and incohesive. It is worth repeating that the effusion cell temperature for the NaCl is only 480°C. Even in the relatively lower temperature range of 350-400°C, desorption of the NaCl is rapid. Because the GaAs in this region does not completely cover the NaCl. As a result, the NaCl layer is much thinner (<10 nm) in this region compared to the expected NaCl thickness (~75 nm, based on calibrations done at 150°C). This highlights the importance of quickly realizing a complete capping layer, which is exacerbated at higher temperatures.

The SEM of the RHEED exposed area (Figure 18(b)) is distinctly different. The interfaces and surfaces of the material in this region are much smoother. The GaAs is fully cohesive, enabling protection of the alkali halide from desorption. The NaCl layer (dark region) is significantly thicker (~55 nm) but still thinner than expected; some will still have sublimated during heating to the nucleation temperature and prior to achieving complete coalescence. Additional work has shown that the RHEED exposure increases the nucleation density of GaAs islands;[13] this would lead to faster coalescence of a full film, protecting the NaCl from further continuous desorption during the GaAs deposition.

EBSD orientation maps were also taken to look at the crystallinity of the GaAs overlayer in both regions (Figures 18(c,d)). The black areas are unindexable in the EBSD analysis due to weak Kikuchi patterns. This could be attributed to poor crystallinity from the presence of surface defects but more likely it is due to roughness of surface features. Using the traditional co-deposition method results in the presence of large {122} grains (some >1.5 µm) in the area without RHEED exposure. The degree of unindexable area also correlates with the larger roughness

observed in this region. The smoother film in the RHEED exposed area results in a lower degree of unindexable area and is mostly (100) oriented. However, there are still areas registering as {122}, albeit significantly smaller in size. The misoriented grains in both regions are the same as the inclusions observed in Figure 17(d). This provides good evidence for why they are also observed in the thicker films. Precisely why only a single 90° rotation of these grains are observed and why they are less prevalent in areas exposed to the RHEED is not known. They may be related to small miscuts, even on 0±0.1° wafers, or deposition on an actively desorbing surface. Because any misorientation propagates through thicker films and can get even bigger with the tapered columnar grain structure observed earlier, a seed layer without any misorientations must be obtained.

2.3.3. Migration enhanced epitaxy of the nucleation layer

In an effort to achieve better crystallinity in the low temperature seed layer, Sample D was grown using a migration enhanced epitaxy (MEE) technique to promote adatom mobility (Table 1). Alternate pulses of Ga (2 ML) followed by As with 0.5s wait times between each were repeatedly supplied until an overall GaAs thickness of ~66 nm was accumulated. The effective growth rate of MEE (<4 nm/min) is significantly slower than co-deposition (33 nm/min), because growth is Ga-limited in this regime and the supply of Ga is limited due to the shutter sequencing, as well as time lost to shutter transients. Thus, the temperature for this step was reduced slightly to 350°C. If repeated at 375°C (same as used for co-deposited GaAs), too much NaCl loss occurred prior to realizing complete coverage of a GaAs film. The MEE step was followed by ~33 nm of co-deposition at 400°C to look for evidence of NaCl desorption at higher temperatures concurrent with further GaAs growth.

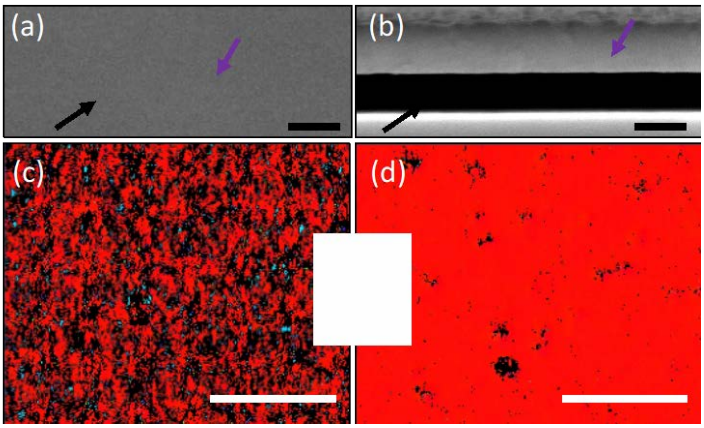

Figure 19: SEM images of Sample D, GaAs on NaCl layers using MEE (a) without and (b) with RHEED exposure (scale bars 100 nm). Purple and black arrows mark the GaAs overlayer and NaCl, respectively. EBSD orientation maps showing primarily (100) oriented films for (c) without and (d) with RHEED exposure (scale bars 5 μm)

Cross section SEM of the regions without RHEED exposure is shown in Figure 19(a). Here, the GaAs layer is chunky, not fully conformal and the NaCl thickness ranges from nearly none to ~30 nm. Comparing the same region of the co-deposited sample in the previous section (Figure 18(a)), the roughness is lower, and the size of the cohesive islands seems to be slightly larger. This suggests that MEE, while still proceeding in a 3D growth mode, does slightly enhance lateral growth allowing for larger island formation. This results in better protection of the NaCl in

these covered areas, and a comparatively thicker NaCl than the previous case. However, with the deposition time being significantly longer, in areas between GaAs islands the exposed NaCl continuously desorbs until none is left.

In the area with RHEED exposure (Figure 19(b)), the cross-section SEM appears largely similar to the same region discussed in the previous section for the co-deposited sample. However, the NaCl layer is ~20nm thicker, and is approximately equal to the target thickness. While this is likely in part due to the lower temperature of the MEE step, the area without RHEED exposure shows that significant desorption can still occur if not completely capped. Thus, we suspect that with the increased nucleation rate due to the exposure to RHEED in this area, coupled with enhanced lateral island growth from MEE, the NaCl is overall capped more quickly in this region compared to traditional co-deposition.

The EBSD orientation maps of the area without RHEED exposure (Figure 19(c)) still shows some small misoriented inclusions, but not nearly as large as those shown in the previous section. In the region with RHEED exposure there is significantly less unindexable signal (Figure 19(d)), and a solely (100) oriented film with no additional orientations observed. The growth of additional thicker high temperature (580°C) GaAs on these low temperature MEE templates is a subject of future work. However, it is expected that by using this single orientation template the crystallinity would persist throughout continued deposition. Similar to that which was shown in Section 2.3.2, the non-indexable areas should be reduced and a clean (100) film without misoriented inclusions should be observed. The work in this section has established a method for obtaining GaAs films with a crystalline surface orientation matching that of the substrate on top of a continuous NaCl layer and will be improved upon in the next.

2.3.4. Metal modulated epitaxy of the nucleation layer

The use of MEE shown in the previous section yielded promising results. However, the effective growth rate is very slow, which presents an issue that will be discussed in more depth in section 2.6. Metal modulated epitaxy (MME) is proposed here as another method for achieving monocrystalline GaAs. However, because the growth sequence allows for longer Ga-shutter open times, the effective growth rate of MME can be higher than MEE. To perform MME, only the Ga shutter is opened/closed and there is a continuous flux of As. However, the As-flux is less than the stoichiometric Ga-flux for the given As-valve position, so that with prolonged Ga exposure the surface becomes metal rich. This transition is clearly observable at 580°C by monitoring the transition of the surface reconstruction from the As-rich (2×4) to the Ga-rich (4×2). The Ga-flux was held constant, and the As-valve was tuned so that the transition from the As-rich to Ga-rich surface occurred ~5 seconds after the Ga-shutter was opened. This calibration was done prior to the buffer layer deposition for each MME growth.

Table 3: Growth parameters for GaAs films grown on NaCl thin films using MEE and MME

	NaCl Deposition		GaAs Nucleation				Intermediate GaAs				High Temperature GaAs			
	Time (min)	Temp (°C)	Time (min)	As/Ga	Doping	Temp (°C)	Time (min)	As/Ga	Doping	Temp (°C)	Time (min)	As/Ga	Doping	Temp (°C)
Sample E	30	150	17	MEE	uid	350	2	1	uid	400	9	1.68	Si	580
Sample F	30	150	4	MME	uid	350	2	1	uid	400	9	1.68	Si	580
Sample G	30	150	4	MME	Si	350	2	1	Si	400	9	1.68	Si	580
Sample H	30	150	4	MME	Si	350	--	--	Si	--	9	1.68	Si	580

Another set of samples will be discussed in this section using the same separate nucleation and growth scheme with the As-adsorb (outlined in Section 2.3.2) are tabulated in Table 3 Each sample consists of ~90 nm of NaCl deposition at 150°C, which is subsequently exposed to As while moving the RHEED beam. The nucleation scheme for Sample E is similar to Sample D from the previous section, MEE at 350°C and then ~66 nm of intermediate GaAs deposition at 400°C (a little thicker than previously). However, this sample is now heated to 580°C and 300nm of n-GaAs is deposited. Sample F is similar to the first, but the layer at 350°C is instead deposited using MME. During this nucleation a cycle of opening the Ga-shutter for 10s and then closing it for 10s (to consume the excess Ga on the surface), is repeated 12 times to yield a thickness approximately equal to that which is deposited by MEE. Sample G is similar to Sample F except that all of the GaAs is doped with Si. Finally, Sample H is the same as Sample G but without the secondary 400°C GaAs deposition.

Figure 20 shows the RHEED patterns at (1) the end of the nucleation section and (2) at the end of growth for each sample with cross-sectional SEM images for areas (3) with RE and (4) with NRE. First, looking at Sample E (Figure 20(a)), bright streaky spots signify a smooth surface (for where the RHEED was exposed) with the presence of some shadow spots and chevrons. This is very similar to the pattern at the end of the 350°C sample from section 2.3.3 (Figure 19) (which is not shown). Bright spots are still maintained but the RHEED pattern dims slightly after the high temperature growth step (Figure 20(a2)) signifying an increase in roughness of the film; large scale undulations can be seen in the corresponding SEM (Figure 20(a3)). The area with RE also shows the presence of a NaCl layer beneath the GaAs. In contrast, the area with NRE shows no NaCl, only large voids beneath a rougher GaAs film (Figure 20(a4)). There is also evidence of fusion with the substrate in these areas which is not surprising when comparing to samples from previous sections (2.3.2 and 2.3.3), as the ≤400°C deposition in the area with NRE was not a continuous film and there was already evidence of NaCl desorbing.

Looking at Sample F (Figure 20b)) where the nucleation layer was switched from MEE to MME does not reveal any drastic differences from the MEE case, which considering the >4× increase in effective growth rate using MME is promising when it comes to capping the NaCl layer more quickly. The RHEED pattern at the end of the MME step is overall brighter compared to the MEE case, but the relative brightness of the shadow spots is also higher. Again, the pattern dims overall but the shadow spots more so relative to the primary spots signifying an increase in roughness, but an improvement in the crystallinity. The SEM looks very similar to that which was shown in the previous case, full NaCl underneath a GaAs film in the RE area and a rougher film over voids with some fusion to the substrate in the area with NRE.

Sample G (Figure 20(c)) only differs from Sample F because the low temperature GaAs layers were doped with Si. The addition of a dopant was not done in an effort to improve the crystallinity or morphology, although that was a possibility. More so, it was done to provide a simpler scheme for device processing as the whole section above the NaCl would be n-GaAs and not require a precise timed etch step to expose the doped layer for the front contact. The device and processing schemes will be discussed more in Sections 2.5 and 2.6. The RHEED pattern after the MME deposition step looks similar to the previous case but dims substantially by the end of growth. It is unlikely that this is due to the addition of Si; rather, there was slight delamination at one of the edges of this sample which is more likely due to oscillations in the sample temperature during the high temperature step. The SEM images from the areas with RE and NRE look similar to previous cases with full NaCl layers, and voids and fusion observed in each area, respectively.

Sample H (Figure 19(d)) repeats Sample G without the 400°C deposition. As expected, the early RHEED pattern looks similar, as this step is the same. But without the intermediate deposition the spots in the pattern remain brighter than previous cases, and even slight streaking is observable signifying a smoother film. The SEM images are again, very similar to previous cases, but the GaAs film is expectedly thinner, as the ~66 nm of GaAs at 400°C was omitted. In the area with NRE, the voids are also much smaller than the previous samples. In the RE area the MME step results in a material that is thick and cohesive enough to protect the NaCl, while the area with NRE must still be more discrete islands. Without the 400°C deposition, even more NaCl is allowed to desorb from the surface prior to further GaAs deposition at 580°C. This results in a bare GaAs surface, and simply homoepitaxy, when exposed to Ga and As. It is worth noting that all these areas with full NaCl layers (i.e., in the RHEED exposed areas) lifted off as will be discussed in the following section and identical schemes used in Samples F, G, and H were used as templates for the deposition of PV devices, which will be discussed in Section 2.5.

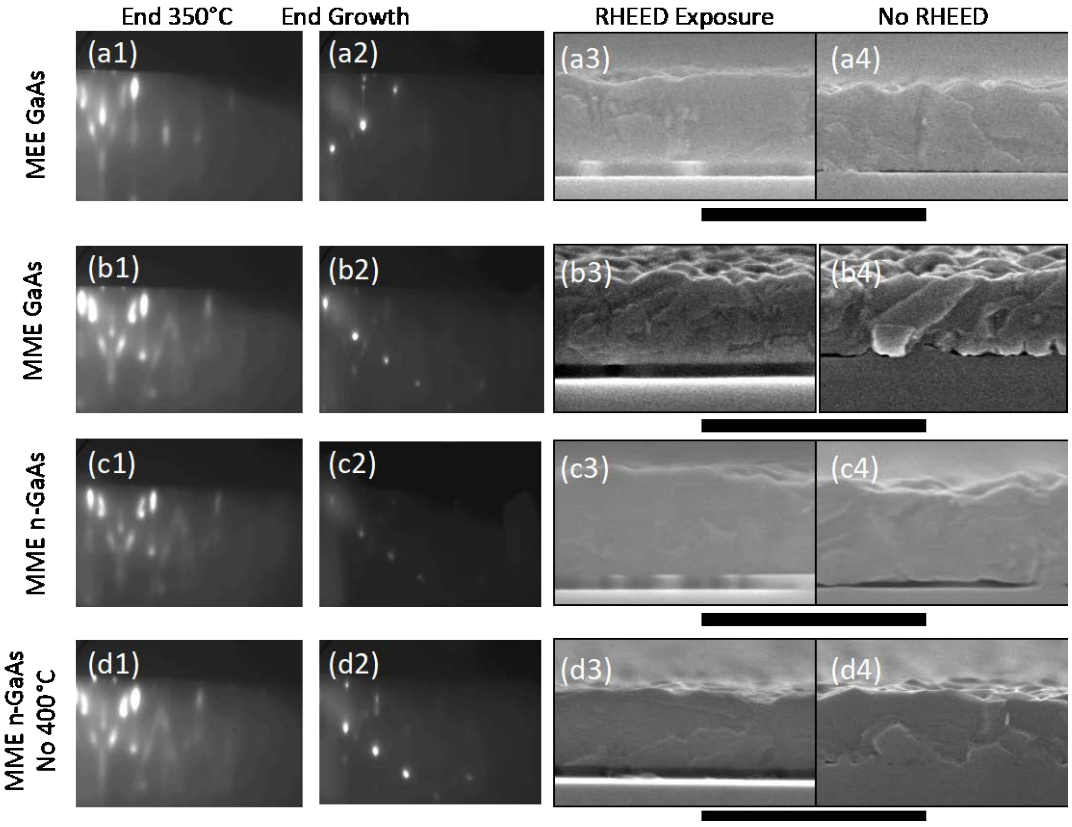

Figure 20: Comparison of MEE and MME growths outlined in Table 2. (a) (Sample E) MEE nucleation of GaAs (b) (Sample F) MME nucleation of GaAs, (c) (Sample G) MME nucleation of n-GaAs, with 400°C secondary deposition and 9 min n-GaAs deposition at 580°C. (d) (Sample H) MME nucleation of n-GaAs and 9 min n-GaAs deposition at 580°C.
RHEED images for (1) the end of the nucleation layer at 350°C and (2) at the end of n-GaAs deposition at 580°C. SEM images of (3) areas with RHEED exposure and (4) areas with no RHEED exposure. Scale bar for SEM images is 1 μm

2.3.5. Section summary

A wide range of growth conditions for GaAs on NaCl were tested. It was found that GaAs grows on NaCl in a 3D island growth mode and NaCl desorbs from the substrate very quickly at temperatures >300°C. Thus, maintaining a continuous NaCl film requires rapid formation of a continuous GaAs layer without negatively influencing the crystallinity of the overlayer. Nucleation of the GaAs was shown to be enhanced through exposure of the bare NaCl to the RHEED electron-beam prior to GaAs deposition and separately nucleating GaAs at a lower temperature. The use of alternate growth techniques such as MEE and MME were shown to yield improvements in the crystalline quality. Eventually, monocrystalline GaAs templates on continuous NaCl layers were realized. The importance of maintaining a continuous NaCl layer cannot be stressed enough, as will be shown in the following section, it is imperative to the removal of the overlayer from the substrate.

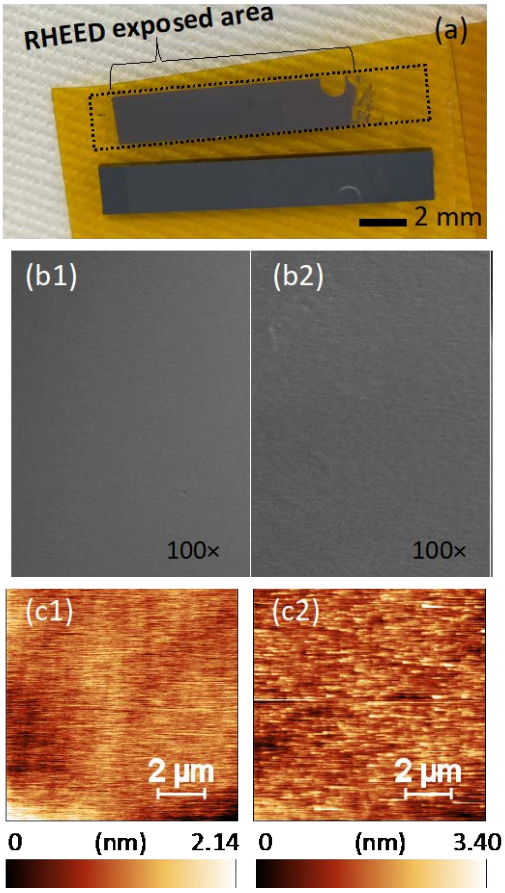

Figure 21: (a) Image of substrate (top) with separated GaAs overlayer (bottom) on Kapton tape, the outline of where the entire piece was originally attached is outlined by the dotted line. (b) 100× Nomarski images and (c) AFM images of (1) a substrate after buffer layer growth and (2) after film liftoff

2.4. Removal of semiconductor films from the substrate

The GaAs overlayer is attached to Kapton tape and placed in room-temperature water to test separation from the parent substrate. Over 200 samples were tested and as long as there is a cohesive NaCl layer, it is rapidly dissolved in the water, with NaCl films as thin as nominally 3

nm facilitating near immediate liftoff. It is also worth noting, when using thicker NaCl layers a water dip is not always necessary, and the overlayer can be simply peeled from the substrate. We hypothesize that this mechanism more closely resembles cleaving of the softer NaCl material because both the lifted overlayer and the substrate have a slight iridescence which immediately disappears from both after rinsing in water.

Figure 21(a) shows a piece cleaved from Sample B (taken from the right side of Figure 17(a)) after separation of the GaAs film from the original wafer. The substrate (above) is placed back on the tape, growth side up for display purposes. The area that was originally attached to tape, prior to placement in water, is outlined below by the black line. The central region was exposed to the RHEED and maintained a continuous NaCl layer. Thus, it was easily separated from the substrate, with the now exposed face being the side of the overlayer that once interfaced with the NaCl. As discussed in Section 3.2.1, the edges of the sample were never exposed to RHEED, had a thinner and less cohesive NaCl, thus subsequently fusing to the substrate and inhibiting liftoff.

Additionally, the films from both Samples C and D lifted off completely and uniformly over the entire area tested. This is promising, as the highly (100) oriented areas exposed to RHEED maintained a continuous NaCl layer under a complete GaAs film, which should protect the NaCl from any desorption when heating to 580°C. Interestingly, the areas that were not exposed to RHEED also lifted off in these samples, despite not having a continuous NaCl layer. This suggests that while the NaCl could completely desorb from underneath discrete GaAs islands, the islands simply sit on the substrate and do not fuse with the substrate unless exposed to higher temperatures.

Nomarski images of the buffer layer grown on a GaAs wafer and the surface after liftoff of a GaAs film are compared in Figures 21(b1, b2). These, coupled with 10×10 μm atomic force microscopy (AFM) scans in Figures 21(c1,c2), show that the original buffer layer is locally very smooth (rms roughness of 0.27 nm). After deposition and removal of NaCl and GaAs layers the rms roughness increases by only 0.2 nm, there are large areas without any obvious surface defects, and looks largely similar to the buffer layer surface. This is with only a short time (<10 s) in water, dried with N_2, and no other cleaning or surface preparation. More deliberate cleaning steps and an additional buffer layer regrowth would be expected to further improve the surface which is ultimately promising for reuse of the substrate.

2.5. Growth of solar cell devices on GaAs/NaCl/GaAs templates

After monocrystalline films on NaCl were demonstrated (Section 2.3), the next step was to use these templates for growth of photovoltaic devices. Devices were grown using both MBE and HVPE (Figure 22). The device structures are not changed in this study, the main variables changed between samples discussed in this section are all related to the MBE template. The one exception is the change in temperature of the grown cells by HVPE. For this reason, no specifics are given for the layers which are changed in the MBE template layer (the NaCl thickness or the temperatures and thicknesses of the low and high temperature GaAs overlayers).

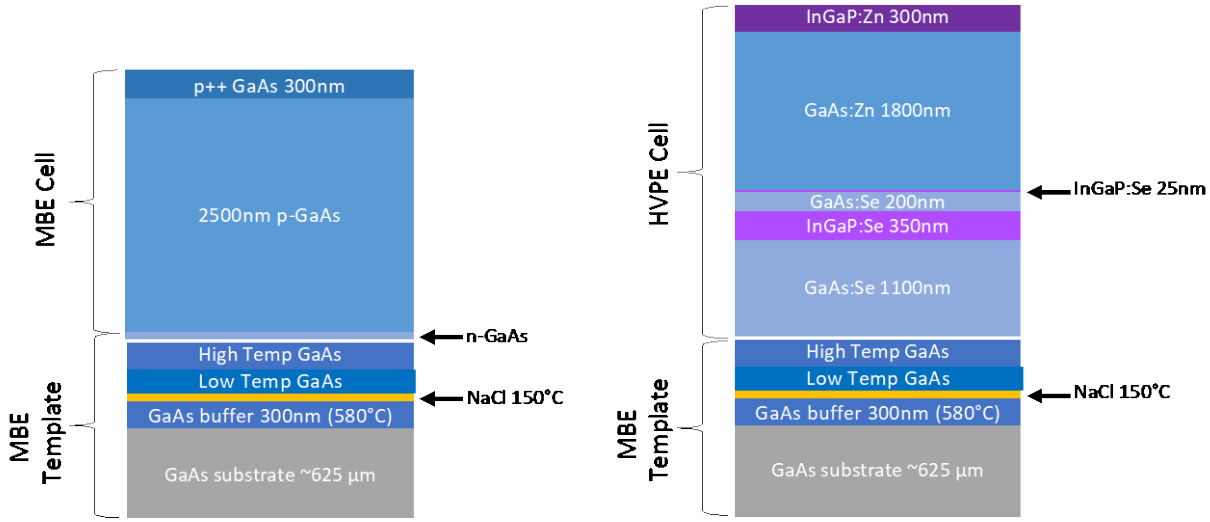

Figure 22: Schematics of all-MBE and the (B) HVPE cell heterostructures grown on MBE-grown templates

For the MBE-grown cell structure is a simple homojunction cell is grown on the template without any stop in growth. A Si-doped n-type buffer layer is deposited first to improve the crystallinity of the material prior to deposition of the device layers, which also functions as the n-GaAs emitter. Because there were no calibrations for MBE-grown InGaAs or AlGaAs etch stop layers, the study here focuses more on improvements in crystallinity than device characteristics. A thick Be-doped p-GaAs collector is deposited next followed by a highly p-type doped GaAs back contact layer.

For the HVPE-grown cell structure, the MBE-template layer is removed from vacuum for transfer to the HVPE system. A standard recipe for a rear heterojunction cell grown directly on GaAs substrates was used. A 1.1 µm n-GaAs buffer layer is grown followed by an InGaP etch-stop layer. After the etch stop a 200 nm n-GaAs emitter followed by a 25 nm n-InGaP etch stop layer is deposited before the 1.8µm Zn-doped p-GaAs collector. The final layer is a 300 nm p-InGaP back contact layer.

2.5.1. All-MBE cells

Here we will look at all-MBE grown cells deposited on the templates identical to the MME samples discussed in Figure 20 (Samples F, G, and H). Regrowth of each of these templates was done with an additional 500 nm n-GaAs buffer layer prior to deposition of the device structure all at 580°C.

Figure 23(a) shows the cell grown on a copy of the template Sample F (MME of unintentionally doped (uid)-GaAs, followed by 66 nm of uid-GaAs at 400°C and 300 nm of n-GaAs at 580°C). The additional ~3.5 µm of GaAs accounting for the buffer layer and cell structure are then also grown at 580°C, which using the standard growth rate of 33 nm/min requires nearly two hours to complete. Figure 23(a1) shows an image of the sample after removal from the chamber. The RHEED was swept across the entire sample (incoming from the bottom of the image) and shadows from the sample holder (and especially from the clip) are visible near the bottom of the sample. However, the bulk of the area is relatively similar to the surrounding areas, and a small amount of delamination is visible. The region of the sample outlined by the black dotted line is cleaved and the top surface attached to Kapton tape and submerged in water.

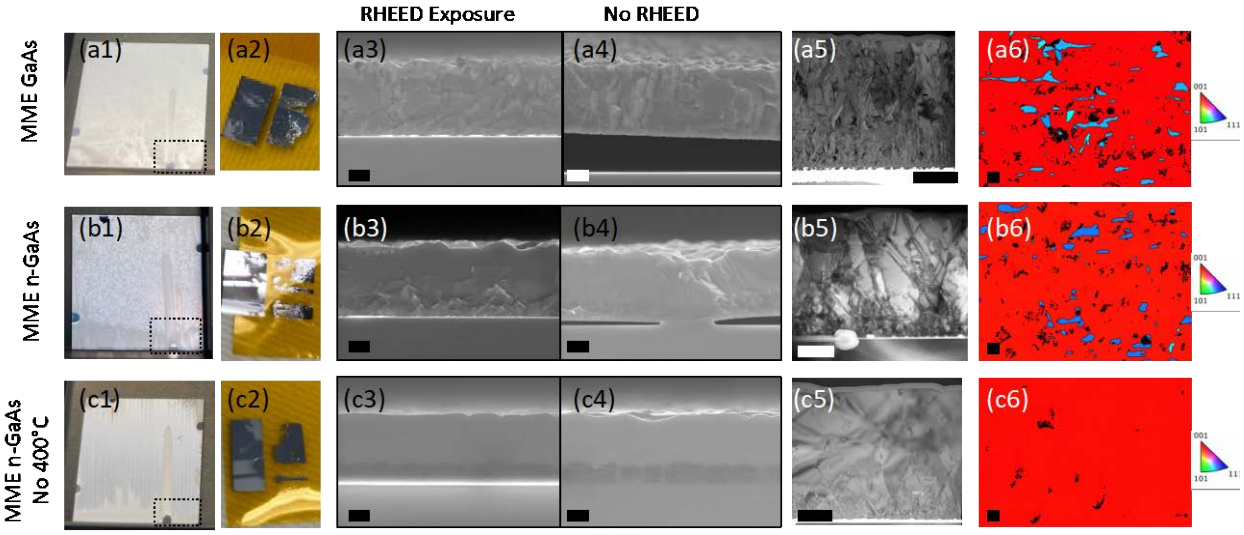

Figure 23: All-MBE cells grown on the templates from Section 2.3.4 (a) MME of uid-GaAs, (b) MME of n-GaAs, and (c) MME of n-GaAs without a 400°C step. (1) images of the 2×2 cm samples after removal from the chamber. (2) images of the cleaved section from (1) showing the device layers (right) attached to Kapton tape after removal from the substrate (left). Cross section SEM images from areas (3) with RHEED exposure and (4) without RHEED exposure. (5) TEM images from areas with RHEED exposure. (6) plan-view EBSD from areas with RHEED exposure. The scale bars for SEM, TEM, and EBSD images are all 1 μm.

Figure 23(a2) shows the cell device layers which remain attached to the Kapton tape on the right, next to the substrate which was reattached to the left for comparison. This area is notably, and deliberately, from a non-uniform area of the sample. Areas where the RHEED was blocked by the sample clip or heavily shadowed (bottom right of the sample) were not removed as completely as areas that were exposed to the RHEED. However, there was some liftoff from these areas, which was unsurprising as delamination was also observable in these areas by eye. When looking at these areas using cross section SEM (Figure 23(a3,a4)) the reason behind this discrepancy is obvious. In areas exposed to RHEED there is a complete NaCl layer beneath the device. Conversely, in areas without RHEED exposure, delamination and large gaps between the device and the substrate are observed. This delamination is also coupled with, but not able to be shown in SEM images of the same scale, fusion of the overlayer to the substrate. This will be the subject of discussion in Section 2.6.

A TEM image of the RHEED exposed area (Figure 23(a5)) shows the tapered grain structure similar to what was observed in Figure 17. The NaCl layer was not observed in this image, but small grains are near the bottom and columnar grains propagate upward, with larger grains near the surface. Plan-view EBSD images are also taken from the RHEED exposed area and reveal a largely (100) oriented surface. However, two different blue grains are also observed similar to Figure 14 which are both related to different orientations of {122} grains. Curiously these misoriented inclusions seem to have a particular geometry with long edges aligned closely to a [110] direction.

Figure 23(b) shows the same cell structure grown on a similar template, but this time all the GaAs in the template layer is doped with Si (repeat template sample (G)). The image of the

sample post-growth (Figure 23(b1) again shows the same shadowing of the RHEED beam from the sample holder. There is a similar amount of delamination in the areas at the edge of the RHEED exposure (near bottom of sample), but it does not show the same degree of delamination in the RHEED exposed area. This is not likely due simply to the inclusion of the Si in the low temperature GaAs layers, but rather is attributed to maintaining a more stable temperature throughout the deposition of the high temperature layers. There are also some darker spots observable in the RHEED exposed area, more details will be given on these features in Section 2.6. When attempting liftoff of this sample, the RHEED exposed areas are able to be removed, while areas where the RHEED beam was shadowed are not able to be lifted off (Figure 23(b2)).

Cross section SEM of the RHEED exposed area (Figure 23(b3)) reveals a full NaCl layer beneath the GaAs cell. Interestingly, the cleaved area for this sample is much smoother near the top, additionally there are areas which are very flat as well. In areas with NRE (Figure 23(b4)), the large gaps between the substrate and film are not observed. There is still no evidence of a NaCl layer, and fusion between the film and the substrate is frequently observed. TEM images of the RE area (Figure 23(b5)) are similar to the previous sample. However, the grains appear larger at both the interface with the NaCl and near the top surface. EBSD images (Figure 23(b6)) reveals again a largely (100) surface, and two {122} grains. However, in this case one seems to dominate over the other. It is not yet known whether this difference in crystallinity between is real or the result of these techniques looking at localized areas which may present similar differences in the same sample. If it is real, it is also not known if it is due to the addition of Si to the low temperature layers or to discrepancies in the way the RHEED is manually moved across the surface during the As-adsorb step.

The final All-MBE grown cell discussed here uses the template without the 400°C deposition step (repeat of template Sample H). Figure 23(c1) shows the image of the device after removal of the chamber, again revealing distinctly different regions where the RHEED was shadowed (at the bottom of the sample and clip region) compared to the remainder of the area where RHEED was moved across the sample. However, this sample also reveals distinct vertical lines, which are indicative of the manual moving of the RHEED beam across the surface. Again, only the areas exposed to RHEED can be removed from the substrate (Figure 23(c2)).

Cross section SEM images of this sample (Figures 23(c3,c4)) reveal very smooth cleaved edges. The RHEED area shows a full NaCl layer beneath the solar cell device layers. Because of this smooth cleave, the contrast differences between the n-type layer (darker) and the p-type layer (lighter) of the solar cell device are discernable. The surface in this area is also smoother than the previous cases, with no large facets observed but there still is some observable roughness. In the area without RHEED exposure, there are no large voids like the previous samples. In this case only very small holes are observed where the NaCl once was and are not visible at this magnification. Because of the lack of additional 66 nm of GaAs deposition at 400°C in this sample, the coverage of the NaCl in the areas without RHEED exposure was very limited. This resulted in desorption of nearly all the NaCl prior to further deposition at 580°C, and essentially a homoepitaxial cell was deposited in this area. However, this area also has a higher degree of surface faceting and roughness than the area with a complete NaCl layer.

For the template without a 400°C deposition, TEM images of the RHEED exposed area (Figure 23(c5)) show something different. No columnar grain structure is observed, instead the area is epitaxial. Separate TEM imaging of only the template growth (Sample H, Figure 24(c3)), reveals that the starting template layer is epitaxial as well. Thus, this shows that if a

monocrystalline, epitaxial template can be provided, a similarly crystalline cell can be achieved as well, while still maintaining the NaCl layer. The first ~150 nm of GaAs near the interface of the NaCl is highly defective; after ~550 nm the material looks significantly better and continues to improve with further growth. Because the initial 350°C MME deposition is only ~66 nm thick, this highlights the importance of a buffer layer grown at more standard conditions prior to growth of the actual cell structure. There are still defects observable in the cell portion of the device, but it is possible that these could be engineered out. EBSD looks at larger areas than TEM and shows that the surface is wholly (100) oriented (Figure 23(c6)). It is worth nothing that the unindexable areas here, and in the other EBSD images in this figure, are due to the shadowing present from surface roughness, and not a lack of crystallinity. Cross section EBSD was also performed on this sample (not shown) and did not reveal the presence of any other grain orientations at the interface with the NaCl.

Epitaxial GaAs homojunction devices were grown on continuous NaCl layers using MBE. These device layers were lifted off from the parent substrate by submerging in water. The removed films were able to be fully processed, but the presence of small holes in the removed films results in shorts in the end devices. These problems and methods taken to address them are covered more completely in Section 2.6.

2.5.2. HVPE-cells on MBE-templates

Solar cell devices were also grown using HVPE on MBE grown templates. Because this involves transfer of the template layer from the MBE to the HVPE system, only templates that were first verified to be able to lift off were selected for subsequent HVPE-cell deposition. However, not all samples that could lift off were able to be used as templates as the number of HVPE runs that could be performed was limited. Figure 23 shows the use of two samples discussed in earlier sections and the changes that happened with subsequent HVPE growth at 650°C and 600°C.

The first example uses Sample B as a template, the TEM images of which were discussed previously in Figure 17, for HVPE growth at 650°C. Cross section SEM images of this sample from areas with RHEED exposure reveals that a NaCl layer is present underneath the GaAs overlayer in the area with RHEED exposure prior to HVPE growth (Figure 24(a1)). We also saw in Figure 21 that this region was able to be removed from the substrate by attaching the sample to Kapton tape and submerging in water. Without RHEED exposure, fusion is observed in some locations, but wide pores are also visible (Figure 24(a2)). For comparison to the HVPE grown cell, EBSD of the RHEED exposed area of the starting template is displayed again (Figure 24(a3)), showing mostly (100) surface with small {122} inclusions. A portion of this template was set aside for the characterization just mentioned, and the remainder (~1.5×2 cm) was transferred to the HVPE system.

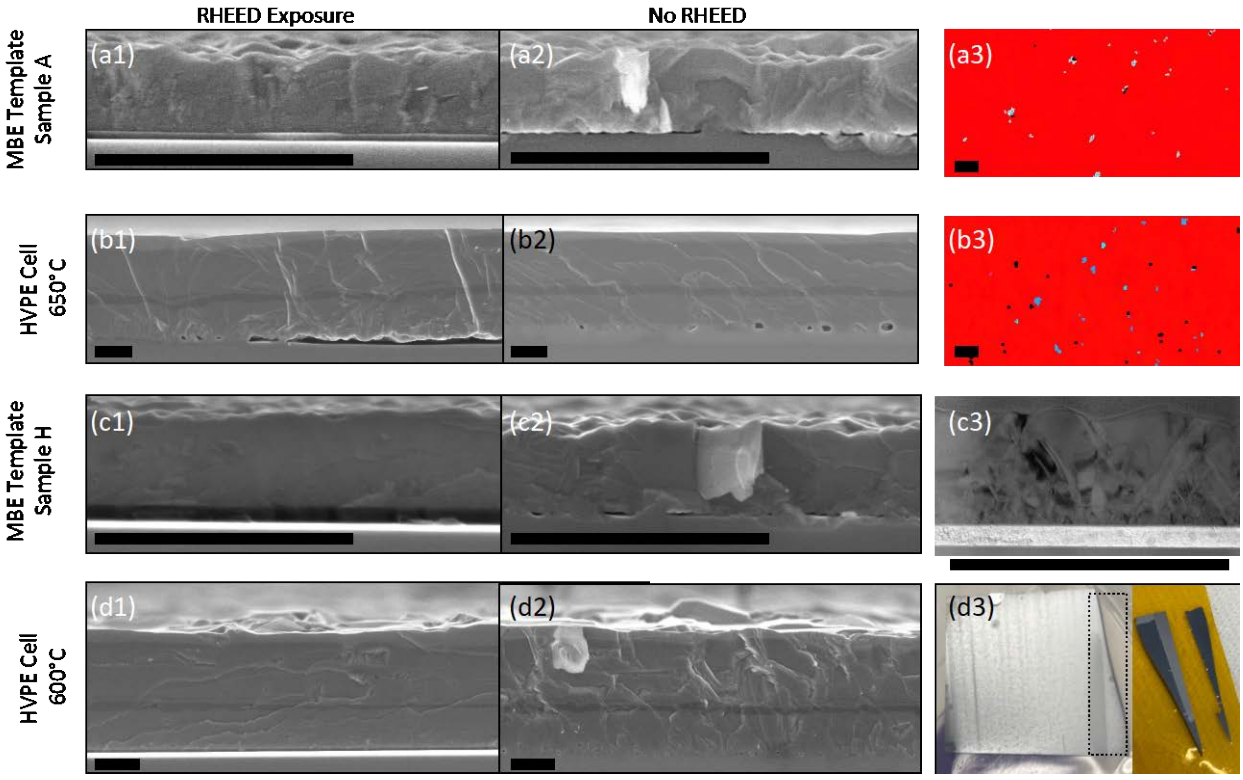

Figure 24: Cross section SEM images from (1) areas with and (2) without RHEED exposure during template growth. (a) Sample B (from Table 1) with (a3) plan view EBSD of the MBE-grown template. (b) HVPE cell grown on top of Sample B at 650°C, (b3) plan view EBSD of the HVPE-grown cell; (c) Sample H (from Table 2) with (c3) cross section TEM of the MBE-grown template. (d) HVPE cell grown on top of Sample H at 600°C, (d3) image of sample post HVPE-grown cell and region of sample that was removed and tested for liftoff using Kapton tape method. All scale bars are 1 μm

The solar cell device was grown on this sample using HVPE at 650°C. Additionally, because a standard recipe for growth on as-received GaAs wafers was being used, the sample was heated to and left at 650°C for 5 min to desorb the presence of any oxide on the surface. This temperature is 70°C hotter than the high temperature GaAs growth on NaCl layers that was performed exclusively using MBE. Cross section SEM images from areas with and without RHEED exposure both show significant changes in the morphology of the sample near what used to be the interface with the NaCl. In the regions where RHEED was exposed to the template, and there was a continuous NaCl layer prior to HVPE growth, fusion with the substrate is now observed along with wide pores (Figure 24(b1)). In areas where prior to HVPE growth there was no NaCl, but wide pores were observed, now only very small holes are seen, and most of the GaAs layer has fused with the substrate (Figure 24(b2)). Both areas show a darker contrast band corresponding to the InGaP etch stop layer; thus, the actual device portion of this structure lies above that line. The EBSD data shows a mostly-(100) oriented surface with {122} inclusions, similar to the template, suggesting that even the additional >3 μm of GaAs did not grow out the existing conclusions. Because of the lack of a NaCl layer these films were no longer able to be removed from the substrate.

The entire time the sample is at elevated temperature for the HVPE growth is ~20 minutes. Not shown but worth mentioning, is that after discovering this a separate template was grown via MBE and annealed *in-situ* at 650°C for 5 minutes. This sample also showed a transition in the interface morphology similar to the one observed during the HVPE growth. This suggested that it was the elevated temperature that was causing disappearance of the NaCl and increased fusion of the film with the substrate, not the HVPE growth chemistry or other conditions.

Knowing that the reason for the morphology changes for the HVPE growth at 650°C was likely due to temperature, a separate run was performed at 600°C. Additionally, because these samples are quickly transferred from one system to another and achieving continuous NaCl layers was more important that the defect density of the overgrown film at this point, the oxide desorb step was also omitted. The template layer chosen to discuss in this study is Sample H (Table 2 and Figure 20(d)). Cross section SEM images of the template layer (Figure 24(c1,c2)) are copied from Figure 20(d3,d4) so that they can be compared to the subsequent HVPE growth. Figure 24(c3) shows a cross section TEM image of the template layer prior to HVPE growth. Crystalline NaCl is observed beneath an epitaxial (albeit highly defective) GaAs film. Additionally, because this template was the basis for the epitaxial all-MBE cell (section 2.5.1, Figure 23(c)), we believed it would function as an ideal template for HVPE growth.

The cross-section SEM images after growth of an HVPE-cell on Sample G are shown in Figures 24(d1,d2). Now, in the areas where there was previously a continuous NaCl layer, the NaCl layer is still there. In areas where there was no NaCl, and just small voids, small voids are still seen. Thus, by lowering the temperature of the HVPE growth we were able to keep the continuous NaCl layers and achieve fairly smooth films. However, some large defects can be seen which will be discussed in the following Section 2.6. Figure 24(d3) shows an image of the cell after HVPE growth, which shows a similar silver-grey color to the samples with all-MBE grown cells shown in Figure 23, and vertical streaks from the manual scanning of the RHEED beam can also still be seen. The area marked by the dotted line was cleaved and used to rest for the ability to lift off the HVPE grown cell using the Kapton tape method. The right image shows the removed device (right) next to the substrate that was reattached to the tape face up (left). The portion of the sample that had the continuous NaCl layer was able to be removed easily from the substrate, but the area that was shadowed by the clip was not. No tests were performed on this sample to verify the crystallinity of the cell area, instead it was sent off for device processing. However, based on previous observations, it seems reasonable to suggest that because the same epitaxial template which yielded the epitaxial all-MBE cell was used, a similar result was achieved.

2.5.3. Section summary

Monocrystalline solar cell structures were grown on MBE-grown templates both by using MBE (without a vacuum break) and by HVPE (requiring transfer to another chamber). Areas that maintained a continuous NaCl layer were able to be removed from the substrate. These regions were all areas that were exposed to the RHEED beam during the deposition of the template layers. HVPE growth at 650°C resulted in disappearance of the NaCl, even in the regions where they were present in the template that was used. However, by lowering the temperature to 600°C the NaCl layers were maintained, and liftoff was enabled. The growth of a cell structure using MBE takes considerably longer than by HVPE, and this extended time at elevated temperature can cause some defects that will be discussed in the following section. Nevertheless, the growth of monocrystalline solar cell devices that were able to be nearly-immediately removed from the substrate is a promising result.

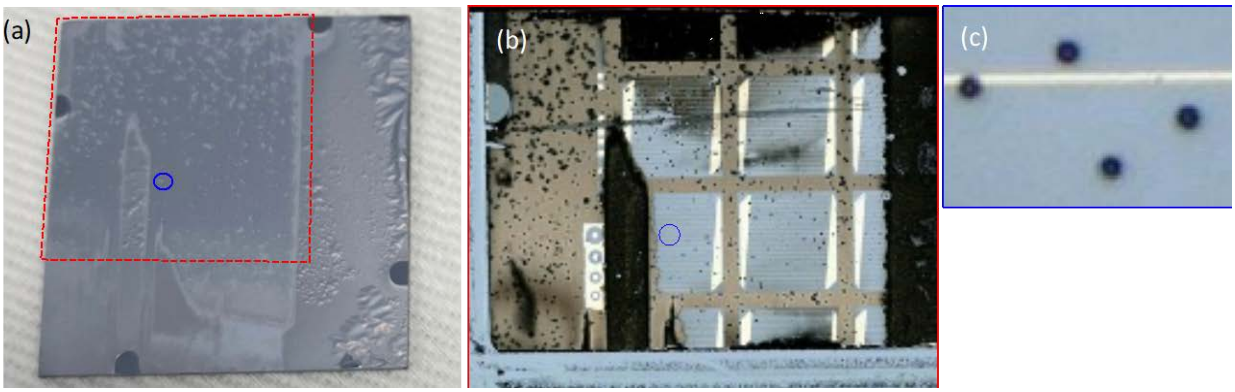

Figure 25: Images of (a) an as-grown all-MBE cell, (b) the fully processed device removed from substrate marked by the red area in the previous image, (c) and a magnified image showing hole present on grid line that is taken from the area marked by the blue circles.

2.6. Large-scale defects in GaAs growth on NaCl thin films

The work discussed up until this point has outlined the steps taken to achieve the growth of monocrystalline photovoltaic devices and subsequent removal of the device layers from the substrate. However, this section will highlight the difficulties that occur with fabrication of a full device. The propensity for the formation of holes in the overlayer film when exposed to elevated temperature results in electrically shorted devices. Here we will also discuss the possible formation mechanisms and the steps taken to reduce the density of these defects.

2.6.1. Observation and origins of hole-like defects

Devices grown either by MBE or HVPE were processed very similarly. To prevent dissolution of the NaCl, no post-deposition cleaning was performed. The process began by depositing a back contact consisting of 1/50/400 nm Ti/Au/Ag onto the top of the sample using a Temscal FC2000 e-beam evaporator. The metal-coated side of the sample was then mounted to a polished silicon handle using Loctite eccobond 931, a general-purpose epoxy which was cured on a hotplate at 120°C. The samples were then placed in deionized water for 5 minutes for dissolution of the NaCl layer. If this was not enough to facilitate liftoff, the samples were sonicated for 1-3 minutes. If no liftoff had occurred after 3 minutes, liftoff was initiated by pressing of a razor blade against the silicon/metal interface at approximately a 45° angle. The difficulty in removal of the substrate in these cases is due to the occasional fusion of the overlayer to the substrate that occurs with prolonged exposure of the stack to elevated temperatures. The GaAs template and pre-cell buffer layers were removed using a 2:1:10 volumetric solution of NH_4OH:H_2O_2:H_2O. For all-MBE cells, this etch was timed to expose the front contact layer. In the case of HVPE grown cells, the material was removed down to the InGaP etch stop layer which was subsequently removed using HCl to expose the front contact layer. Front grids were patterned using standard photolithography techniques. The Ni/Au front grids were electroplated using Watts Nickel and Transene TSG-250 Sulfite Au solutions. The Ni was plated at 2.15 mA/cm^2 for 30 s and the Au was plated at 2.15 mA/cm^2 for 120 s followed by 300 s at 4.30 mA/cm^2. Standard photolithograph was again used to pattern 5×5 mm mesas. A 2:1:10 volumetric solution of NH_4OH:H_2O_2:H_2O was used to remove the GaAs (and HCl for the InGaP if applicable) down to the back contact.

Figure 25(a) shows an image taken of an all MBE-grown cell. The area marked by the red box was exposed to RHEED and is the area of the sample that was chosen to be processed. In this area there are light contrast spots, a small area of contrast is marked by the blue circle. The areas to the right of the red square shows a large degree of delamination, which is also observable inside the area that was chosen to be processed because of the shadowing of the RHEED beam caused by the sample clip. The fully processed film is shown in Figure 25(b) showing 5×5 mm device mesas with contacts attached to a rigid Si handle. Many dark spots are visible in this image which closely correlate to the light spots in the previous image. Looking closer at the highlighted spot (Figure 25(c)) reveals a quartet of small holes near one of the grid fingers with the leftmost one enabling direct contact to the back contact.

The purpose of displaying this sequence of images is to show that these defects cause contrast variations in nearby areas which are visible by eye, even if they are too small to discern individually. These variations in contrast can be seen in images of other samples that had extended high-temperature growth sections (Figure 23, Figure 24). However, samples that were purely low temperature appear much more specular and even under Nomarski contrast imaging or plan-view SEM, there is little evidence of the formation of these defects or increased long-range roughness. Because growth of a device requires some elevated temperature, a closer investigation of these holes was performed.

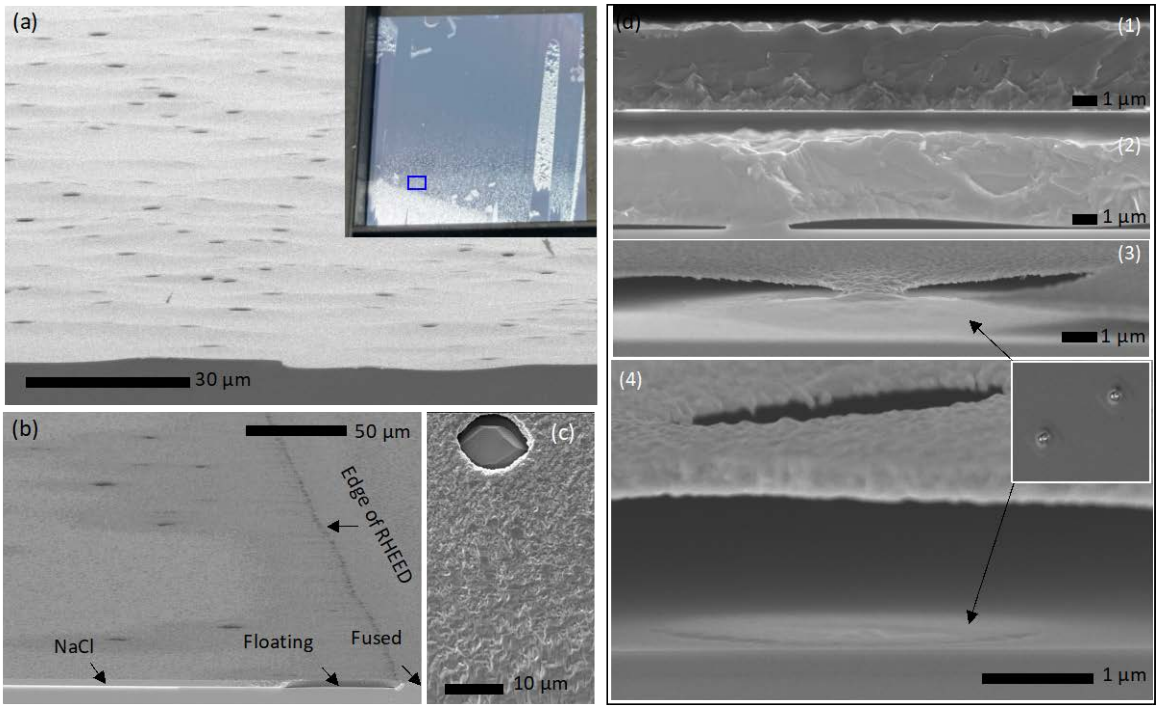

Figure 26: Images of holes in various samples. (a) tile view SEM showing an extremely high density of holes near the edge of the RHEED exposed area (inset). (b) title view SEM image near the edge of where the RHEED was shadowed by the sample holder clip with cleaved edge visible. (c) plan view image of a hole, (d) Different cross section SEM images showing (1) flat film with continuous NaCl, (2) area with no NaCl present, a small amount of bonding to the substrate, but no delamination, (3) area with fusion and delamination around the bonded area, (4) area where the film completely separated from the substrate; (inset) Nomarski image of a substrate after removal of the overlayer, the faceted areas are related to the shapes seen in (3) and (4).

Figure 26 shows images taken of several different samples and regions that have various stages of hole formation. Figure 26(a) shows a tilt view SEM image from the portion of the sample outlined by the blue box (inset). There is an extremely high density of holes in this area, being only tens of microns apart. The holes are all quite uniform in size at the top of mounds similar to a volcano. Looking at the inset, one can see that the density of holes this area is higher than the area near the top of the sample, and lower than the area near the bottom which has nearly delaminated completely. This change is directly related to the RHEED beam which comes in from the bottom of the sample. The area near the bottom left (which is nearly delaminated) was largely shadowed by the sample holder, and the delaminated streak near the right edge is from the clip shadow. It is worth noting that similar samples were grown with a 90° rotation after the RHEED exposure, and prior to GaAs deposition, and showed no directional dependence due to non-uniformities in the Ga or As flux. At the very least, any dependence on the impinging species (and thus local V/III ratio) was completely masked by the effect of the RHEED beam.

Figure 26(b) shows a tilt-view SEM image taken near the area where the RHEED was shadowed by the clip. The area on the right side of the image shows the top of the film where the RHEED was shadowed. The bottom shows the cleaved edge of the sample, and the remainder of the image shows the surface of the film exposed to RHEED. Looking at the cleaved edge, where the RHEED was shadowed, the grown material is fused to the substrate. Moving left, there is no NaCl, and the overlayer is floating above the substrate; this correlates with the darker contrast surface which surrounds the visible holes and spans the entire length of the border between RHEED-exposed and the RHEED-shadowed areas. This border also shows a high frequency of much smaller holes right at the interface between the fused and floating areas. Moving further left, the bright contrast at the interface between the film and substrate is NaCl, and the surface above this area is lighter than the areas surrounding the hole. Figure 26(c) shows a much steeper angle (nearly plan view) SEM image of one of the holes, and a change in surface roughness/morphology can be seen moving closer to the hole. Where the observable difference in contrast of the surface near the holes in the previous image is due to this difference in roughness, or something else like impurities is not known. But the width of the darker area (corresponding to a floating layer) from a hole is quite uniform within a single sample.

Figure 26(d) shows a series of images related to this fusion, floating, and delamination process taken from different samples and regions so that all parts can be seen. Some generalizations can be made from looking at many samples, which can be represented by these figures, and are outlined here:

(1) In areas where there is no fusion with the substrate observed there is a full NaCl layer. Said in another way, if there is a full NaCl layer, there is no fusion. This is the case for the majority of the RHEED exposed area in carefully controlled samples. These areas can be lifted off easily and completely.

(2) In the case of any amount of fusion of the overlayer with the substrate, there is no NaCl in the surrounding area, only voids. Areas where there is more frequent fusion, the voids are less-elongated, smaller, less frequent, or not observed (homoepitaxy), are deemed to be *fused*. Areas without frequent fusion, where the spacing between the film is <~1μm, are termed *floating*, such as in this figure. This represents areas near the border of sharp differences in the presences of RHEED, such as shadows created by the sample clip, or with samples that had very thin initial NaCl layers. These areas are sometimes able to be removed from the substrate but result in holes in the film or peeling of the substrate as will be discussed in Section 2.6.2.

(3) Where fusion has occurred at a single point and a hole in the film is present, the film begins to strongly peel away from the substrate. This case is not observed very frequently and lies between *fusion* and full *delamination.*

(4) *Delamination* occurs in the case when the film is no longer attached to the substrate in the near vicinity. No NaCl is observed in this region, and it is coupled with the presence of a hole. The presence of multiple holes often signifies large areas of delamination which occurs during growth (up to multiple millimeters, as seen in Figure 25(a)). This increase in large scale roughness is also coupled by a distinct darkening in the RHEED pattern during growth due to shadowing of the RHEED from the film itself.

The inset of Figure 26(d4) shows a Nomarski image of a substrate surface after removal of the overlayer. Faint square edges, aligned with <100> directions are observed around areas of fusion and can be seen to some degree in the SEM images as well. In the center of the square is a bright spot, likely part of the film that remains attached to the substrate, which will be discussed more in the conversation surrounding Figure 28. In the case of hole formation early in the growth, continued GaAs deposition can result in direct homoepitaxial growth through those holes, as seen in Figure 26(c).

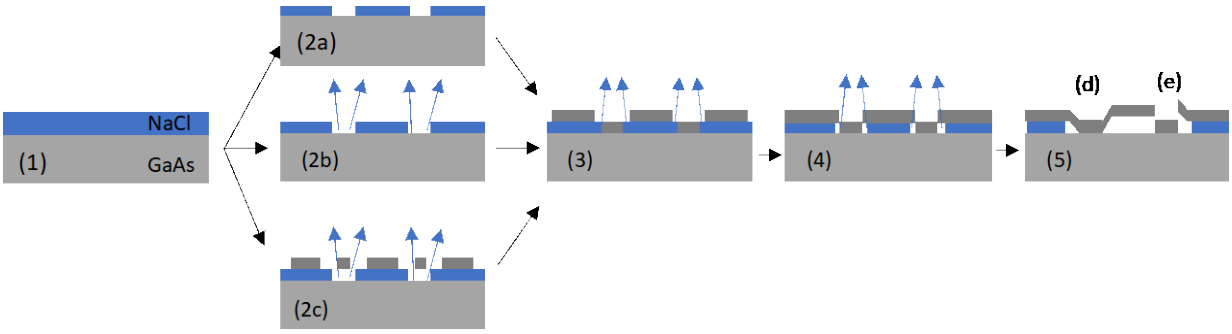

Figure 27: Proposed mechanisms of formation of the holes. (1) Starting with NaCl (blue) on the GaAs substrate (light grey), holes can form in the NaCl layer from (2a) existing pinholes in the NaCl growth, (2b) during the heating of the sample, of (2c) when depositing the GaAs overlayer (dark grey), in which case (2c.2) the islands that were once on the NaCl fall to the substrate. (3) further GaAs deposition results in areas with fusion and/or homoepitaxy. (4) NaCl continuously leaks out before the overlayer completely seals the NaCl which results in (5) (d) pockets of no salt near fused and/or near (e) delaminated areas

Using the generalizations presented above, possible mechanisms of formation of these holes, which are detrimental to the fabrication of a working device are proposed in Figure 27.

(1) The process starts with a NaCl (blue) film on the GaAs substrate (light grey)

(2) Holes form in the NaCl layer, which can be presented by three extreme cases:
   a. There are existing pinholes in the NaCl
   b. NaCl desorbs only during heating of the sample prior to GaAs deposition, exposing bare GaAs
   c. NaCl desorbs only during deposition of the GaAs film (dark grey)

(3) Further time and deposition results in GaAs islands falling to the substrate and/or direct homoepitaxy of GaAs all while any exposed NaCl continues to desorb.

(4) Prior to coalescence of GaAs, NaCl continuously leaves the substrate through the gaps between islands (especially during higher temperature growth). resulting in areas without

NaCl in close proximity to either islands that had fallen to the substrate or homoepitaxial areas.

(5) Coalescence occurs and the resulting morphology is dependent on the density of the gaps in NaCl, fusion of the GaAs overlayer to the substrate, and time spent at elevated growth temperatures
    d. Coalescence suppresses further NaCl desorption. The result is a fused location surrounded by an area where NaCl desorbed prior to coalescence.
    e. Additional time at high temperature, or a higher density of holes enables more NaCl to desorb between gaps and complete coalescence does not occur (such as Figure 26(d3). It is not known whether continuous flow of NaCl out of these holes prevents coalescence or if pressure of volatized NaCl builds up in the voids resulting in an eventual volcano like features that are observed in Figures 26(a,b). However prolonged time at elevated temperatures (even during continuous growth) results in an increase in the density of these volcano-like features.

A few more points of note regarding specific steps in this process are outlined here as well.

1. Regarding step 2: we know from previous sections that the NaCl actively desorbs at elevated temperature, thus holes are likely forming as a combination of 2b and 2c. Thus, the contribution from a 2a is less likely, especially with thicker NaCl layers.
2. Regarding step 3: while direct epitaxy could occur during the low temperature nucleation, fusion of islands that may fall onto the substrate does not occur until exposed to higher temperature.
3. Regarding step 5: The formation of a volcano seems to require the initial presence of a void, as it does not seem to happen spontaneously in areas that have continuous NaCl layers. However, perhaps this could occur with extended or higher temperature exposure, like observed in the HVPE growth at 650°C.
4. Regarding step 5: In regions where the distance that NaCl desorbs prior to complete coalescence is larger than the spacing between fused areas, holes are present and large area delamination occurs.

2.6.2. Reduction in the density of hole-like defects

Based on these proposed mechanism and observations discussed earlier in this section, the key to avoiding formation of holes in the removed films lies first with the ability to minimize the formation of holes in the NaCl layer and fusion with the substrate. This is a problem in itself, as fusion can result in ripping holes in the film as will be discussed later but is also the first step to formation of the volcano like defects which already present a hole. The first two things to be most important in this process are the thickness of the NaCl layer, and the time it takes to effectively create a coalesced film on the NaCl. It is worth noting here, that the RHEED patterns at the end of any growths discussed in this section were very similar to what was observed for the epitaxial templates discussed in previous sections, but detailed characterization of all samples was not possible.

Table 4 outlines the growth parameters for samples discussed in this section. All samples build on the structure of the MME template which provided the epitaxial all-MBE cell (Sample H, Table 3), with NaCl deposition at 150°C, manual RHEED sweep for As-adsorption, MME growth of n-GaAs at 350°C, and ~800nm of n-GaAs at elevated temperature (approximately the thickness of the buffer layer for the cell structure). A thicker elevated temperature step was made to give better estimation of how the material would behave with prolonged high temperature growth. Even

in the growth of a full cell structure (~2 hours) most significant changes in the RHEED pattern occurred within the first 20 minutes, which was still during the buffer layer growth. The changes usually observed were the reduction of any secondary spots and a darkening of the pattern, which correlate to improvement of the crystallinity (as mentioned in previous sections) and increase in large scale roughening/delamination/hole formation, respectively.

For each of these samples the As-valve position for the MME section was calibrated so that the transition from an As-rich surface to a Ga-rich surface occurred in ~5s. It must be noted that the growth rate noted in the table is the growth rate during co-deposition, and the real growth rate of MME is dependent on the shuttering sequence. For example, for Sample I in a single MME sequence the Ga-shutter is open for 5s and closed for 10s, and the co-deposition growth rate is 33 nm/min. Thus, growth only occurs for 1/3 the total time, so the effective growth rate is only 11 nm/min. Another example for Sample O, the co-deposition growth rate is 53 nm/min, and the Ga open and closed times are 45 and 10s, respectively, so the effective growth rate is ~43 nm/min.

Figure 27 shows Nomarski images of the surfaces of Samples H-N, with the primary variables being the NaCl thickness and the effective growth rate of the MME section. The result of decreasing the NaCl thickness (Samples I-K) is obvious. With a nominal NaCl thickness of 180 nm (Sample H, thicker than any samples discussed during or after Section 2.3.3), each dark spot is a single volcano-like defect (like Figure 26)

(d4)) with a density of ~122×10^3 cm^{-2}. Close inspection reveals that areas of delamination between some of these holes are connected. However, the regions between these volcanoes are flat and, based on additional SEM measurements (not shown), the GaAs overlayer is likely intimately interfaced with NaCl in these areas. Reducing the NaCl thickness to 90 nm (similar to previously discussed Samples E-H) results in a >4× decrease in the density (to ~28×10^3 cm^{-2}) of these defects. Because of this, the bridging of delamination between volcano-like holes is also significantly reduced, and the area interfacing NaCl is increased. Further decreasing NaCl thickness to 30 nm shows an additional 13.6× reduction in the density down to ~2083 spots cm^{-2}, nearly a 60× decrease in the density from Sample I. Additionally, a number of these observed defects are not full holes/volcanoes, and are still somewhat attached to the film, something closer to what is shown in Figure 26(d3).

Table 4: Growth parameters for samples focused on reducing the density of holes in the GaAs overlayer

	NaCl Deposition		MME Nucleation of n-GaAs at 350°C						High Temperature n-GaAs		
	Time (min)	Temp (°C)	MME cycles	Ga-open time (s)	Ga-closed time (s)	Real growth rate (nm/min)	Effective growth rate (nm/min)	Thickness (nm)	Time (min)	As/Ga	Temp (°C)
Sample I	60	150	24	5	10	33	11	66	24	1.68	580
Sample J	30	150	24	5	10	33	11	66	24	1.68	580
Sample K	10	150	17	5	10	33	11	100	24	1.68	580
Sample L	10	150	17	5	10	53	18	75	24	1.68	580
Sample M	10	150	17	5	10	53	18	66	24	1.68	580
Sample N	10	150	17	10	10	53	27	70	24	1.68	580
Sample O	10	150	17	45	10	53	43	80	24	1.68	580

The NaCl thickness obviously plays an important role in the formation of these defects. Thicker layers may cause more issues due to the increased amount of volatile material trapped below the GaAs surface, or increased strain. Regardless, thinner layers yield more promising results; however, further reducing the NaCl thickness results in difficulty achieving liftoff with these growth parameters. It must be noted that for Sample K the thickness of the MME layer was

increased to 100 nm, because when a similar 66 nm thick layer was used, lift off was not achievable. We hypothesize that this is due to holes forming in the NaCl during GaAs deposition and getting direct bonding to the substrate (Figure 27, step 3 & 5d).

To minimize NaCl loss during the GaAs deposition, the effective growth rate was increased first by simply increasing the Ga flux supplied during the Ga-open portion of the MME cycle. The As-valve position was still calibrated so that the surface transitions form As-rich to Ga-rich in ~5s, and the MME cycle times remained the same. However, the number of cycles was changed to more closely match the thicknesses in Samples I and J. Sample L was similar to Sample J, but with a 1.6× higher effective growth rate. With this higher effective growth rate, the density was reduced to 4323 cm^{-2} (6.5× lower). The features here seem to be a mixture of full and partial volcano-like defects. When combining this with thinner NaCl (Sample M) the density is further reduced to 417 cm^{-2}, a 5× decrease compared to the previous best (Sample K) and nearly 300× reduction compared to Sample I. No full volcano-like defects are observed in this case, only smaller partial-volcanoes with much smaller regions of delamination surrounding them. Additionally, the thickness of the nucleation layer in Sample M is the same as Samples I and J (thinner than Sample K), but still enables liftoff. Increasing the rate at which the NaCl is capped decreases the time the NaCl can desorb, thus minimizing the fusion with the substrate and subsequent defects, and still maintaining the ability to remove the overlayer.

In several growths that are not discussed, rapid roughening and spontaneous delamination of the overlayer was observed, directly through the viewport and by dimming of the RHEED pattern, during the growth of the high temperature section if the temperature crept up above 590°C. Thus, for subsequent samples, including Samples N and O, the high temperature section was held closer to 560°C rather than 580°C to keep this from happening. Further decreasing the temperature could help control the formation of these defects, but it may be at the cost of decreased crystallinity.

The effective growth rate was further increases for additional samples by increasing the time the Ga-shutter remains open. Because the As-valve position remained calibrated to give an As-rich to Ga-rich transition time of ~5s, this increased amount of Ga results in more Ga-rich growth conditions. For Samples N and O, the amount of time the surface is Ga-rich is approximately 5 and 40s, respectively. This contrasts with previous samples which had only a Ga-rich surface for a few moments. Sample N shows an increase in both the size of the defects and the density (to 1198 cm^{-2}). While most of the defects observed are partial-volcanoes, one full-volcano is seen in this image. Sample O further increases the effective growth rate to 43 nm/min (nearly 4× higher than the original case) and yields a defect density and characteristics identical to Sample L, although the surface between defects may be slightly rougher. The long shutter times for Sample O, are possibly more closely in line with traditional co-deposition than MME. So, according to observations in Section 2.3, it is possible that the crystallinity of this sample in particular could be worse.

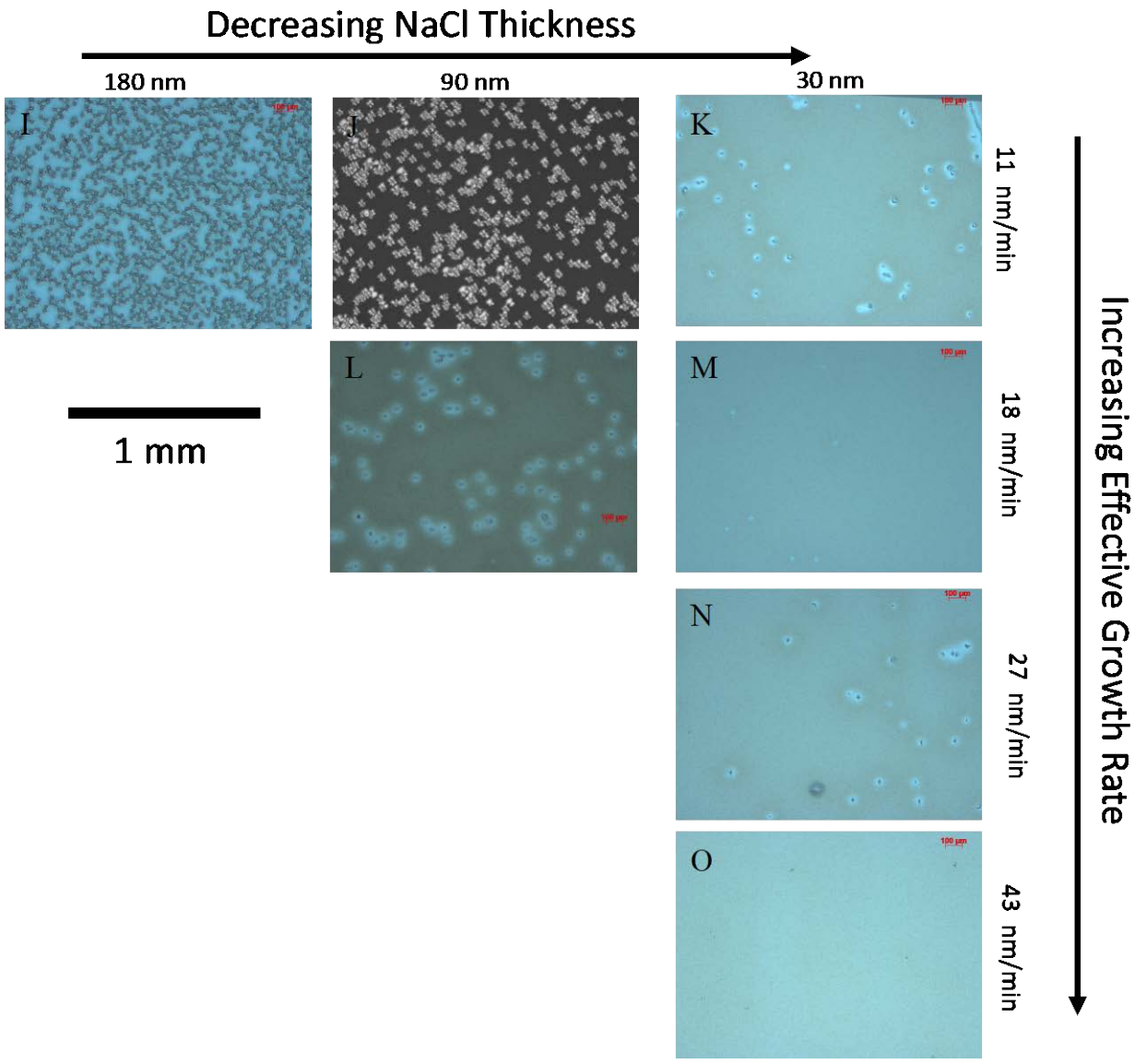

Figure 27: 5× Nomarksi images for the samples in Table 4 showing the effects of decreasing the NaCl thickness and increasing the effective growth rate. The scale bar pertains to all micrographs.

Improvements were also seen in the number of full-volcano defects when growing a device using the same template structure (Sample H) when comparing HVPE (Figure 24(d)) to MBE (Figure 23(c)). At the end of the template growth, volcano-like defects are already present, which are not healed during the growth of the MBE-cell. However, in the HVPE-grown cell, large-scale features of similar size are still observed, but they do not show delamination or holes. Despite the higher temperature used for HVPE (600°C) compared to MBE (580°C), the faster growth rate suppresses further hole formation and can even close off existing ones. Whether this is due to suppressed desorption of the NaCl or simply decreased time spent at elevated temperature is not known. However, the limited number of samples where HVPE-grown cells were attempted on templates that did not have these defects (thinner, exclusively low temperature GaAs overlayers)

did not lift off easily. Thus, more work is required to find the right overlayer thickness without increasing defect formation or sacrificing the crystalline properties for eventual transfer to HVPE.

The overlayer from Sample M was separated from the substrate using an epoxy bonding method to a rigid substrate without placement in water, and images of the film side that once interfaces the NaCl are shown in Figure 29. In this case, removal required insertion of a wedge between the substrate and film to facilitate separation. The low magnification image (Figure 29(a)) shows the entire 5×10 mm piece that was removed from the substrate; marks can be seen on the right side of the sample revealing damage from the wedge. Looking at the higher magnification images (Figures 29(b,c)) reveals a defect density that is $>1\times10^9$ higher than what Nomarski showed on the top surface (Figure 28(M)). The defects on the bottom surface are only hundreds of microns apart and have strong 90° angular features surrounding them, with edges parallel to <100> directions. It is worth repeating that the density of these features can vary significantly across a single sample because of the non-uniformity in the RHEED beam, as was seen in the inset of Figure 26(a), which makes careful quantitative analysis difficult.

Most of the square features are 30-50 μm and have one or two different features in the center: a hole in the removed film and/or a piece of the substrate attached to the removed film, marked by black and white arrows, respectively. This sample is roughly equivalent in thickness as buffer layers for the devices discussed in the previous section processing a device, which would be etched away. But both features provide difficulties with processing a working device and are obviously detrimental to the direct reuse of the parent wafer. In the case of the holes in the lifted-off film, this means the substrate has a piece of the film still attached. This is what is observed on substrates when removing the film using the Kapton tape method, as direct bonding of the film to the substrate is stronger than the "bonding" of the tape to the film. Using the epoxy bonding method results in a very strong bond to the film, and when forcefully removed can pull pieces of the substrate off, leaving small pits in the original wafer. It is possible that improvements in the latter can be made through working on the transfer method.

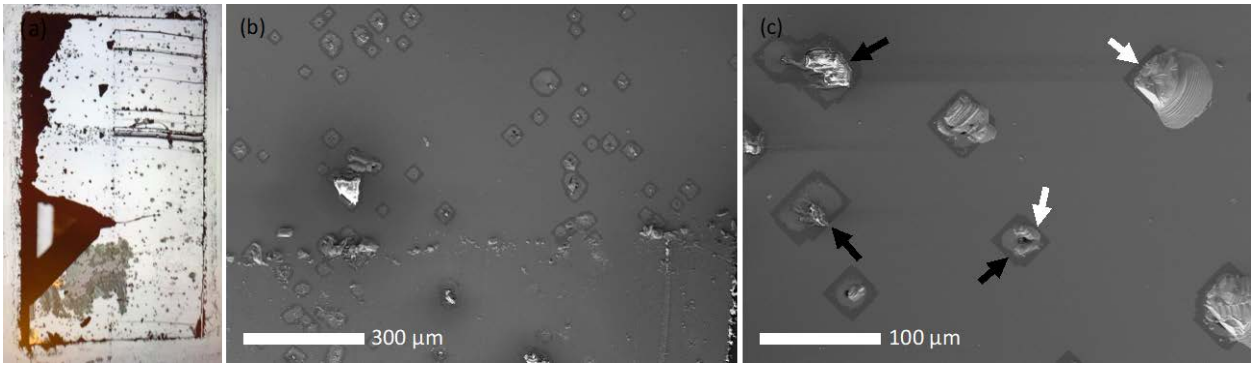

Figure 29: (a) Optical microscopy and SEM images at (b) 100×, and (c) 300× magnification of the film from Sample M removed from substrate using epoxy bonded technique without submersion in water. Black and white arrows mark holes in the removed layer and portions of the substrate attached to the removed layer, respectively

2.6.3. Section summary

Substantial reductions in the large-scale defects which hamper the fabrication of working devices can be achieved through engineering of the template layer. While variables such as growth

rate and salt thickness were shown to play an important role, additional things which are harder to quantify also made a difference. The rate at which the NaCl is heated to the deposition temperature of GaAs was chosen to be 20°C/min for all samples in this section. However, the actual time taken to actually heat to this temperature (350°C for Samples I-O, and other samples not discussed here) ranged from 14-18 minutes. This discrepancy is largely due to delays at low temperature, but when the total deposition time is comparable to the variation in heating time, and the NaCl layer is uncapped, it is impossible to discount this completely. On a similar note, to avoid any delay in capping of the initial exposed NaCl, the GaAs nucleation started as soon as the target temperature was reached, resulting in eventual increases of 10-25°C, throughout the course of the low temperature growth. Growth temperature oscillations of ±10°C were also seen during the longer high temperature growth step, could also cause inconsistencies.

However, the hardest thing to control completely, is consistent sweeping of the RHEED beam during the As-adsorb step at low temperatures. The variation within a single sample due to non-uniformities in the manual sweeping process is clearly apparent, so there are affects between samples. Within a single sample these variations were eventually minimized by stepping the RHEED in very small increments (across the sample perpendicular to the RHEED beam), watching the phosphor screen directly for complete dimming of the diffraction pattern at each step, and incorporating movement of the beam in the direction parallel to the RHEED beam. As was discussed in previous sections, the presence of the RHEED beam is crucial, but exactly what is happening is not fully understood. By employing a separate electron flood source designed for large area irradiation and better dosage control large improvements could be made in the uniformity, reduction in defects, and ease of investigation.

3. Final Discussion and Conclusion

3.1. Discussion of the effects of exposure to the RHEED beam

The RHEED effects of only three samples of GaAs on NaCl are shown in the previous section, but a large number of samples (>200, listed in Section 5.1.3) have been systematically grown and analyzed including some that deposit Ge directly on NaCl surfaces (Section 5.1.1). They reveal that the effects of RHEED are quite complex, and neither exclusively beneficial nor detrimental. Some general observations and conclusions are outlined below:

(1) The presence of RHEED roughens NaCl. This effect is likely reduced with reducing the accelerating voltage, but then the pattern is too dim to be interpreted. This effect also seems to be more pronounced at higher temperatures i.e., at 15 kV it takes ~180s for the RHEED pattern to transition from streaky to spotty at 300°C, but at 150°C even after exposure for significantly longer times the RHEED is unchanged. Previous reports have suggested that the electron beam results in dissociation and desorption of the NaCl.[6,15] This could also be why imaging bare NaCl layers under highly focused electron beams in SEM and TEM results in the changes and destruction of the NaCl discussed in Section 2.2. Unfortunately, most other *ex-situ* techniques to look at more subtle changes between areas with RE cannot be used on bare NaCl films because the NaCl degrades appreciably in the presence of water vapor, even in the amount present in the air.

(2) RHEED and delamination. The presence of the RHEED sometimes causes delamination. This is most frequently observed at the edges of the RHEED exposed areas. For samples with deposition temperatures >350°C, the area with RE shows a complete NaCl layer beneath a GaAs overlayer, while the area with NRE shows frequent fusion to the substrate. Delamination is somewhat obviously not observed in areas that have frequent fusion to the

substrate, but it is also never observed in the regions that have a complete NaCl layer. However, at the transition between these two regions, the film is occasionally observed to be pulling away from the substrate; there is no NaCl and the fusion to the substrate is less frequent. For samples which use the As-sweep technique, this is thought to occur because this transition region only somewhat protects the NaCl due to less enhanced GaAs nucleation compared to areas with longer, more deliberate RE. Thus, this area has larger islands, which the NaCl sublimates out from underneath during prolonged high temperature steps, resulting in larger voids. This is especially true for films with thin nucleation layers heated to high temperatures for thicker (>300 nm) high temperature grown layers. This effect is also observed in the case with prolonged RHEED exposure. But in this case, it could be the result of the RHEED roughening the film, discussed in the previous point, to the extent that holes are formed completely though the NaCl layer, which allows for less frequent fusion of the overlayer to the substrate and subsequently delaminates.

(3) Excessively long RHEED exposure times do not enhance crystallinity of GaAs. While some beneficial effects may be gleaned from selective exposure, prolonged exposure never seemed to give desirable results. This could be due to surface roughening or related to the higher degree of polycrystallinity observed in areas with RE. Constant exposure during the GaAs deposition resulted in a more polycrystalline material and sometimes spontaneous delamination of the film during growth.

(4) The presence of RHEED enhances As-adsorption. As discussed in section 2.3.1.c.ii, arsenic preferentially condenses where the RHEED beam is present. The reason is not fully understood, but it is possible this is from a slightly rougher surface facilitating nucleation points, or from a change in surface charge promoting adhesion of As adatoms. As the temperature is increased, this amorphous As layer has to desorb before the NaCl surface atoms can, so in some way it can protect the NaCl at elevated temperatures. However, they both begin to desorb at similar temperatures, so the impact is limited. Related to the previous points, if the bare NaCl is exposed to the RHEED beam for too long the overlayer tends to delaminate from the substrate.

(5) The presence of RHEED promotes nucleation of GaAs on NaCl. This seems to be true not just during the actual nucleation step, but even exposure prior to opening the Ga shutter with the As adsorption. It is not known whether this is due to slight roughening of the NaCl or from the actual As-adsorption itself as it may not necessarily be fully desorbed by the time the Ga shutter is opened. However, this enhanced nucleation rate is one of the key benefits of RHEED for the formation of higher quality GaAs films on NaCl because swift formation of a complete GaAs layer is crucial to enable higher temperature depositions without sublimation of the NaCl layer.

(6) RHEED affects the crystallinity of GaAs grown on NaCl using traditional co-deposition techniques. In the cases discussed above it is possible that RHEED (or at least the As adsorption) is a cause of the highly textured GaAs overlayer because RE areas have more of the {322} grains than areas that are not exposed. For some samples such as the one where GaAs was deposited continuously from 250-580°C (Figure 7(c)), EBSD revealed that areas with RE showed grain sizes >5 μm, while the grains in areas with NRE were only a few hundred nanometers. However, there were no grains oriented commensurate to the underlying substrate or NaCl layer in either area. This could be related to previous studies on electron beam annealing of amorphous GaAs,[16,17] but these studies were done with much higher accelerating voltages.

3.2. Thoughts for the future

By the end of this project, monocrystalline templates and photovoltaic devices were achieved, and successfully removed from the substrate. However, because the bulk of the work in this project was focused on achieving single crystalline GaAs templates, no information on the density of other defects (such as threading dislocations) was obtained. Additionally, the large-scale defects which inhibited the fabrication of working devices, need to be addressed. Looking back, there are many things for this material system that were not able to be explored (fully or sometimes even at all) during this project which could be fruitful for future work to address the outstanding issues.

3.2.1. With existing equipment

There are several things that could benefit from additional study, both in an effort to achieve working devices, through reducing the density of defects (large-scale and small), and to understand interesting scientific phenomena. Several directions that can be explored without needing to buy or install additional equipment are outlined below:

Improving the MBE templates:

1. *Incorporation of additional atomic species*. Limited work was done on the incorporation of Bi in the low temperature GaAs nucleation layer. However, this work was only done prior to achieving monocrystalline templates. A thin layer of Bi is known to act as a surfactant, enhancing adatom mobility and improving surface roughness. Even with the addition of Bi, the previous work still resulted in three-dimensional island growth. Combining Bi with the existing procedures that gave epitaxial material that may help with achieving faster coalescence of smoother films to reduce the large area defects. Through the addition of Bi, the lattice constant of the material is also increased, so it is possible that higher quality material (with regards to lower threading dislocation density) could be achieved. Something that was not explored was the addition of In or Al to the GaAs nucleation layer. Growth of InAs on GaAs also shows formation of a wetting layer which could be favorable if something similar forms on NaCl. The addition of In would also increase the lattice constant and, being more stable at high temperatures than GaAsBi, could be grown at higher temperatures, not just nucleation.
2. *Growth rate (real and effective).* While an increased growth rate was shown to be a promising direction in Section 2.6 for reducing the volcano-like defects, the effects on surface roughness and crystallinity were not thoroughly investigated. Additionally, further space exists to explore the differences in changing the effective growth rate using MME or other shutter pulsing techniques and compared to increased Ga-flux in a usually As-limited growth window. This also ties into the next point regarding the As/Ga ratio and combining with the high growth rates that could be offered in HVPE.
3. *As/Ga ratio*. The As/Ga ratio is necessarily quite transient in the MME (and MEE) growth procedures and could use a more thorough investigation. Most co-deposition growths at low temperature were concentrated around a As/Ga ratio of 1 erring on the side of As-rich. However, the MME scheme showed promising results (at least with regards to the large-scale defects) operating while in or near a Ga-rich regime.
4. *Substrate cleaning*. All substrates employed in this study were used as-received. SIMS measurements showed the incorporation of impurities during the growth of low temperature growth of GaAs on NaCl, such as Ca and O, which should not be present in the chamber along

with elevated amounts of Na and Si. Similar results were also seen in growths of low temperature GaAs, where Na and Si should not be in the chamber either. These impurities seem to float on the surface and are only incorporated in the growth of poor-quality GaAs. Because the GaAs nucleation is the poorest quality (because of the material mismatch as well as temperature), it is possible that high amounts of impurities could be incorporated thus impacting the nucleation dynamics, coalescence, and crystallinity.

5. *Cycled NaCl deposition*. An alternative method that may also provide some degree of cleaning the surface is to grow a NaCl layer >10 nm at low temperature (such as 150°C) and then heat the substrate to desorb the NaCl. Another GaAs buffer layer could be grown at normal 580°C conditions as well. This is related to the previous suggestion, as it might clean the surface, in select growths where NaCl was deposited and desorbed multiple times, the RHEED pattern when returning to high temperature was slightly brighter than it was previously. A slightly different method would only desorb some of the NaCl and then deposit more NaCl either at this higher temperature or after cooling back down to lower temperature. Because of differences in the lattice constant due to thermal expansion, there could be interesting effects of depositing NaCl at different temperatures, which may be more related to multiple salts, to be discussed in Section 3.2.3.
6. *Substrate miscut and orientation*. Substrate miscut was also a variable that was also explored, but only prior to discovering a procedure that yielded monocrystalline material on GaAs (100)±0.1° substrates. There were differences between samples using miscut up to 10°, but because the samples were not monocrystalline, it is possible that the differences are just due to local fluctuations in crystalline texture or grain size. However, this would be something worth revisiting with the conditions known to give epitaxial GaAs overlayers on NaCl thin films. Because there are symmetry differences between GaAs and NaCl, similar to growth of GaAs on Ge or Si, if the step edges were maintained through the NaCl layer a miscut could be useful in the suppression of antiphase domains and possibly yield in better coalescence of islands if they similarly oriented.
7. *Ultra-thin low temperature GaAs*. As a method to enhance nucleation of GaAs beyond just RHEED, doing a very short deposition of GaAs at low temperature could yield more closely spaced nuclei. This could be a sub-monolayer deposition, or because of the Volmer-Weber growth mode will result in islands anyway, just a very small amount which would act as seeds for further intermediate temperature (such as 350°C) GaAs deposition. However, if this layer is too thick it will likely cause a reduction in crystallinity.
8. *Ramp rates between sections after NaCl*. Mentioned as a possible source of discrepancies in Section 2.6.3, this is another thing that could be investigated as a potential method to reduce the number of holes in the NaCl, subsequent fusion of the GaAs to the substrate and formation of the large-scale defects. Only ramp rates of 20°C/min were used, except for a select few samples in the early portion of the project. A balance must be struck when increasing the temperature. Initializing the increase in temperature too quickly results in overcompensation of the heater, and rapid desorption of the NaCl layer, even at lower "real" temperatures. Additionally, a faster ramp rate often results in overshooting the target temperature more, subsequently attempting to nucleate GaAs at higher temperatures (which is slower) with higher NaCl desorption. Ramping the temperature too slowly results in prolonged times required to reach the desired temperature. While there is no overcompensation from the heater at low temperatures and less overshoot of the desired nucleation, the total amount of time spent above a temperature where NaCl is desorbing is higher when ramping more slowly. The ramp rates

before and after the GaAs nucleation do not have to be the same, and higher/lower rates could be used for different sections depending on the needs of that section.

9. *RHEED effects*. Throughout this entire project, we constantly learned new ways that the RHEED affected the growth of GaAs on NaCl. While careful studies are hard to do with existing setup (refer to section 3.2.2 for details on an electron flood source), effects have been observed, but are still not well understood. Combining the RHEED with other atomic species (like listed in (1)) could have additional outcomes.

For templates transferred to HVPE:

10. *Improvement of original template*. The results of HVPE-grown cells could undoubtedly be improved through refinement of the MBE-grown template. Because the volcano-like defects which are detrimental to device fabrication seem to be realized most during the high temperature MBE step, developing a way to do an exclusively low-temperature MBE-grown designed specifically for transfer to an HVPE system. Previous samples testing this were unable to be removed from the substrate, so figuring out where the NaCl is going during this process must be understood. The surface is free from holes prior to transfer, but perhaps because the low temperature templates consist of thinner films, holes develop upon heating in the HVPE chamber or during the early stages of growth. Maybe this is tied to the rate of temperature increase as mentioned in (8).
11. *Amorphous As cap prior to transfer*. The only HVPE-grown cells that were successfully removed from the substrate were grown at 600°C and omitted the oxide desorption step at 650°C. However, the formation of an oxide between transfer of bare GaAs and even the propensity for contaminants on the surface are unavoidable. However, the template could be capped with an amorphous As layer, which would be removed upon heating to ~325°C. This layer would protect from the formation of a surface oxide and keep the GaAs surface clean for subsequent growth.
12. *Lower temperature growth*. Finally, HVPE growth occurs at higher temperatures compared to MBE, and as the previous sections all discussed, elevated temperatures cause issues in this system. If the growth temperature of HVPE could be lowered, even at the cost of a slight reduction in growth rate, better results may be achievable. Or at least initially capping the MBE template with a thicker lower temperature HVPE grown material before growing a buffer layer at more ideal conditions.

There is a scanning tunneling microscope (STM) connected *in-vacuo* to the MBE chamber which could allow for answering of some interesting questions pertaining to the NaCl layer, which is temperamental when it comes to *ex-situ* experiments.

13. *Look at NaCl surfaces with STM*. The surface structure and crystallinity of bare NaCl layers and nuclei grown on GaAs could be investigated. This could be coupled with growth on different GaAs surface reconstructions, to see where the other orientations discussed in Section 2.1.2 come from. Additionally, one could investigate what actually happens to the NaCl layer upon exposure to the RHEED beam, after As-condensation at low temperature, and after desorption of the amorphous layer. Is the NaCl surface after As condensation and desorption the same as it is with RHEED exposure without As? A closer investigation of the GaAs nuclei on NaCl layers could also be done to see if there are preferential locations or features for nucleation of GaAs islands.

3.2.2. Wide area electron irradiation source

While currently using the RHEED as a diagnostic tool and an important piece of the growth parameters, it is impossible to separate the effects of an electron beam with the *in-situ* characterization. If a main goal of future work in this area is to achieve devices, a commercially available electron flood source would be required. This would allow for uniform irradiation over areas large enough to fabricate a device. Additionally, being able to have precise dose control would enable more quantitative studies on the effects of an electron source.

3.2.3. Double Ionic Salt Heterostructure (DISH)

The work done to achieve GaAs growth on thin NaCl films has inspired an idea using a highly lattice mismatch double-ionic-salt-heterostructure (DISH) to enable growth of III-V materials on large area Si wafers, as well as reuse of the parent Si substrate. The area of DISHs is still relatively unexplored. It is known that lattice matched semiconductors will grow epitaxially, with limited formation of extended defects, and that lattice mismatched semiconductors (such as GaAs on Si) is extremely difficult, and results in the formation of many extended defects. Epitaxial growth of nearly lattice matched LiBr on Si (1.1% lattice mismatch) has been observed previously,[4] as has NaCl on GaAs ((100) surface) (<1% lattice mismatch) as shown in this report. Unsurprisingly, deposition of ionic salts on highly lattice-mismatched semiconductors, such as KBr on GaAs ((100) surface) (+16% lattice mismatch), is not epitaxial. However, with the prior deposition of a lattice matched salt the second highly lattice mismatched can be epitaxial. This was shown with the demonstration of an epitaxial and fully relaxed 2 nm KBr film on GaAs by inserting a 2 nm NaCl layer.[5] In other words, within 4 nm of material the lattice constant was changed from 5.65Å to 6.60Å. This project would attempt to utilize a DISH consisting of Si/LiBr/NaCl/GaAs. The growths of Si/LiBr and NaCl/GaAs have both been demonstrated but combining the unique relaxation properties of ionic salts to grow GaAs on Si in this way has not been shown. How the upper ionic salt is grown, bonds, and relaxes with respect to the lower materials is important to understanding what types of defects will be present in future overlayers. There are no reports in the literature of growth of lattice matched semiconductor material on a DISH, which would permit growth and liftoff of highly mismatched materials.

Developing the understanding of the deposition and defect characteristics in highly mismatched ionic materials could lead to technology allowing for integration of III-Vs with Si, substrate recycling, and thinner wafer templates and devices. By using separate ionic salts with tunable lattice constants, this project could have implications such as:

- Reusable substrates → reduce this cost in multiple technologies
- Templates of composition-tailored ternary compounds ($In_xGa_{1-x}As$, $Al_xGa_{1-x}As$, etc.) or binary compounds (InP, InSb, etc.) which do not exist or are fragile
- Ultra-thin template layers → reduce material and energy waste of typical bulk substrates
- Scale III-Vs to 450 mm → enable large area III-V growth
- III-V integration with Si → beyond renewable energy

3.2.4. High-temperature stable salt

Many of the issues in this project are a result of the high vapor pressure of NaCl, and low thermal stability. Using a different salt, which could have a lower solubility in water, that is more stable at temperatures conducive to GaAs growth it might be worth studying. If incorporated into a DISH, mentioned in Section 3.2.3, the lattice matching conditions may not be as strict. Additionally, incorporation of another atomic species in the semiconductor material may also

allow for a more finely tuned lattice matching condition with a bit of flexibility around the higher thermal expansion coefficients of ionic salts and desired growth temperatures.

4. REFERENCES

[1] K. Saiki, A. Goda, and A. Koma, Japanese Journal of Applied Physics, Part 2: Letters **36**, (1997).
[2] K. Saiki, Y. Nakamura, and A. Koma, Surface Science **269**, 790 (1992).
[3] N. Nishida, K. Saiki, and A. Koma, Surface Science **304**, 291 (1994).
[4] K. Saiki, Y. Nakamura, N. Nishida, W. Gao, and A. Koma, Surface Science **301**, 29 (1994).
[5] Y. Nakamura, K. Saiki, and A. Koma, Journal of Vacuum Science & Technology A: Vacuum, Surfaces, and Films **10**, 321 (1992).
[6] F. Cosandey, Y. Komem, and C.L. Bauer, Thin Solid Films **59**, 165 (1979).
[7] F. Tang, T. Parker, G.C. Wang, and T.M. Lu, Journal of Physics D: Applied Physics **40**, (2007).
[8] A. Ichimiya and P. Cohen, *Reflection High Energy Eelctron Diffraction* (Cambridge University Press, 2004).
[9] E. Kneedler, B. Jonker, P. Thibado, R. Wagner, B. Shanabrook, and L. Whitman, Physical Review B - Condensed Matter and Materials Physics **56**, 8163 (1997).
[10] T.H. Myers, A.J. Ptak, B.L. VanMil, M. Moldovan, P.J. Treado, M.P. Nelson, J.M. Ribar, and C.T. Zugates, Journal of Vacuum Science & Technology B: Microelectronics and Nanometer Structures **18**, 2295 (2000).
[11] B.L. Vanmil, A.J. Ptak, N.C. Giles, T.H. Myers, P.J. Treado, M.P. Nelson, J.M. Ribar, and R.D. Smith, Journal of Electronic Materials **30**, 785 (2001).
[12] R.C. Myers, B.L. Sheu, A.W. Jackson, A.C. Gossard, P. Schiffer, N. Samarth, and D.D. Awschalom, Physical Review B - Condensed Matter and Materials Physics **74**, 1 (2006).
[13] B.J. May, J.J. Kim, P. Walker, H.R. Moutinho, W.E. McMahon, A.P. Ptak, and D.L. Young, ACS Omega **in-prep**, (n.d.).
[14] B.J. May, J.J. Kim, P. Walker, H.R. Moutinho, W.E. McMahon, A.J. Ptak, and D.L. Young, Journal of Crystal Growth **in-review**, (n.d.).
[15] A. Friedenberg and Y. Shapira, Surface Science **87**, 581 (1979).
[16] M.W. Bench, I.M. Robertson, and M.A. Kirk, MRS Proceedings **235**, 27 (1991).
[17] X. Yang, R. Wang, H. Yan, and Z. Zhang, Materials Science and Engineering B **49**, 5 (1997).
[18] S. Sharma, C.A. Favela, S. Sun, and V. Selvamanickam, Conference Record of the IEEE Photovoltaic Specialists Conference **2020-June**, 0744 (2020).
[19] A.J. Shuskus and M.E. Cowher, *Fabrication of Monocrystalline GaAs Solar Cells Utilizing NaCl Sacrificial Substrates* (1984).

APPENDIX

4.1.1. Deposition of germanium on NaCl

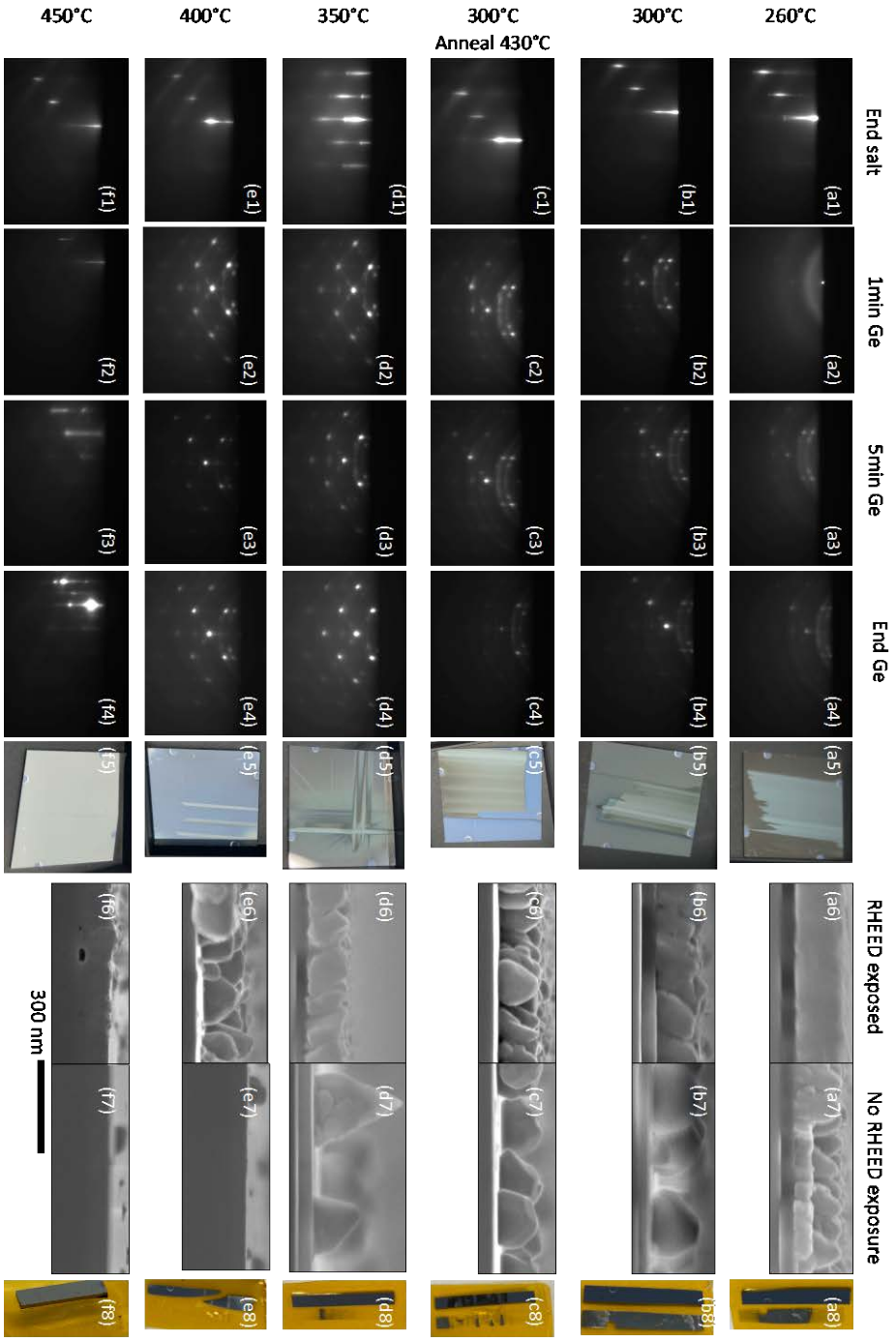

Figure 30: 20-minute Ge depositions on NaCl films on GaAs substrates with deposition beginning at 150°C and continuously until the Ge nucleation is started. (a) ~20min total salt followed by Ge deposition at 260°C, (b) ~23min total salt followed by Ge deposition at 300°C (c) ~23min total salt followed by Ge deposition at 300°C and annealed at 430°C for 5 minutes (d) ~24.5min total salt followed by Ge deposition at 350°C (e) ~49min total salt followed by Ge deposition at 400°C (f) 83 min total salt followed by Ge deposition at 450°C. RHEED images taken at (1) the end of NaCl deposition, just prior to (2) 1 minute into, (3) 5 minutes into, and (4) at the end of Ge deposition. (5) Images of the samples after removal from the chamber showing streaks from the presence of the

RHEED beam throughout growth. (6) Ge films attached to Kapton tape after removal from the substrate via placement in water (lower) and the GaAs substrate (upper). Cross-section SEM images of areas (7) with RHEED exposure and (8) without RHEED exposure (scale bar is the same for all images)

The deposition of elemental Ge on NaCl thin films on GaAs substrates was also investigated because Ge has a similar lattice constant to NaCl and GaAs, but since it is only a single atomic species, there are no added complications with stoichiometry, flux-matching, or overpressures of another volatile species which could affect the growth mode. GaAs films have also been demonstrated on NaCl films previously with the use of Ge interlayers.[18,19] A similar growth scheme as outlined in Figure 8 is used. NaCl was deposited at low temperatures for a t_{NaCl} and continuously for an additional t_{ramp1} before T_{GaAs1} was reached. Then once the temperature stabilized, Ge was deposited for 20 minutes. The sample was cooled immediately after Ge deposition. A series of growths was performed varying the T_{GaAs1} of Ge from 260-450°C and analyzed using RHEED (along a [110] direction) and cross section SEM. The very clear discrepancy in areas with RHEED exposure (WRE) and areas with no RHEED exposure (NRE) in this simpler growth system was where we realized the importance of the presence of an electron beam.

For the sample with T_{GaAs1}=260°C (Figure 30(a)) the NaCl pattern prior to deposition is still bright and streaky. Upon opening the Ge shutter the pattern quickly dims and after 60s (Figure 30(a2)) the pattern shows diffuse rings meaning the film is highly polycrystalline. After 5 minutes, the wide blurry rings begin to give way to more discrete rings and spots (Figure 30(a3)); but with more time the pattern does not change, except for an overall slight dimming. The initial nucleation is likely highly polycrystalline, and at these low temperatures possibly somewhat amorphous as well, and although further deposition seems to suggest a more crystalline layer, the grains are very small and randomly oriented. The 5th column shows images of the sample after removal from vacuum, and here the RHEED exposed area can be seen clearly in the central region. Cross section SEM for areas with RE and with NRE are shown in Figures 30(a6 and a7), respectively. The area WRE shows the darker NaCl film completely covered by a dense Ge film. In the area with NRE there is still a NaCl layer of similar thickness. However, the Ge overlayer, while still mostly covering the NaCl, is very rough with significant variations in height. One thing that was not mentioned in the main text as it is outside the scope of this work is the ability of the NaCl to function as a water-soluble release layer. The final column of this figure (Figures 30(a8-f8) shows a piece of the sample that was cleaved off and had the Ge attached to Kapton tape. The substrate and tape were submerged in water, where the NaCl would rapidly dissolve allowing for near-immediate removal of the Ge overlayer. Figure 30(a8) clearly shows the central (area WRE) lifted off. The edge areas are less dark because the thickness of the Ge is still transparent, but this region also lifted off.

Similar growth and analysis of a sample with T_{GaAs1}=300°C was performed (Figures 30(b)). The starting NaCl is similar to the previous sample, but the initial Ge deposition no longer shows blurry rings. Instead, the pattern is very spotted with more discrete rings. Thus, when grown at this temperature the Ge has a higher degree of short-range ordering. Further growth results in dimming of the rings and the shadow spots, while the primary spots (which would match up with NaCl) become brighter (Figure 30(b4)). This suggests that with further growth a more textured film is being achieved, and with further growth maybe even something approaching single-crystalline could be achieved. Because it would be nucleated on material consisting of multiple orientations, it would likely have a high defect density. Again, looking at the sample after removal from the chamber the area WRE can be clearly differentiated in the center (Figure 30(b5)).

Cross section SEM shows that the film in the central area WRE is not quite a cohesive film, and although the thickness is similar to the previous case, there is the appearance of discrete columnar islands. In the area with NRE, the islands are much more discrete and further apart. But again, with continuous NaCl layers beneath, the tape peeled easily from the substrate either with or without placement in water and the Ge can be seen still stuck to the tape (Figure 30(b8)).

The previous sample is repeated again, except with an additional anneal at 430°C for 5 minutes in an effort to coalesce islands and achieve more crystalline material (Figures 30(c)). Unsurprisingly, the first three RHEED patterns look nearly identical as the growths are identical up until this point. However, the pattern after the annealing (Figure 30(c4)) dimmed considerably, with no apparent reduction in the relative brightness of the rings or shadow spots. Signifying that the crystallinity was not improved and the film just got rougher. The image of the sample after removal from the chamber shows the left half of the sample exposed to RHEED clearly. SEM no longer shows the presence of a NaCl layer in either area. Instead, Ge islands are simply sitting on the GaAs substrate surface. The density of islands in the area WRE is higher than the area with NRE, but because neither area had a conformal film to protect the NaCl for heating to high temperatures, the NaCl desorbs away. When attempting to remove the Ge islands from the substrate (Figure 30(c8)) it was more sporadic. Perhaps some NaCl existed some places that were not imaged in SEM, facilitating removal, while in other regions the Ge fused to the substrate and could not be lifted off.

Another sample was grown, now increasing T_{GaAs1} to 350°C (Figures 30(d)). The RHEED pattern of the NaCl is again bright and streaky. But after the first minute of Ge deposition, the pattern is slightly different than previous cases. There are not full rings, rather they are broken into spots, often intersecting the symmetric shadow spots about the primary. The primary spots are very bright and show chevrons connecting them. This indicates a more textured film than the previous cases. With further growth, the primary spots get relatively brighter compared to the rings and shadow spots as well signifying an improvement of the crystal structure. The lines from the RHEED exposure can be seen again, including marks from when the sample was rotated 90° during growth (Figure 30(d5)). The SEM images still show continuous NaCl layers in both areas WRE and NRE (Figures 30(d6,7)). In the area WRE the Ge more closely resembles a film of approximately the target thickness, while outside of the RHEED-exposed area the density of the islands is much lower. These discrete islands also can be much taller than expected and are extremely faceted. This suggests that the Ge adatoms can move around on the NaCl surface until they find an existing Ge island to help grow. When attempting to remove the overlayer from the substrate as shown in Figure 30(d8), the tape peeled easily from the substrate. There is a clear line where the area was exposed to the RHEED. Moving away from that, the dark color fades. This is because of the dense film where the RHEED was and moving away from this region the density of the Ge islands decreases, until they are no longer visible with a camera.

The RHEED patterns when increasing T_{GaAs1} to 400°C (Figures 30(e1-4)) are similar to the previous case. And while streaks can be seen on the sample from the presence of the RHEED beam (Figure 30(e5)), the SEM images reveal discrete islands (Figure 30(e6)), and nothing resembling a full film. The nucleation rate of Ge on NaCl at these temperatures must be lower, and the NaCl is definitely desorbing faster. Even with a longer initial NaCl deposition (t_{NaCl}) of 30 min, there is no NaCl present underneath these Ge islands. Additionally, in the area with NRE, neither a NaCl layer nor Ge islands are really observed. It is likely that in this area the nucleation density of Ge is

so low that the NaCl fully desorbs and heteroepitaxial Ge is deposited directly on the GaAs. Attaching the sample to tape was not able to remove any material that was visible to the eye.

A final sample with t_{NaCl}=60 minutes was done using a T_{GaAs1}=450°C (Figures 30(f)). The RHEED pattern of the NaCl layer at this temperature is still streaky but starting to blur, which is understandable because the substrate temperature is almost equivalent to the effusion cell temperature. After closing the NaCl and opening the Ge for 60 seconds, the pattern has dimmed further as the sample was roughening as Ge was going down on an actively desorbing surface. With continued growth, the pattern begins to reveal spotty streaks and eventually finishes with a bright pattern that has rotational symmetry (Figure 30(f4)). However, unlike the previous samples the area WRE is barely discernable in Figure 30(f5). Cross section SEM reveals why; in the area WRE it appears only slightly rougher than the area with NRE. Small voids are present under the surface at a depth approximately equal to the target Ge layer. This would suggest that the area with NRE (Figure 30(f7)) is heteroepitaxial Ge on GaAs, and that the layer on top of the voids in the area WRE is also Ge that formed only fast enough for some NaCl to sublime out leaving behind a pore. Attempted removal of material from this substrate (Figure 30(f8)) unsurprisingly yielded no results.

List of samples grown

Date	Sample	Wafer	NaCl Temp	NaCl time	Overlayer Temperature(s)	BI Temp
			(°C)	(min)	(°C)	(°C)
190709A		(100)	100	15	580	
190709B		(100)	200	15	580	
190712A		(100)	100	poly	380-580	
190717A		(100)±0.1°	100	15	~430-580	
190717B		(100)±0.1°	100	15	430-580	
190719A		(100)±0.1°				
190724A		(100)±0.1°	150	15	380-580	
190724B		(100)±0.1°	175	15	380-580	
190802A		(100)±0.1°	175	15	430-580	
190808A		(100) 2°->(1-10)	175	15	~450-580	
190813A		(100) 2°->(1-10)	100	30	375-580	
190813B		(100) 2°->(1-10)	250	15	430-580	
190821A		(100) 2°->(1-10)	100	15	430-580	
190821B		(100) 2°->(1-10)	100°	15	430-580	
190827A		(100) 2°->(1-10)	100	15	430-580	
190827B		trolley3	100	15		
190904A		(100)±0.1°	100	30	430-580	
190905A		(100)±0.1°	100	30	430-580	
190905B		(100)±0.1°	100	30		
190919A		(100)±0.1°	100	30	100	
190930A		(100)±0.1°	100	30	100-580	
191002A		(100)±0.1°	110	30	110-580	
191008A		(100)±0.1°	110	30	200-580	
191008B		(100)±0.1°	110	30	300-580	
191018A		(100)±0.1°	110	30	250-580	
191018B		(100)±0.1°	110	10	110-580	
191111A		(100)±0.1°	x	x		
191112A		(100)±0.1°	x	x		
191113A		(100)±0.1°	x	x	250	500
191114A		(100)±0.1°	110	10	250	500
191114B		(100)±0.1°	x	x	250	
191120A		(100)±0.1°	110	10	250	500
191120B		(100)±0.1°	x	x	250	550
191122A	EE266	(100)±0.1°	110	10	250-580	500
191122B	EE267	(100)±0.1°	110	10	fast 250-580	
191204A		(100)±0.1°	110	10	250/325-580	
191204B		(100)±0.1°	110-325	10+9	325-580	
191204C		(100)±0.1°	x	x	250-580	
191220A	manual	(100)±0.1°	x	x		
191223A	manual	above substr.	110-325	10+6+4	360	
191226A	EE271	(100)±0.1°	110-325	10+9.5	354	500
191226B	EE272	(100)±0.1°	110-325	10+10	364	
191227A	EE273	(100)±0.1°	110-325	10+8.75	344	
200110A	EE274	(100)±0.1°	110-300	10+15	300	
200113A	EE275	(100)±0.1° GaAs	x	x	300	550
200128A	EE276		x	x	310	580
200204A	EE277		x	x	310	595
200205A	EE278		x	x	310	630
200225A	EE279		x	x	310	550
200226A	EE280		x	x	250	550
200226B	EE281		x	x	310	
200228A	EE282		x	x	250	550
200302A	EE283	(100)±0.1°	x	x	250	575
200302B	EE284	(100)±0.1°	x	x	250	575
200303A	EE285	(100)±0.1°	110	10	250	550
200303B	EE286	(100)±0.1°	110	10	250	
200306A	EE287	(100)±0.1°	110	10	250	550
200311A	EE288	(100)±0.1°	110	10	250	550
200311B	EE289	(100)±0.1°	110	10	250	550
200316A	EE290	(100)±0.1° GaAs	110	60+11	350	
200316B	EE291	(100)±0.1°	110	60+11	400	
200317A	EE292	(100)±0.1°	110	60+13	450	
200317B	EE293	(100)±0.1°	110	60+12	500	
200318A	EE294	(100)±0.1°	110	180+11	450	
200320A	EE295	(100)±0.1° GaAs	110	180+12	500	
200323A	EE296	(100)±0.1°	110	180+11	550	
200324A	EE297	(100)±0.1°	110	240+12	550	
200325A	EE298	(100)±0.1°	110	240+12	550	
200514A	EE299	(100)±0.1° GaAs	110	10	110	
200515A	EE300	(100)±0.1°	110	10	110	
200525A	EE301	(100)±0.1°	110	10	110	
200525B	EE302	(100)±0.1°	110	10	110	
200527A	EE303	(100)±0.1° GaAs	110	10	110,110	
200609A	EE304	(100)±0.1° GaAs	110	10	250	
200629A	EE305	(100)±0.1° GaAs	175	5	175	
200629B	EE306	(100)±0.1°	x	x	175	500
200630A	EE307	(100)±0.1°	175	5	175	500
200715A	EE308	(100)±0.1° GaAs	175	5	175,300-380	500
200715B	EE309	(100) 2°->(111)A	175	5	175	500
200721A	EE310	(100)±0.1°	175	5	175,300	500
200721B	EE311	(100) 2°->(111)A	175	5	175,300	500
200727A	EE312	(100) 2°->(111)A	175	5	175	500
200727B	EE313	(100) 2°->(111)A	175	5	175,300	500
200729A	EE314	(100) 10°->(111)A	175	5	175,300	500
200729B	EE315	(100) 2° ->(111)A	175	5	175,300,400	500
200803A	EE316	(100)±0.1°	175	3	175,300	500
200803B	EE317	(100) 10°->(111)A	250	5	250,300	500
200805A	EE318	(100)±0.1°	175	3	175,300	575
200805B	EE319	(100)±0.1°	175	2	175,300	500
200805C	EE320	(100) 10° ->(111)A	225	5	225,300	500
200814A	EE321	(100)±0.1°	200	5	200,300	500
200814B	EE322	(100)±0.1°	175	3	175,300	500
200819A	EE323	(100)±0.1°	x	x	580->200	
200819B	EE324	(100)±0.1°	x	x	175	
200901A	EE325	Si	100°	60	x	
200914A	EE326	(100)±0.1° GaAs	175	3	175	500
200914B	EE327	(100)±0.1°	175	3	175	500
200930A	EE328	(100)±0.1° GaAs	175	3	175	500
200930B	EE329	(100)±0.1°	175	3	175	500
201008A	EE330	(100)±0.1° GaAs	175	3	175	500
201008B	EE331	(100)±0.1°	175	3	175	500
201013A	EE332	(100)±0.1°	175	3	175,300	500
201013B	EE333	(100)±0.1°	175	3	175,300	500
201014A	EE334	(100)±0.1°	150	3	150,300	500
201014B	EE335	(100)±0.1°	150	3	150,300	500
200803A copies		(100)±0.1°	175	3	175,300	500
200803A copies		(100)±0.1°	175	3	175,300	500

Date	Sample	Wafer	NaCl Temp	NaCl time	Ge Temp,time	GaAs Temp,time	Bi Temp
			(°C)	(min)	(°C,min)	(°C,min)	(°C)
210209A		(100)±0.1°	20	10	20, 30m		
210210A		(100)±0.1°	20	10	20, 30m		
210210B		(100)±0.1°	--	--	20, 30m		
210216A		(100)±0.1°	150	5	150, 10m		
210216B	EE336	(100)±0.1°	200	5	200, 10m		
210217A	EE337	(100)±0.1°	150	5	150, 10m		
210301A	EE338	(100)±0.1° GaAs	175	10	175, 20m		
210302A	EE339	(100)±0.1°	175	10	175, 20m		
210302B	EE340	(100)±0.1°	175	60	175, 20m		
210303A	EE341	(100)±0.1°	175	10	175, 20m		
210303B	EE342	(100)±0.1°	150-250	10+9.75	250, 20m		
210308A	EE343	(100)±0.1°	150-250	10+9.75	250, 20m		
210308B	EE344	(100)±0.1°	150-300	10+14	300, 20m		
210309A	EE345	(100)±0.1°	150-350	10+14.5	350, 20m		
210309B	EE346	(100)±0.1°	150-300	10+13	300, 20m		
210310A	EE347	(100)±0.1°	150-400	30+19	400, 20m		
210310B	EE348	(100)±0.1°	150-450	60+23	450, 20m		
210315A	EE349	(100)±0.1°	150-350	10+>15	350, 60m		
210315B	EE350	(100)±0.1°	--	--	350, 20m		
210316A	EE351	(100)±0.1°	150-350	10+>12	350,20m		500
210316B	EE352	(100)±0.1°	150-250	10+11	250/350, 15s/20m		
210317A	EE353	(100)±0.1°	150-350	10+15	350, 60m	580, 3m	
210331A	EE354	(100)±0.1° GaAs	150-300	10+12	300/350, 15s/20m		
210331B	EE355	(100)±0.1°	150-300	10+12	--	400, 3m	
210401A	EE356	(100)±0.1°	150-350	10+15	350,20m	580, 9m	
210402A	EE357	(100)±0.1°	150	10		150 As, 2m, GaAs 340-580	
210402A	EE358	(100)±0.1°	150-300	10+x	300, 20m		550
210402B	EE359	(100)±0.1°	150-300	10+x	300, 20m ttl		

Date	Sample	Wafer	NaCl Temp	NaCl time	GaAs Temp,time
			(°C)	(min)	(°C,min)
210403A	EE360	(100)±0.1°	150	10	*350-580, 15m*
210403B	EE361	(100)±0.1°	150	10	*400-580, 15m*
210405A	EE362	(100)±0.1°	150	10	*450-580, 15m*
210405B	EE363	(100)±0.1°	150	10	*425-580, 15m*
210415A	EE364	(100)±0.1°	150	10	350-410, 3m, 580, 9m
210415B	EE365	(100)±0.1°	150	20	*425-580, 15m*
210416A	EE366	(100)±0.1°	150	10	350-410, 3m, 580, 9m
210416B	EE367	(100)±0.1°	150	10	*350-580, 15m*
210419A	EE368	(100)±0.1°	150	10	*350-580, 15m*
210422A	EE369	(100)±0.1°	150	10	*350-580, 15m*
210422B	EE370	(100)±0.1°	150	60	*450-580, 15m*
210428A	EE371	(100)±0.1°	150	20	*425-580, 15m*
210428B	EE372	(100)±0.1°	150	10	350-410, 1m, 580, 9m
210430A	EE373	(100)±0.1°	150	15	*400-580, 15m*
210430B	EE374	(100)±0.1°	150	10	350-410, 2m, 580, 9m
210505A	EE375	(100)±0.1°	150	15	400-460/580, 3/9m
210505B	EE376	(100)±0.1°	150	10	350, ~2min
210518A	EE377	(100)±0.1°	150	10	350, 1min
210518B	EE378	(100)±0.1°	150	10	350, ~1min
210524A	EE379	(100)±0.1°	150	15	400-460/580, 3/9m
210524B	EE380	(100)±0.1°	150	10	350, ~12min
210525A	EE381	(100)±0.1°	150	15	375-435/580, 3/9m
210525B	EE382	(100)±0.1°	150	10	350, ~17min
210610A	EEman1	(100)±0.1°			
210611A	EE383				
210617A	EE384	(100)±0.1°	150	15	150, 1min
210622A	EE385	(100)±0.1° C	150	10	350, ~17m, 580 9m
210627B	EE386	(100)±0.1°	150	10	350/400/580, 17/1/3m
210629A	EE387	(100)±0.1° C	150	25	400-460, 3m, 580, 9m
210629B	EE388	(100)±0.1°	150	25	350/400/580, 17/1/3m
210713A	EE389	(100)±0.1° C	150	25	375-435, 3m
210713B	EE390	(100)±0.1°	150	25	350/400, 17/1m
210723A	EE391	(100)±0.1° C	150	25	300/400, 17/1m
210723B	EE392	(100)±0.1°	150	25	300/400/580, 17/1/0m
210727A	EE393	(100)±0.1° C	--	--	--
210809A	EE394	(100)±0.1° C	150	35	300/400, 17/9m
210809B	EE395	(100)±0.1°	150	35	300/400/580/650, 17/9/9/5m
210818Acell	EE396	(100)±0.1° C	150	35	300/400/580 17/9/12+cell
210825Acell	EE397	(100)±0.1° C	150	35	300/400/580 18/9/9+cell
211004A	EE398	(100)±0.1° C	150	30	350/400/580, 17/2/9
211004B	EE399	(100)±0.1°	150	30	350/400/580, 17/2/9
211005A	EE400	(100)±0.1° C	150	30	350/400/580, 6/2/9
211005B	EE401	(100)±0.1° C	150	30	350/400/580, 4/2/9
211007Acell	EE402	(100)±0.1° C	150	30	350/400/580, 4/2/24+cell
211007B	EE403	(100)±0.1° C	150	30	350/400/580, 4/2/9
211008Acell	EE404	(100)±0.1° C	150	30	350/400/580, 4/2/24+cell
211008B	EE405	(100)±0.1° C	150	30	350/400/580, 17/2/9
211011A	EE406	(100)±0.1° C	150	30	350/400/580, 4/4/9
211011B	EE407	(100)±0.1° C	150	30	350/580, 4/9
211012Acell	EE408	(100)±0.1° C	150	30	350/580, 4/24+cell
211012B	EE409	(100)±0.1° C	150	30	350/580, 6/9
211108A	Eeman	(100)±0.1° C	150	30	bare salt
211109A	EE410	(100)±0.1° C	150	30	350/580, 6/24
211112A	EE411	(100)±0.1° C	150	30	350/540, 6/24
211112B	EE412	(100)±0.1° C	150	10	350/580, 6/24
211116A	EE413	(100)±0.1° C	150	30	350/580, 6/24
211116B	EE414	(100)±0.1° C	150	60	350/580, 6/24
211117A	EE415	(100)±0.1° C	150	30	350/580, 6/24
211117B	EE416	(100)±0.1° C	150	10	350/580, 9/24
211122A	EE417	(100)±0.1° C	150	10	350/580, 6/24
211122B	EE418	(100)±0.1° C	150	10	350/580, 4/24
211124A	EE419	(100)±0.1° C	150	10	350/560, 2.6/24
211124B	EE420	(100)±0.1° C	150	10	350/560, 4/4+24
211129A	EE421	(100)±0.1° C	150	10	350/560, 1.5/24
211129B	EE422	(100)±0.1° C	150	10	350/560, 1.5/24*
211201A	EE423	(100)±0.1° C	150	10	350/560, 4/4+22.5
211201B	EE424	(100)±0.1° C	150	10	350/560, 4/16
211223A	EE425	(100)±0.1° C	150	5	350, 5
211223B	EE426	(100)±0.1° C	150	5	350/560, 5/24
211228A	EE427	(100)±0.1° C	150	5	350, 10
211228B	EE428	(100)±0.1° C	150	5	350/540, 10/24
211230A	EE429	(100)±0.1° C	150	7.5	350/540, 10/24
211230B	EE430	(100)±0.1° C	150	7.5	350/540, 10/24
220104A	EE431	(100)±0.1° C	150	5	350/540, 4/5
220104B	EE432	(100)±0.1° C	150	5	350/540, 2.6/5
220105A	EE433	(100)±0.1° C	150	5	350/540, 8/5
220105B	EE434	(100)±0.1° C	150	5	350/540, 4/5